U.S. DEPARTMENT OF COMMERCE
National Technical Information Service

PB-267 100

EXPLORE-I: A River Basin Water Quality Model

Battelle Pacific Northwest Labs, Richland, Wash

Prepared for

Environmental Protection Agency, Washington, D C Office of Research and Monitoring

Aug 73

BIBLIOGRAPHIC DATA SHEET

1. Report No.

2.

3. Recipient's Accession No.

4. Title and Subtitle

EXPLORE I: A River Basin Water Quality Model

5. Report Date
August 1973

6.

7. Author(s) R.G. Baca, W.W. Waddel, Charles R. Cole
Albin Brandstetter, D.B. Cearlock

8. Performing Organization Rept. No.

9. Performing Organization Name and Address

Battelle-Northwest
P.O. Box 999
Richland, WA 99352

10. Project/Task/Work Unit No.

11. Contract XXXX No.
68-01-0056

12. Sponsoring Organization Name and Address

Environmental Protection Agency
Office of Monitoring & Research

13. Type of Report & Period Covered
Final

14.
EPA

15. Supplementary Notes

16. Abstracts

A dynamic river basin water quality model, EXPLORE was developed to simulate the dynamics of water flow and quality in rivers, estuaries shallow lakes and impoundments. The model will handle several boundary conditions such as weirs, dams, loops, diversions and discharges in addition to tidal flows and the occurrence of tidal flats. The water quality module consists of a multiparameter transport submodel with various other submodels which describe the chemical-biological kinetics of the system. A total of 16 water quality parameters can be modeled simultaneously. Testing and verification of the EXPLORE river basin model was conducted on the Willamette River Basin in Oregon. This basin was chosen because the Willamette is a large river with a tidally influenced reach, several major tributaries and considerable flow regulation, thereby encompassing a wide range of hydraulic conditions. The following appendicies were also prepared A-Literature Review, B - User's Manual, C - Programmer's manual.

17. Key Words and Document Analysis. 17a. Descriptors

17. Algae
Biochemical oxygen demand
Dissolved oxygen
Ecology
Estuaries
Lakes
Limnology
*Mathematical Models
Reservoirs
*Rivers
*Water Pollution
Water quality

17b. Identifiers/Open-Ended Terms

Ecological models
Limnological models
River basin water quality models
Wastewater management
*Water quality planning
*Willamette River (Oregon)

17c. COSATI Field/Group

18. Availability Statement
Release unlimited

19. Security Class (This Report)
UNCLASSIFIED

20. Security Class (This Page)
UNCLASSIFIED

21. No. of Pages
125

22. Price
PC A06 | MF A01

FORM NTIS-35 (REV. 10-73) ENDORSED BY ANSI AND UNESCO. THIS FORM MAY BE REPRODUCED USCOMM-DC 8265-P74

PB 267 100

REPRODUCED BY
NATIONAL TECHNICAL
INFORMATION SERVICE
U. S. DEPARTMENT OF COMMERCE
SPRINGFIELD, VA. 22161

EXPLORE-I: A RIVER BASIN WATER QUALITY MODEL

by

Robert G. Baca
William W. Waddel
Charles R. Cole
Albin Brandstetter
Dennis B. Cearlock

PACIFIC NORTHWEST LABORATORIES
a division of
BATTELLE MEMORIAL INSTITUTE
Battelle Boulevard
Richland, Washington 99352

for the

Office of Research and Monitoring
ENVIRONMENTAL PROTECTION AGENCY

Project #211B00557
Contract #68-01-0056

August 1973

SUMMARY

Battelle-Northwest has developed a comprehensive mathematical water quality model, EXPLORE-I, for use in river basin planning and water resource studies. This generalized river basin water quality model can predict the hydrodynamics and water quality dynamics for rivers, well mixed estuaries, and thermally stratified reservoirs. The model has been set up, calibrated, and verified, using historical hydraulic and water quality data, on a portion of the Willamette River Basin consisting of major tributaries and a thermally stratified reservoir.

The EXPLORE-I model is an extended and modified version of the Storm Water Management Model, receiving water component, which was developed for studies of DO/BOD dynamics. The EXPLORE-I model predicts the flows and stage in the general water system in addition to the transport and interaction of the following water quality parameters:

- Carbonaceous Biochemical Oxygen Demand
- Nitrogenous Biochemical Oxygen Demand
- Benthic Biochemical Oxygen Demand
- Total Organic Carbon
- Refractory Organic Carbon
- Sedimentary Phosphorus
- Soluble Phosphorus
- Organic Phosphorus
- Ammonia Nitrogen
- Nitrite Nitrogen
- Nitrate Nitrogen
- Organic Nitrogen
- Toxic Compounds
- Phytoplankton
- Zooplankton
- Dissolved Oxygen

CONTENTS

Page

SUMMARY iii

FIGURES vii

TABLES x

SECTION I: EXPLORE I: A RIVER BASIN WATER QUALITY MODEL 1

SECTION II: PROJECT OBJECTIVES AND ORGANIZATION 5

SECTION III: MODELING APPROACH 7

  Specie Continuity 10
  Fundamental Assumptions of the Model 10

SECTION IV: WATER QUALITY SUBMODELS 13

  Biochemical Oxygen Demand 13
  Benthic Oxygen Demand 16
  Total Organic Carbon 17
  Nitrogen Model 18
  Phosphorus Model 20
  Photosynthesis and Respiration of Suspended Algae 22
  Photosynthesis and Respiration of Attached Algae and Benthic Plants 23
  Dissolved Oxygen 23
  Planktonic Algae Model 26
  Toxic Compounds 28

SECTION V: HYDRAULIC MODEL SELECTION 31

  Hydraulic Models Considered 31
  Model Selection 32

SECTION VI: RESERVOIR MODEL SELECTION 41

  Reservoir Models Considered 41
  Model Selection 42
  Description of the Reservoir Model 42
  Problems Encountered 63

Preceding page blank

Page

SECTION VII: VERIFICATION OF EXPLORE-I RIVER BASIN CODE ON THE WILLAMETTE RIVER BASIN 65

Verification of Hydraulic Code 66
Verification of Quality Model 83

SECTION VIII: MODEL VERIFICATION ON DETROIT RESERVOIR 103

Problems Encountered in Calibration 103
Program Testing 106

SECTION IX: PROGRAM SYNOPSIS, CAPABILITIES, AND LIMITATIONS 113

River Basin Program 113
Reservoir Simulation Program 114
Application of the EXPLORE-I Model 115

REFERENCES 117

ACKNOWLEDGMENTS 121

FIGURES

NO.		PAGE
1	WILLAMETTE BASIN	4
2	CHARACTERIZATION OF THE WATER QUALITY PROBLEM: PHENOMENOLOGICAL INTERRELATIONSHIPS AND SOURCES OF POLLUTION	8
3	CONCEPTUAL REPRESENTATION OF THE WATER SYSTEM	9
4	INTEGRATED SUBMODELS	14
5	ALGAL NITROGEN MODEL	18
6	ALGAL PHOSPHORUS MODEL	20
7	FACTORS AFFECTING THE DISTRIBUTION AND FATE OF TOXIC MATERIALS IN WATER	29
8	CHANNEL-JUNCTION DEFINITION FOR COMPUTATIONAL MESH	35
9	ILLUSTRATION OF TEMPERATURE - INFLOW RELATIONSHIP FOR THE DEEP RESERVOIR HYDROTHERMAL MODEL	43
10	DISCRETIZATION OF A RESERVOIR GEOMETRY	52
11	CONCEPTUALIZATION OF A WITHDRAWAL ZONE	56
12	ILLUSTRATION OF WITHDRAWAL LAYER CONFIGURATIONS	58
13	TEMPERATURE AND DENSITY STRUCTURE FOR APPLICATION OF CRAYA'S CRITERIA	59
14	WILLAMETTE RIVER BASIN SIMULATION FROM SALEM TO PORTLAND	68
15	PREDICTED WATER SURFACE ELEVATION FROM WILLAMETTE FALLS TO SALEM	75
16	WATER DEPTH VERSUS RIVER MILE FROM SALEM TO PORTLAND	75
17	VELOCITY PROFILE FROM SALEM TO PROTLAND	76
18	DIAGRAM ILLUSTRATING SMALL TRIBUTARY CHANNEL CONFIGURATION	77
19	EFFECT OF DEOXYGENATION COEFFICIENT, k_1, ON PREDICTED BOD VALUES	89

FIGURES (continued)

NO.		PAGE
20	CALIBRATED BOD MODEL	90
21	PREDICTED AND OBSERVED DATA FOR BOD AT RIVER MILE 71.9 FOR PERIOD 1 - 12 SEPT. 1967	92
22	PREDICTED AND OBSERVED DATA FOR BOD AT RIVER MILE 34.4 FOR PERIOD 1 - 12 SEPT. 1967	92
23	PREDICTED AND OBSERVED DATA FOR BOD AT RIVER MILE 16.6 FOR PERIOD 1 - 12 SEPT. 1967	93
24	EFFECT OF REAERATION COEFFICIENT k_2 ON PREDICTED DISSOLVED OXYGEN LEVELS	94
25	CALIBRATED DISSOLVED OXYGEN MODEL	94
26	VERIFICATION OF DISSOLVED OXYGEN MODEL WITH AUGUST 1967 DATA	96
27	VERIFICATION OF DISSOLVED OXYGEN MODEL WITH JUNE 1967 DATA	96
28	PREDICTED AND OBSERVED DATA FOR DISSOLVED OXYGEN AT RIVER MILE 71.9 FOR PERIOD 1 - 12 SEPT. 1967	97
29	PREDICTED AND OBSERVED DATA FOR DISSOLVED OXYGEN AT RIVER MILE 34.4 FOR PERIOD 1 - 12 SEPT. 1967	97
30	PREDICTED AND OBSERVED DATA FOR DISSOLVED OXYGEN AT RIVER MILE 16.6 FOR PERIOD 1 - 12 SEPT. 1967	98
31	CALIBRATED NITROGEN MODEL	98
32	VERIFICATION OF NITROGEN MODEL WITH AUGUST 1967 DATA	99
33	VERIFICATION OF NITROGEN MODEL WITH JUNE 1967 DATA	99
34	CALIBRATION OF PHOSPHORUS MODEL	100
35	VERIFICATION OF PHOSPHORUS MODEL WITH AUGUST 1967 DATA	101
36	VERIFICATION OF PHOSPHORUS MODEL WITH JUNE 1967 DATA	101

FIGURES (continued)

NO.		PAGE
37	DETROIT RESERVOIR: MODEL STUDY AREA	104
38	DETROIT RESERVOIR: TEMPERATURE SURVEY STATIONS	105
39	INITIAL CONDITIONS	107
40	UPSTREAM INFLOW (BOUNDARY CONDITIONS)	108
41	RESERVOIR QUALITY SIMULATION OF DISSOLVED OXYGEN	109
42	RESERVOIR QUALITY SIMULATION OF CARBONACEOUS BOD	109
43	RESERVOIR QUALITY SIMULATION OF PHYTOPLANKTON	110
44	RESERVOIR QUALITY SIMULATION OF ZOOPLANKTON	110
45	RESERVOIR QUALITY SIMULATION OF TOXIC COMPOUNDS	111
46	RESERVOIR SIMULATION OF TEMPERATURE	111

TABLES

NO.		PAGE
1	WATER QUALITY PARAMETERS MODELED IN EXPLORE-I	15
2	SUMMARY OF DATA SOURCES USED IN MODEL CALIBRATION ON WILLAMETTE RIVER BASIN	66
3	TABULATION OF THE USGS FLOW DATA USED IN VERIFICATION RUNS	70
4	TABULATION OF CLACKAMAS RIVER INFLOW DATA	71
5	TUALATIN RIVER FLOW RATIOS AND FLOW VALUES USED TO SIMULATE THE SEPTEMBER 1967 AND JUNE 1967 FLOW PERIODS	72
6	STABILITY CHART CALCULATED BY USING THE WRE STABILITY CRITERION	79
7	STABILITY CHART CALCULATED FROM EQUATION 105	80
8	STABILITY CHART CALCULATED FROM EQUATION 105	81
9	STABILITY CHART CALCULATED FROM EQUATION 105	82
10	DATA USED FOR CALIBRATION AND VERIFICATION OF EXPLORE-I WATER QUALITY MODEL	85
11	DISCHARGE DATA FOR EXPLORE-I VERIFICATION ON WILLAMETTE RIVER BASIN	88

SECTION I

EXPLORE I: A RIVER BASIN WATER QUALITY MODEL

INTRODUCTION

The management of water resources in a river basin is a complex task. Sufficient quantities of water must be maintained with the proper levels of quality to satisfy many diverse and often conflicting needs. Uses such as irrigation, power generation, and disposal of municipal and industrial wastes may affect the water quality adversely. Other uses, such as domestic or industrial supplies, recreation, and sport and commercial fishing may require relatively high levels of quality. Past development of water management policy has primarily been determined on a first-come, first-served basis because the many pressures of competitive uses did not exist. Today the nation no longer enjoys the luxury of dividing the water resources on a haphazard basis but must instead develop and apply management policies which consider all uses, both for the present and for the future.

A tool which can help resource managers immensely is the ability to quantitatively describe the behavior and interactions of various water quality parameters in a river basin system. Mathematical modeling represents an efficient method for predicting such water quality levels. The mathematical model is a flexible and economical tool which can be tailored to each river system as required.

The mathematical model EXPLORE-I was developed by Battelle-Northwest for the Environmental Protection Agency to serve as a management tool in the allocation of water resources in a river basin. EXPLORE-I is a synthesis of a number of existing hydraulic and water quality models which have shown reliability in the past. These models were identified in an extensive literature review and were incorporated into a single model which enables the resource manager to obtain and overall perspective of various allocation schemes.

EXPLORE-I is capable of simulating a number of hydraulic regimes in either a dynamic or steady state mode. These regimes are

- streams and rivers,
- shallow lakes, and
- estuaries or tidally influenced rivers.

The behavior and interactions of the following water quality parameters can be studied for the hydraulic regimes listed above.

- Carbonaceous Biochemical Oxygen Demand (BOD)
- Nitrogenous Biochemical Oxygen Demand (BOD)
- Benthic Biochemical Oxygen Demand (BOD)
- Total Organic Carbon (TOC)
- Refractory Organic Carbon
- Sedimentary Phosphorus
- Soluble Phosphorus
- Organic Phosphorus
- Ammonia Nitrogen
- Nitrite Nitrogen
- Nitrate Nitrogen
- Organic Nitrogen
- Toxic Compounds
- Phytoplankton
- Zooplankton
- Dissolved Oxygen

In addition, a second computer model was developed for analysis of water quality in thermally stratified reservoirs. Although the original contract did not require development of a thermal model, the broad scope of the project necessitated the inclusion of a model to predict temperatures and flows in a thermally stratified reservoir. The Deep Reservoir Thermal Model was selected and tested but the results were generally unsatisfactory; an intensive reprogramming effort was required to render the computer model fully operational and capable of specifying temperatures and flows in stratified reservoirs. A Deep Reservoir Water Quality Model was developed and programmed which can readily be interfaced with several existing single segment, thermal hydraulic models.

All program modules of the EXPLORE-I code were applied on the Willamette River Basin in Oregon (Figure 1) to demonstrate that the models work properly and indeed can be used to describe the water quality levels in a general river system.

The main objectives of this research project are summarized in Section II of this report. Sections III, IV, and V provide a detailed discussion of the models used in this program. These models were selected from extensive literature reviews, as described in Appendix A. A summary of the EXPLORE-I code is presented in Section IX. Sections VII and VIII discuss the verification of the program on the Willamette River Basin. Operation and coding details are given in Appendices B and C, User's Manual and Programmer's Manual.

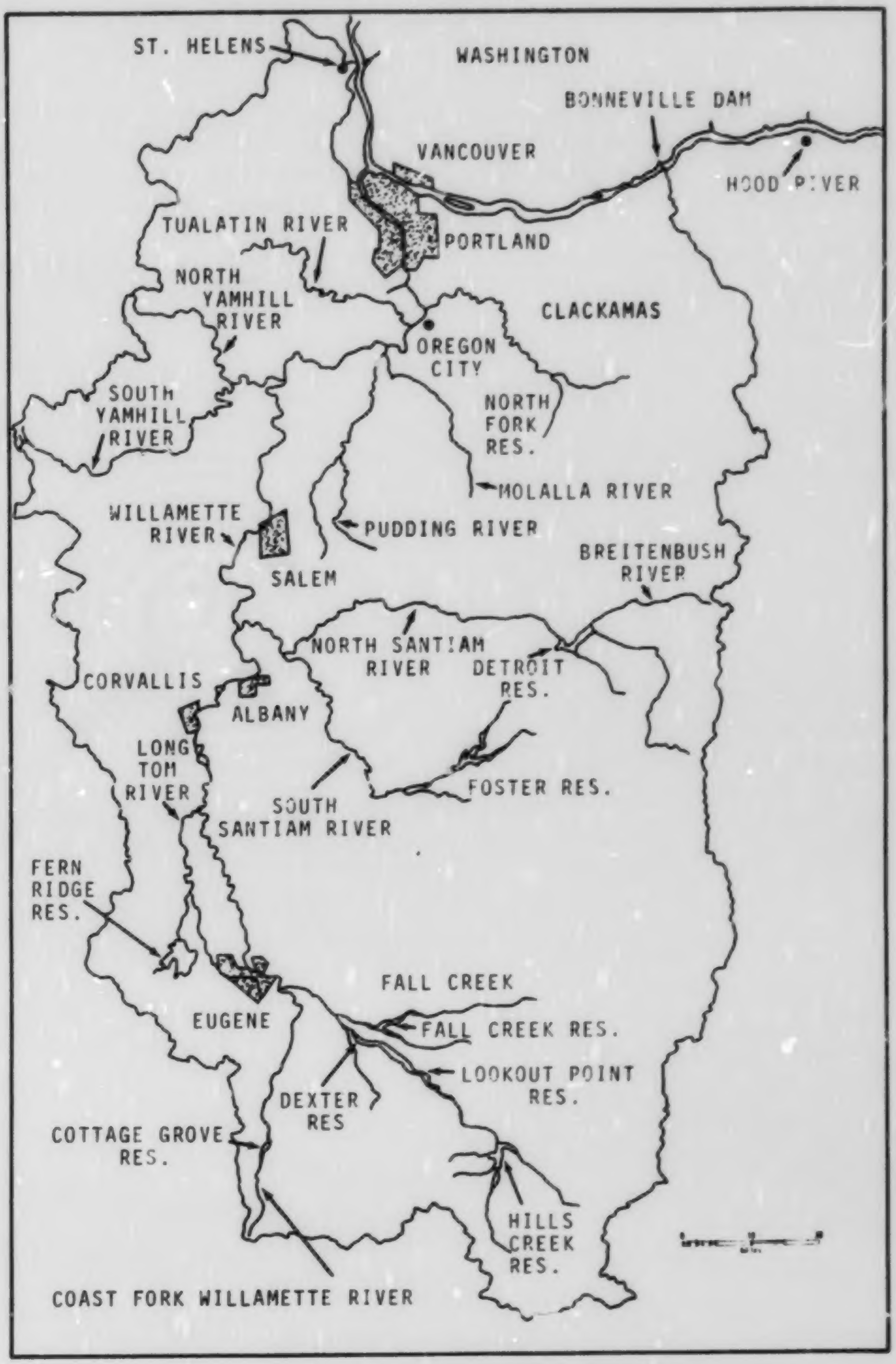
ST. HELENS
WASHINGTON
BONNEVILLE DAM
VANCOUVER
HOOD RIVER
TUALATIN RIVER
PORTLAND
NORTH YAMHILL RIVER
CLACKAMAS
OREGON CITY
SOUTH YAMHILL RIVER
NORTH FORK RES.
MOLALLA RIVER
WILLAMETTE RIVER
PUDDING RIVER
SALEM
BREITENBUSH RIVER
NORTH SANTIAM RIVER
DETROIT RES.
CORVALLIS
ALBANY
LONG TOM RIVER
FOSTER RES.
SOUTH SANTIAM RIVER
FERN RIDGE RES.
FALL CREEK
EUGENE
FALL CREEK RES.
LOOKOUT POINT RES.
DEXTER RES
COTTAGE GROVE RES.
HILLS CREEK RES.
COAST FORK WILLAMETTE RIVER

FIGURE 1. WILLAMETTE RIVER BASIN

SECTION II

PROJECT OBJECTIVES AND ORGANIZATION

This research project had two main objectives: to develop a comprehensive water quality model which could be applied to entire river basins and to calibrate and verify the model on the Willamette River Basin. These objectives have been met with the EXPLORE-I computer model.

The model, which can be applied to any river basin providing the appropriate data is specified, has the following characteristics and capabilities:

- It will describe the spatial and temporal variations of sixteen water quality parameters, characterizing the behavior and interrelationships of dissolved oxygen, biochemical oxygen demand, algal populations, nutrient cycles, and toxic compounds.
- It is applicable to any river basin with widely varying hydraulic regimes.
- It is flexible and can provide both steady and dynamic predictions.
- It is capable of simulating diurnal or long-term periods.
- It is capable of handling constant and/or time varying point or diffuse sources.
- It is capable of simulating any portion of the river basin individually or as a subsystem of a large scale system.
- It is relatively simple to set up and use on a digital computer.
- It can reliably predict the hydromechanics and water quality in river systems, estuaries and thermally stratified reservoirs.

Considerable attention has been given to the computer implementation aspects of this project, e.g., input data checking and defaults, formats and output specifications, etc., to promote and facilitate the routine use of the computer code.

The EXPLORE-I computer model was developed by the staff of the Water Resources Systems Section of the Water and Land

Resources Department, Battelle-Northwest Research Laboratories. The work was performed under the administrative direction of Mr. Dennis B. Cearlock, Manager of the Water Resources Systems Section. Mr. Robert G. Baca organized and coordinated the project and was responsible for the development of the Deep Reservoir modules of EXPLORE-I. Mr. William W. Waddell developed the water quality submodels, incorporated them in the river and estuary modules and contributed substantially to the calibration and verification effort on the Willamette River Basin. Mr. Charles R. Cole extended and applied the river and estuary hydrodynamics module. Dr. Albin Brandstetter provided expert technical guidance in various areas of hydraulics and mathematical modeling.

SECTION III

MODELING APPROACH

A mathematical model consisting of a set of describing equations is an analog of the physical system and processes which it represents. The model is generally constructed so that it will react to various stimuli in the same manner as the real system. However, only those phenomena which are important to the model's objectives need be included in the general formulation and other physical mechanisms may be ignored. In this manner, the total number of variables is reduced to a workable set.

In developing a mathematical model of water quality pertinent concepts from many diverse fields such as hydraulics, hydrology, chemistry, and biology must be organized and integrated into a practical scientific tool. As illustrated in Figure 2, the interrelationships between various phenomena are as diverse and complex in nature as are natural and man-made sources of pollution. Recent research in the fields of water quality and ecology has provided much basic knowledge of individual phenomena and mathematical characterizations of specific cause and effect interrelationships. Many of these relationships have been successfully used to model the key parameters of individual phenomena such as assimilation of organic material, algae growth and death, nitrogen and phosphorus cycles, bacterial decay, reaeration and other mechanisms which dictate the quality of a water body. The list of key parameters grows as the concern for water pollution problems increases. The sixteen basic parameters modeled in this work are discussed in Section IV.

EXPLORE-I effectively combines the water quality models within the framework of a general purpose river basin model. The overall model formulation is partitioned into two basic components, or modules, which can be operated sequentially: the hydromechanics module and the mass transport and water quality submodels module. Two general purpose computer codes, a river and estuary code and a deep reservoir code, were developed. This modular approach allows parallel development and calibration.

The hydromechanics module is formulated on conservation of mass and momentum principles. A simple conceptual representation of the water system such as that illustrated in Figure 3 is used as a computational network to determine the flow and stage history for a river network and/or estuary system. The specific formulation of the hydromechanics module is presented in Section V of this report. A hydromechanics

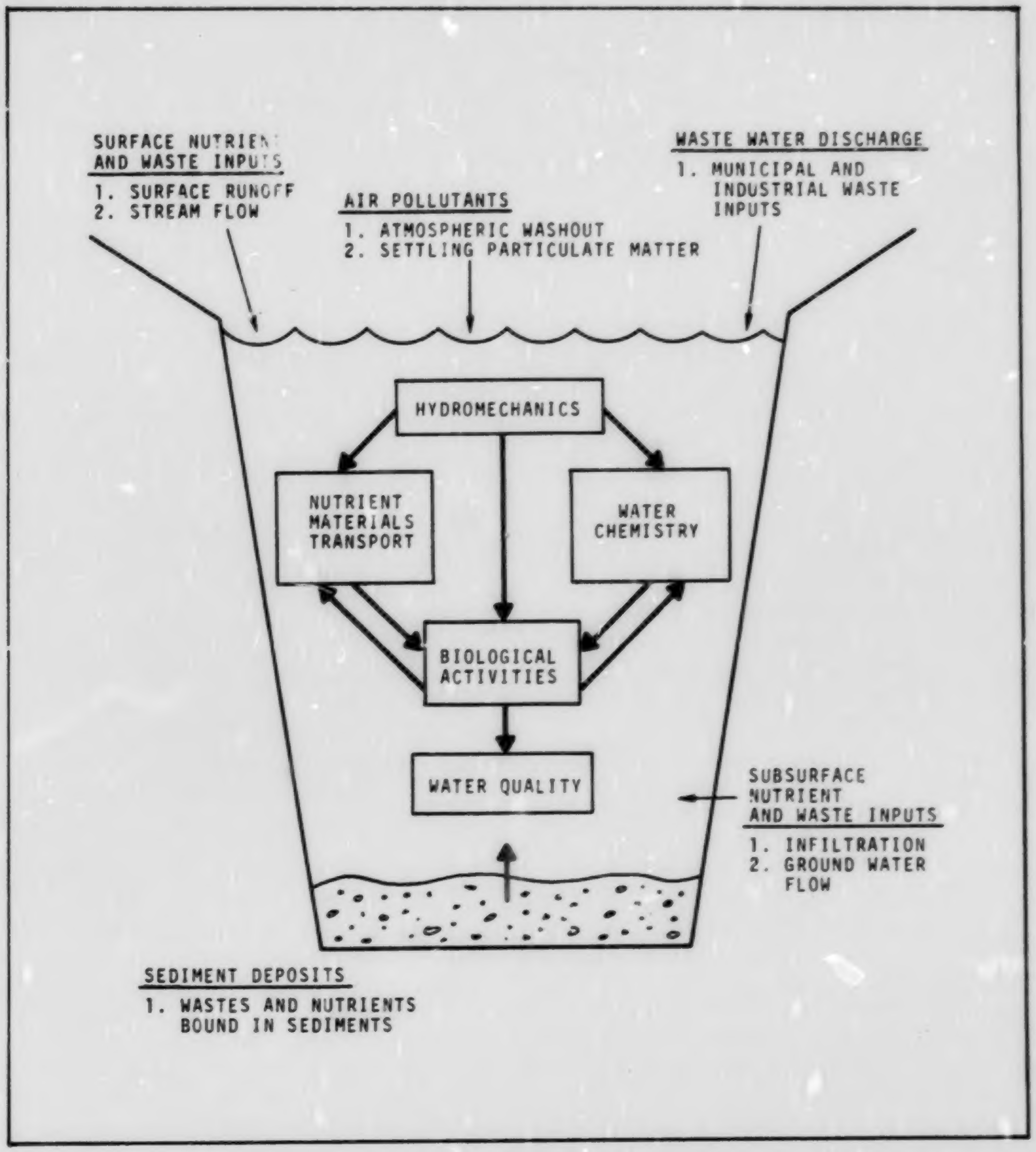
SURFACE NUTRIENT AND WASTE INPUTS
1. SURFACE RUNOFF
2. STREAM FLOW
AIR POLLUTANTS
1. ATMOSPHERIC WASHOUT
2. SETTLING PARTICULATE MATTER
WASTE WATER DISCHARGE
1. MUNICIPAL AND INDUSTRIAL WASTE INPUTS
HYDROMECHANICS
NUTRIENT MATERIALS TRANSPORT
WATER CHEMISTRY
BIOLOGICAL ACTIVITIES
WATER QUALITY
SUBSURFACE NUTRIENT AND WASTE INPUTS
1. INFILTRATION
2. GROUND WATER FLOW
SEDIMENT DEPOSITS
1. WASTES AND NUTRIENTS BOUND IN SEDIMENTS

FIGURE 2. CHARACTERIZATION OF THE WATER QUALITY PROBLEM: PHENOMENOLOGICAL INTERRELATIONSHIPS AND SOURCES OF POLLUTION

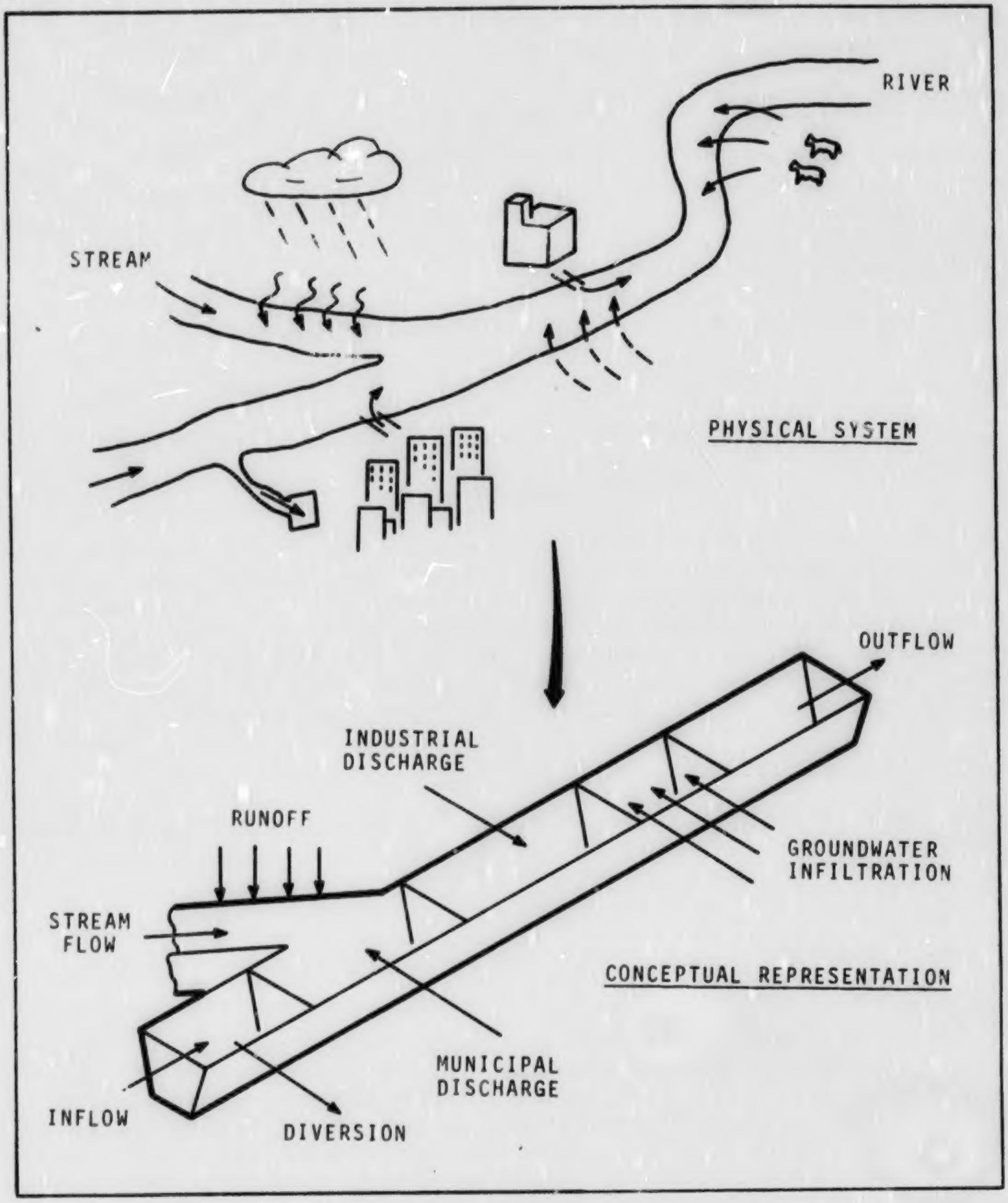
RIVER
STREAM
PHYSICAL SYSTEM
OUTFLOW
INDUSTRIAL DISCHARGE
RUNOFF
GROUNDWATER INFILTRATION
STREAM FLOW
CONCEPTUAL REPRESENTATION
MUNICIPAL DISCHARGE
INFLOW
DIVERSION

FIGURE 3. CONCEPTUAL REPRESENTATION OF THE WATER SYSTEM

module for stratified lakes and reservoirs was also developed to predict flow and temperature patterns. This model is based on an analytic-empirical approach which is discussed in Section VI.

SPECIE CONTINUITY

The mass transport water quality submodels module is formulated from the expressions for specie continuity, i.e., mass balance of a particular constituent or specie. For any biotic or abiotic substance the general mass transfer expression is the sum of individual forms of mass transfers.

$$\begin{aligned}\text{Accumulation} = {} & \text{Advection} + \text{Diffusion} + \text{Import} - \text{Export} \\ & - \text{Settling} + \text{Scour} + \text{Reaeration} - \text{Decay} \\ & \pm \text{Chemical Transformations} \pm \text{Biological} \\ & \text{Transformations} \qquad (1)\end{aligned}$$

The first five terms of this balance are the transport component of the EXPLORE-I model while the remaining terms constitute the water quality submodels. Development of the EXPLORE-I multiparameter water quality submodel involved formulating mathematical expressions for the kinetics of the individual mass transfer mechanisms. Several kinetic expressions have been proposed which vary in range of applicability and level of complexity.

FUNDAMENTAL ASSUMPTIONS OF THE MODEL

In the mass transport/water quality submodels module, two basic assumptions are intrinsic to the EXPLORE-I model. These are:

- diffusion is negligible
- mass transfer is partitioned into simple transport and water quality kinetics

The first of these was assumed for the river and estuary code because of the nebulous nature of hydrodynamic dispersion coefficients. Although literature on the subject is plentiful, no single equation or methodology is currently available which will accurately determine the mixing characteristics of a general water body. In addition, investigations have shown that finite-difference solutions to the advection-diffusion equation can introduce pseudo dispersion effects which completely mask the actual solution. To avoid these difficulties and simplify data input specifications the diffusion term has been ignored.

The second assumption refers to the sequence of computations involved in the solution of the complete equation for specie continuity.

For simplicity and convenience of computer implementation, the solution of the mass balance is partitioned into the sum of individual changes, namely

$$C^{k,n+1} = C^{k,n} + \Delta C^{k,n+1}_{\text{transport}} + \Delta C^{k,n+1}_{\text{kinetics}} \qquad (2)$$

where

$C^{k,n}, C^{k,n+1}$ = concentration of the k^{th} parameter at the old and new time planes, n and n+1 respectively.

$\Delta C^{k,n+1}_{\text{transport}}$ = incremental change on the k^{th} parameter due to simple transport, i.e., advection, import and export, in the n+1 time plane

$\Delta C^{k,n+1}_{\text{kinetics}}$ = incremental change in the k^{th} parameter due to water quality kinetics, i.e., settling, scour, reaeration, decay, and chemical and biological transformations

The incremental change $\Delta C^{k,n+1}_{\text{transport}}$ is obtained by some finite-difference approximation from the solution of the partial differential equation for simple transport of each constituent. The incremental change $\Delta C^{k,n+1}_{\text{kinetics}}$ is determined from the simultaneous solution of the kinetic equations for all constituents by a 4th order Runge-Kutta scheme. Numerical experiments have shown that this form of approximation is adequate and greatly reduces the difficulty of the computational problem. Sections IV, V, and VI present more detailed information on the specific formulation of these modules and their operation.

The EXPLORE-I model is a versatile and useful scientific tool for evaluation of alternative strategies of water quality management. In the hands of experienced analysts and decision-makers, this model can be efficiently used to find sound and economical solutions to complex water pollution problems in many different types of water systems including estuaries and bays, streams and river networks, lakes and reservoirs, and combinations of these. Application of EXPLORE-I is relatively inexpensive, far less than for large-scale sampling programs.

SECTION IV

WATER QUALITY SUBMODELS

The water quality submodels used to describe the reactions of various quality parameters in both the river and estuary and deep reservoir models are discussed in this section. A review of all quality models identified during an extensive literature survey is contained in Appendix A.

In choosing the models for each quality parameter, a number of guidelines were considered. Past successful use of a model was an important criterion, because the purpose of this study was to identify and use the best existing models rather than to develop new ones. In addition, the simplest models which would provide acceptably accurate results were selected. Consideration was also given to the model's ease of calibration with existing water quality data.

The program consists of eleven integrated water quality submodels which predict the behavior of sixteen water quality parameters. A diagram of the relationship between these submodels is shown in Figure 4 and Table 1 provides a list of the sixteen water quality parameters.

BIOCHEMICAL OXYGEN DEMAND

A number of models reviewed treat the biochemical oxygen demand (BOD) reaction in a river system as other than a first order reaction. These models have two things in common: first, they do not predict BOD concentrations with any more accuracy than the first order models. Second, considerably more data are required to determine the large number of coefficients in these models. Hence, a model using first order BOD reactions was adopted.

The carbonaceous and nitrogenous components of BOD were separated to allow individual treatment of each reaction. The BOD equations are written as

$$\frac{dL_c}{dt} = -\left(k_1^c + k_3^c\right)L_c + P_c \qquad (3)$$

$$k_1^c = k_1^c(20)\ \theta_c^{(T-20)} \qquad (4)$$

Preceding page blank

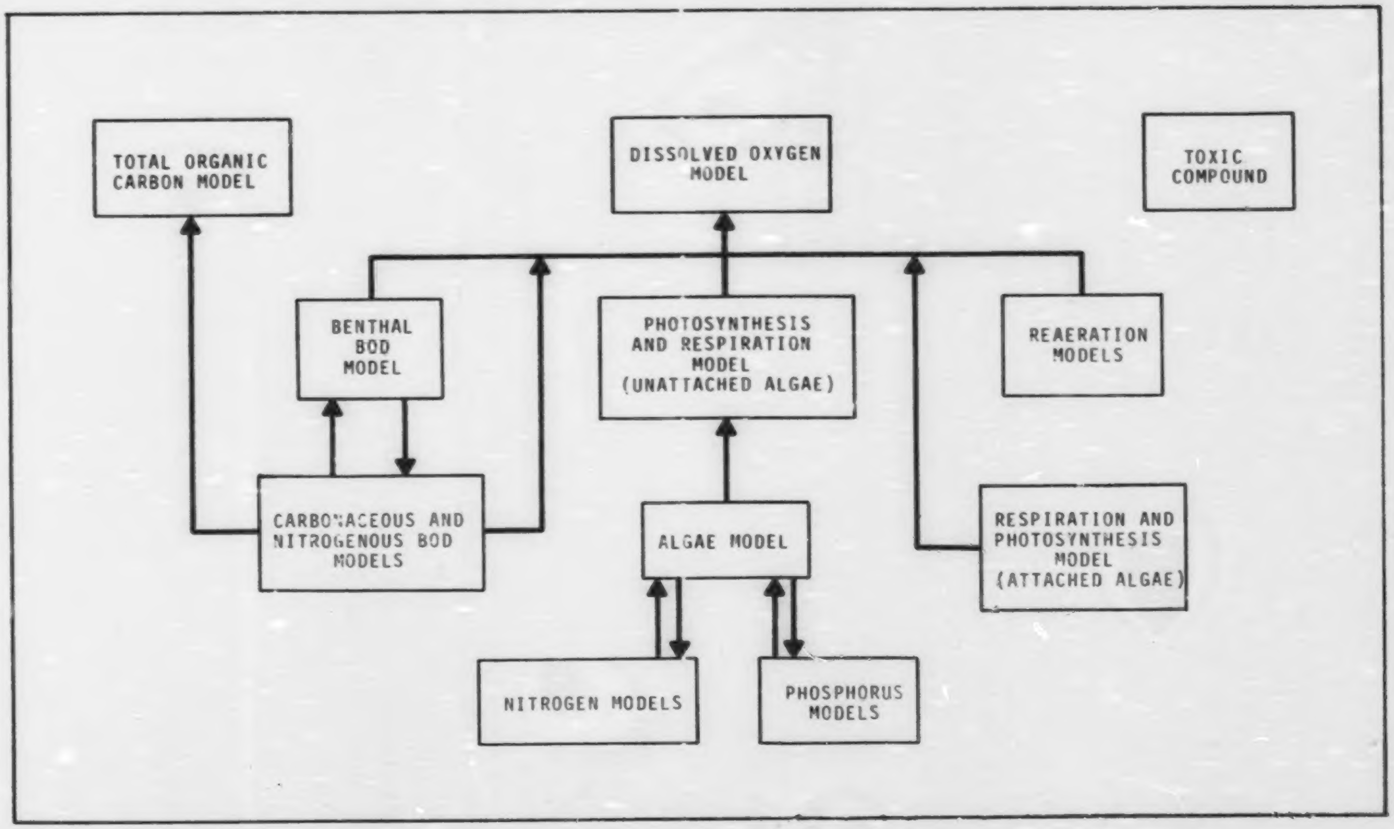
TOTAL ORGANIC CARBON MODEL
DISSOLVED OXYGEN MODEL
TOXIC COMPOUND
BENTHAL BOD MODEL
PHOTOSYNTHESIS AND RESPIRATION MODEL (UNATTACHED ALGAE)
REAERATION MODELS
CARBONACEOUS AND NITROGENOUS BOD MODELS
ALGAE MODEL
RESPIRATION AND PHOTOSYNTHESIS MODEL (ATTACHED ALGAE)
NITROGEN MODELS
PHOSPHORUS MODELS

FIGURE 4. INTEGRATED SUBMODELS

TABLE 1. WATER QUALITY PARAMETERS MODELED IN EXPLORE-I

1. Benthic Oxygen Demand
2. Sedimentary Phosphorus
3. Soluble Phosphorus
4. Organic Phosphorus
5. Carbonaceous BOD
6. Nitrogenous BOD
7. Refractory Organic Carbon
8. Total Organic Carbon
9. Ammonia Nitrogen
10. Nitrite Nitrogen
11. Nitrate Nitrogen
12. Organic Nitrogen
13. Toxic Compounds
14. Phytoplankton
15. Zooplankton
16. Dissolved Oxygen

$$\frac{dL_n}{dt} = - k_1^n L_n \qquad (5)$$

$$k_1^n = k_1^n(20)\ \theta_n^{(T-20)} \qquad (6)$$

where

L_c = carbonaceous BOD, mg/l

k_1^c = deoxygenation coefficient

k_3^c = sedimentation coefficient: 0.0-3.5/day

P_c = scour coefficient: 0.0-0.8 mg/l-day

$k_1^c(20)$ = deoxygenation coefficient at 20°C: 0.1-0.8/day

θ_c = temperature coefficient: 1.02-1.06

T = temperature, °C

L_n = nitrogenous BOD, mg/l

k_1^n = deoxygenation coefficient: 0.1-0.8/day

$k_1^n(20)$ = deoxygenation coefficient at 20°C

θ_n = temperature coefficient: 1.05

c = denotes carbonaceous

n = denotes nitrogenous

Sedimentation and scour terms were included in the carbonaceous BOD equation to allow the use of the model with different waste discharges and in varying hydraulic situations. Since the nitrogenous BOD is normally in a dissolved state these terms were excluded from that equation.

BENTHIC OXYGEN DEMAND

The benthic oxygen demand has been described primarily as a steady state or first order reaction. Because of the success of the first order reaction models a kinetic rate form was chosen for use in this program. The equation is:

$$\frac{1}{H}\frac{dL_d}{dt} = - k_4 \frac{L_d}{H} - P_c + k_3^c L_c \qquad (7)$$

$$k_4 = k_4(20)\ \theta_d^{(T-20)} \qquad (8)$$

where

L_d = areal benthic BOD, mg/m^2

k_4 = deoxygenation coefficient for benthic BOD

$k_4(20)$ = deoxygenation coefficient at 20°C: 0.0-0.8/day

θ_d = temperature coefficient: 1.05

H = average river depth, m

P_c, k_3^c, L_c are defined above

This equation is coupled to the carbonaceous BOD equation through the constants P_c, k_3^c and L_c.

TOTAL ORGANIC CARBON

No models were identified for simulating the reactions of total organic carbon (TOC) during the literature review. The following first order model was developed (see Appendix A) and is used in the program:

$$\frac{dC_T}{dt} = - (M_1 + M_3)\ A_B L_c - M_3 C_T + P_B + P_R \qquad (9)$$

$$M_1 = M_1(20)\ \theta_m^{(T-20)} \qquad (10)$$

$$C_T = A_B L_c + C_R \qquad (11)$$

where

C_T = total organic carbon, mg/l

C_R = refractory organic carbon, mg/l

M_1 = deoxygenation coefficient: 0.1-0.8/day

$M_1(20)$ = deoxygenation coefficient at 20°C

M_3 = sedimentation coefficient: 0.0-3.5/day

A_B = proportionality constant: 10.0

L_C = carbonaceous BOD, mg/l

P_B = scour of degradable organic carbon: 0.0-0.8 mg/l-day

P_R = scour of refractory organic carbon: 0.0-0.8 mg/l-day

θ_m = temperature coefficient: 1.05

This model is related to the BOD model since the rate of reaction depends upon the concentration of carbonaceous BOD.

NITROGEN MODEL

Two nitrogen models have been included in the program. One considers the effects of algae while the second includes ammonia-nitrate dynamics. The algal nitrogen model (Figure 5a) assumes that each reaction can be described by a first order equation. The concentrations

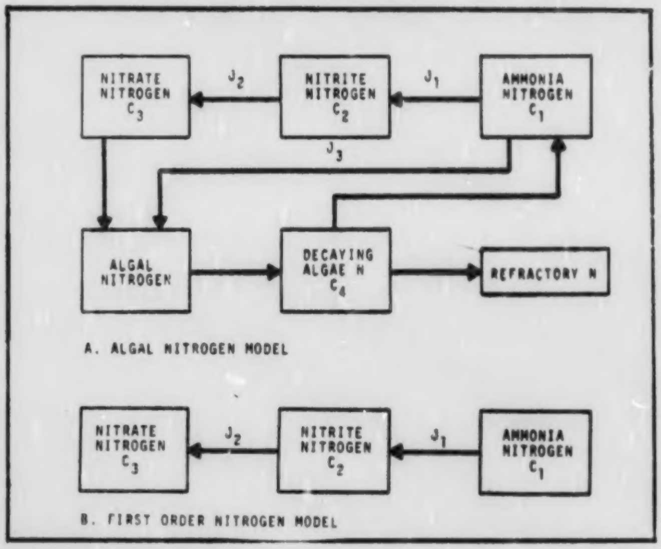
NITRATE NITROGEN C_3
J_2
NITRITE NITROGEN C_2
J_1
AMMONIA NITROGEN C_1
J_3
ALGAL NITROGEN
DECAYING ALGAE N C_4
REFRACTORY N
A. ALGAL NITROGEN MODEL
NITRATE NITROGEN C_3
J_2
NITRITE NITROGEN C_2
J_1
AMMONIA NITROGEN C_1
B. FIRST ORDER NITROGEN MODEL

FIGURE 5. NITROGEN MODELS

of the various nitrogen forms are given by C_i and the rates of reaction are given by J_i. The various nitrogen components were formulated as a first order model for two reasons. First, the relative simplicity of the first order equations with only one constant to be evaluated (along with the boundary conditions) is attractive. Detailed data for regression on a large number of constants will generally not be available. Second, the firt order model has been shown to work satisfactorily, at least under certain conditions. The model is described by the equations:

$$\frac{dC_1}{dt} = - J_1C_1 + J_3C_4 - G_P\ P\ A_{NP} \left[\frac{C_1}{C_1+C_3}\right] \tag{12}$$

$$\frac{dC_2}{dt} = - J_2C_2 + J_1C_1 \tag{13}$$

$$\frac{dC_3}{dt} = J_2C_2 - G_P\ P\ A_{NP} \left[\frac{C_3}{C_1+C_3}\right] \tag{14}$$

$$\frac{dC_4}{dt} = - J_3C_4 + D_PP\ A_{NP} + (D_Z - G_Z)A_{NZ}Z \tag{15}$$

where

C_1 = ammonia concentration, mg/l

C_2 = nitrite concentration, mg/l

C_3 = nitrate concentration, mg/l

C_4 = organic nitrogen concentration, mg/l

J_1, J_2, J_3 = rate constants: 0.1-0.5, 5.0-10.0, 0.1-0.4/day

P,Z = phytoplankton and zooplankton concentrations, mg-C/l

A_{NP}, A_{NZ} = ratio of nitrogen to carbon in phytoplankton and in zooplankton: 0.17, 0.15 mg-N/mg-C

G_P, G_Z = growth rates of phytoplankton and zooplankton,/day

D_P, D_Z = death rates of phytoplankton and zooplankton,/day

P, Z, G_P, G_Z, D_P, and D_Z are formulated in the algae model.

A simple first order ammonia-nitrate model (Figure 5b) has been included in the code for use when algal effects are not to be considered:

$$\frac{dC_1}{dt} = - J_2C_1 \tag{16}$$

$$\frac{dC_3}{dt} = + J_2C_1 \tag{17}$$

PHOSPHORUS MODEL

Three phosphorus models are included in the quality model program. One includes the first order reactions of soluble phosphorus with algae and with the sediments. The second is a first order reaction model between soluble and sediment phosphorus. The third model is a second order decay model for soluble phosphorus.

The algal phosphorus model selected (Figure 6a) is similar to the nitrogen model and assumes that the reactions between the various forms of phosphorus can be described by a first order equation. The concentrations of the phosphorus forms are given by D_i and the rate constants for the reactions are given by I_i.

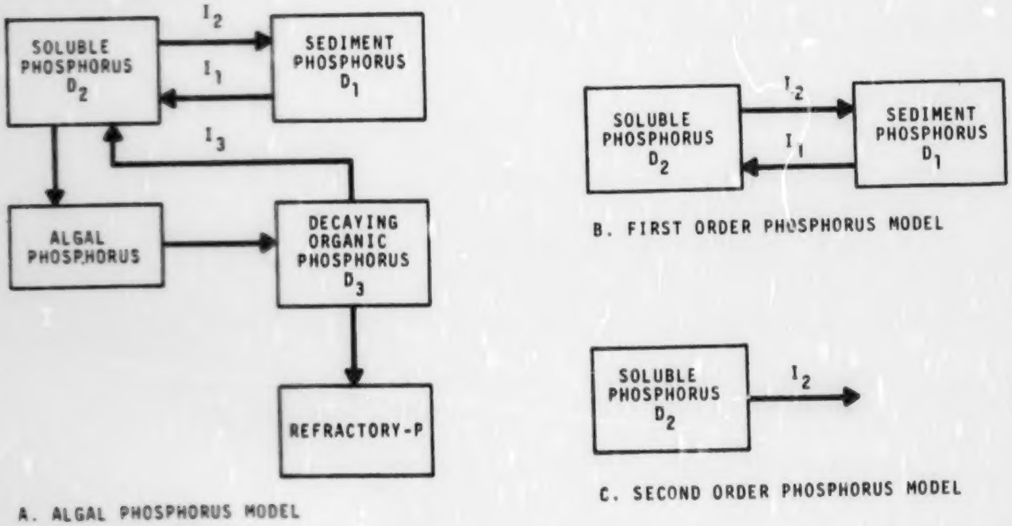
SOLUBLE PHOSPHORUS D_2
I_2
I_1
SEDIMENT PHOSPHORUS D_1
I_3
ALGAL PHOSPHORUS
DECAYING ORGANIC PHOSPHORUS D_3
REFRACTORY-P
SOLUBLE PHOSPHORUS D_2
I_2
I_1
SEDIMENT PHOSPHORUS D_1
SOLUBLE PHOSPHORUS D_2
I_2

A. ALGAL PHOSPHORUS MODEL

B. FIRST ORDER PHOSPHORUS MODEL

C. SECOND ORDER PHOSPHORUS MODEL

FIGURE 6. PHOSPHORUS MODELS

Phosphorus was modeled as a set of first order reactions primarily because no other models were available in the literature. The first order model allows a simple analysis method for phosphorus behavior in cases where sufficient data are available to calibrate the model. In addition, some past work has indicated that first order reactions are applicable to phosphorus behavior in at least some areas.

This model is considerably simpler than most proposed phosphorus cycles because it would not be possible to determine all the rate constants involved in a complicated system. Phosphorus data are usually incomplete and it is very unlikely that enough data would exist to allow a regression analysis on many constants. The equations for this model are:

$$\frac{dD_1}{dt} = - I_1D_1 + I_2D_2 + I_3D_3 - G_PP\ A_{DP} \quad (18)$$

$$\frac{dD_2}{dt} = -I_2D_2 + I_1D_1 \quad (19)$$

$$\frac{dD_3}{dt} = - I_3D_3 + D_PP\ A_{DP} + (D_Z - G_Z)A_{DZ}Z \quad (20)$$

where

D_1 = soluble phosphorus concentration, mg/l

D_2 = sedimentary phosphorus concentration, mg/l

I_1, I_2, I_3 = rate constants : 0.1-0.7/day

P = phytoplankton concentration, mg-C/l

Z = zooplankton concentration, mg-C/l

A_{DP}, A_{DZ} = ratio of nitrogen to carbon in phytoplankton and zooplankton: 0.17, 0.15 mg-N/mg-C

G_P, G_Z = growth rates of phytoplankton and zooplankton,/day

D_P, D_Z = death rates of phytoplankton and zooplankton, /day

P, Z, G_P, G_Z, D_P, and D_Z are formulated in the algae model.

The first order model (Figure 6b) assumes that only reactions between soluble and sedimentary phosphorus occur. This model uses the equations:

$$\frac{dD_1}{dt} = - I_1D_1 + I_2D_2 \qquad (21)$$

$$\frac{dD_2}{dt} = - I_2D_2 + I_1D_1 \qquad (22)$$

where the notation is the same as above.

The second order model (Figure 6c) uses the equation:

$$\frac{dD_1}{dt} = - I_1D_1^2 \qquad (23)$$

PHOTOSYNTHESIS AND RESPIRATION OF SUSPENDED ALGAE

The model chosen to represent the rate of photosynthesis and respiration of suspended algae is a two term harmonic function of the form:

$$(P-R)_s = A_1 \cos(\omega t + \phi) + A_2 \cos(2\omega t + \alpha) \qquad (24)$$

where

$(P-R)_s$ = net rate of photosynthesis and respiration: ±(0.1-2.0), mg/l-day

ω = period, days

A_1, A_2, ϕ, α = constants

This formulation was selected for two reasons. First, it is relatively simple since only three constants need to be determined (A_1,A_2 and the difference $\phi-\alpha$). The success of previous authors in using one, two, and three term periodic functions to model diurnal variations has shown that these relatively simple expressions can be successfully applied. Second, the two term expression is more desirable than the one term expression since with two terms the maximum rate of photosynthesis need not equal the maximum rate of respiration.

An option is provided in the program which allows the user to couple this equation to the phytoplankton density. This is done simply by:

$$(P-R)_s = \beta P \qquad (25)$$

Where P is the phytoplankton concentration and β is a proportionality constant.

PHOTOSYNTHESIS AND RESPIRATION OF ATTACHED ALGAE AND BENTHIC PLANTS

The model chosen to represent the net rate of photosynthesis and respiration of attached algae and benthic plants is identical to that used for the suspended algae model. It is given as

$$(P-R)_a = A_1^a \cos(\omega_a t + \phi_a) + A_2^a \cos(2\omega_a t + \alpha_a) \qquad (26)$$

where

$(P-R)_a$ = net rate of photosynthesis and respiration, ± (0.01-2.00), mg/l-day

ω_a = period, days

$A_1^a, A_2^a, \phi_a, \alpha_a$ = constants

DISSOLVED OXYGEN

Dissolved oxygen (DO) levels in a stream are influenced by a variety of interrelated factors. The more significant factors which contribute to the change in DO levels are: 1) reaeration, 2) bacterial oxidation of organic matter, 3) algal and plant photosynthesis and respiration, 4) benthal demand, and 5) temperature variations.

The rate of reaeration of well mixed pure water is proportional to the oxygen saturation deficiency. Mathematically this can be expressed as

$$\frac{dDO}{dt} = + k_2 (DO_s - DO) \qquad (27)$$

where

DO = dissolved oxygen concentration, mg/l

DO_s = saturated dissolved oxygen concentration, mg/l

k_2 = reaeration coefficient:0.05-16.0/day

The value of DO_s for natural, unpolluted streams can be calculated from the following equation:

$$DO_s = 14.652 - 0.41022T + 0.0079910T^2 - 0.000077774T^3 \qquad (28)$$

where

T = temperature, °C

Four separate models for estimating the reaeration coefficient have been included in the program. These models cover most of the work done on reaeration coefficients.

The first model for the reaeration coefficient is a general velocity-depth model of the form

$$k_2 = r_1 \frac{v^{r_2}}{h^{r_3}} \tag{29}$$

where

k_2 = reaeration coefficient,/day

v = velocity, ft/sec

h = depth, ft.

r_1, r_2, r_3 = constants; 2.0-12.0, 0.6-1.0, 0.85-1.85

The second model is one proposed by O'Connor and Dobbins[1] which is given as

$$k_2 = 1109 \frac{D_m^{1/2} S^{1/4}}{h^{5/4}} \quad \text{for } C < 17 \tag{30}$$

$$k_2 = \frac{(D_m v)^{1/2}}{h^{3/2}} \quad \text{for } C > 17 \tag{31}$$

where $C = \frac{v}{(hS)^{1/2}}$

and

D_m = liquid film diffusion coefficient: 0.01-0.02 ft^2/sec

S = river channel slope

The third model, proposed by Dobbins,[2] is given as:

$$k_2 = \frac{.2772\ C_A A E^{3/8} \coth\left(\frac{BE^{1/8}}{C_4^{\ 1/2}}\right)}{C_4^{\ 3/2} h} \tag{32}$$

where

$$C_4 = 0.9 + \frac{v}{\sqrt{gh}}$$

$$C_A = 1.0 + \left(\frac{v}{\sqrt{gh}}\right)^2$$

$A = 9.68 + 0.054\ (T-20)$

$B = 0.976 + 0.0137\ (30-T)^{3/2}$

$E = 30.\ v\ S$

g = gravitational constant, ft/sec^2

T = temperature, °C

The fourth model was proposed by Thackston and Krenkel[3]:

$$k_2 = 0.000299 \left[1 + \left(\frac{v}{\sqrt{gh}}\right)^{1/2} \right] \sqrt{\frac{Sg}{h}} \tag{33}$$

The temperature dependence of the reaeration coefficient for models one, two and four above is described by the following relationship:

$$k_2 = k_2(20)\ \theta^{(T-20)}. \tag{34}$$

This relationship was chosen because it is based on large amounts of data and has proven reliable in many investigations.

The effects of wind on the reaeration coefficient have been observed; however, only minor theoretical treatments were found. Therefore, wind effects were not included in this model.

With the exception of TOC (the contribution of which is handled through the BOD models) and toxic compounds, all models discussed previously provide input information either directly or indirectly to the dissolved oxygen model. The general equation describing the dissolved oxygen level is

$$\frac{dDO}{dt} = -k_1^c L_c - k_1^n L_n - \frac{k_4 L_d}{H} + k_2 (DO_s - DO)$$

$$+ (P-R)_s + (P-R)_a \qquad (35)$$

where

DO = dissolved oxygen, mg/l

k_1^c, k_1^n, k_4 = deoxygenation rates for carbonaceous, nitrogeneous and benthic BOD, /day

k_2 = reaeration coefficient, /day

$(DO_s - DO)$ = dissolved oxygen deficit

$(P-R)_s, (P-R)_a$ = photosynthesis and respiration rate for suspended and attached algae, respectively

Values for the rate constants and formulation of (P-R) contributions are presented in previous sections of the report.

PLANKTONIC ALGAE MODEL

The model selected for plankton is described by the following relationships:

$$\frac{dP}{dt} = [G_p - D_p]\, P \qquad (36)$$

$$\frac{dZ}{dt} = [G_z - D_z]\, Z \qquad (37)$$

where

$$G_p = F_1 T \left[\frac{2.718\, f}{k_e H} \left(e^{-\alpha_1} - e^{-\alpha_o} \right) \left(\frac{N}{K_n + N} \right) \left(\frac{D}{K_D + D} \right) \right] \qquad (38)$$

$$D_p = F_2 T + C_g Z \qquad (39)$$

$$G_z = A_{zp} C_g K_{mp} \left(\frac{P}{K_{mp} + P} \right) \qquad (40)$$

$$D_z = F_3 T + F_4 \qquad (41)$$

Notation

P = phytoplankton concentration, mg-C/l

G_p = phytoplankton growth rate, /day

D_p = phytoplankton death rate, /day

Z = zooplankton concentration, mg-C/l

G_z = zooplankton growth rate, /day

D_z = zooplankton death rate, /day

N = nitrate-nitrogen concentration, mg/l

F_1 = saturated growth rate of phytoplankton:0.05-0.20 /day-°C

T = temperature, °C

f = photoperiod:0.3-0.7, days

k_e = extinction coefficient:0.15-7.10, /ft

H = depth, ft.

$\alpha_1 = (I_a/I_s) \exp(-k_e H)$

I_a = average incident radiation, ly/day

I_s = saturated radiation, ly/day

K_n = Michaelis constant for total inorganic nitrogen: 0.025, mg-N/l

K_D = Michaelis constant for total phosphorus: 0.006-0.025, mg-P/l

F_2 = endogenous respiration rate of phytoplankton: 0.005, /day-°C

C_g = zooplankton grazing rate: 0.13, 1/mg-C-day

$\alpha_o = I_a/I_s$, fraction of saturation light intensity: 0.5-1.0

A_{np}, A_{dp} = phytoplankton nitrogen-carbon ratio: 0.05-0.17 mg-N/mg-C and phosphorus-carbon ratio: 0.024-0.24 mg-D/mg-C

A_{nz}, A_{dz} = zooplankton nitrogen-carbon ratio: 0.05-0.17 mg-N/mg-C and phosphorus-carbon ratio: 0.024-0.24 mg-D/mg-C

A_{zp} = zooplankton conversion efficiency: 0.6, mg-C/mg-C

K_{mp} = phytoplankton Michaelis constant: 0.06, mg-Chl/l

F_3 = zooplankton endogenous respiration rate 0.01 /day-°C

F_4 = zooplankton death rate due to other causes, /day

D = phosphorus concentration, mg/l

C = carbon

Chl = chlorophyll-A

This model considers two trophic levels (phytoplankton and zooplankton) and two limiting nutrients (nitrogen and phosphorus). If carbon is limiting, then additional Michaelis-Menton terms can be added to Equation 38 to adjust the saturated growth rate.

This model was selected because it is the least complex one available which accounts for all of the pertinent ecological parameters associated with phytoplankton and zooplankton. In addition, the model has been tested successfully in field studies. Average values for a number of the constants have been determined. The remaining constants have to be evaluated through calibration with field data.

TOXIC COMPOUNDS

The literature survey revealed very little information on the modeling of toxic compounds. The behavior of toxic compounds in an aquatic environment is highly variable and depends upon the compound being modeled. A model which would predict the interaction of toxic compounds with sediments, biota and other constituents would be a fine scientific tool but impossible to develop within the scope of this program. Figure 7 illustrates the complexity of the problem and traces the distribution and uptake of toxic materials.

Therefore, a simple n^{th} order decay model was included to describe toxic compounds. This model accounts for any order of decay desired, including zero order, and can easily accommodate nonlinear behavior. The model is given as:

$$\frac{dT_c}{dt} = - aT_c^n \quad (42)$$

where

T_c = concentration of toxic compound

a = rate constant

n = order of decay

This decay model can be used to represent any of the mechanisms of exchange such as chemical transformations, sedimentation, biological uptake, and sorption.

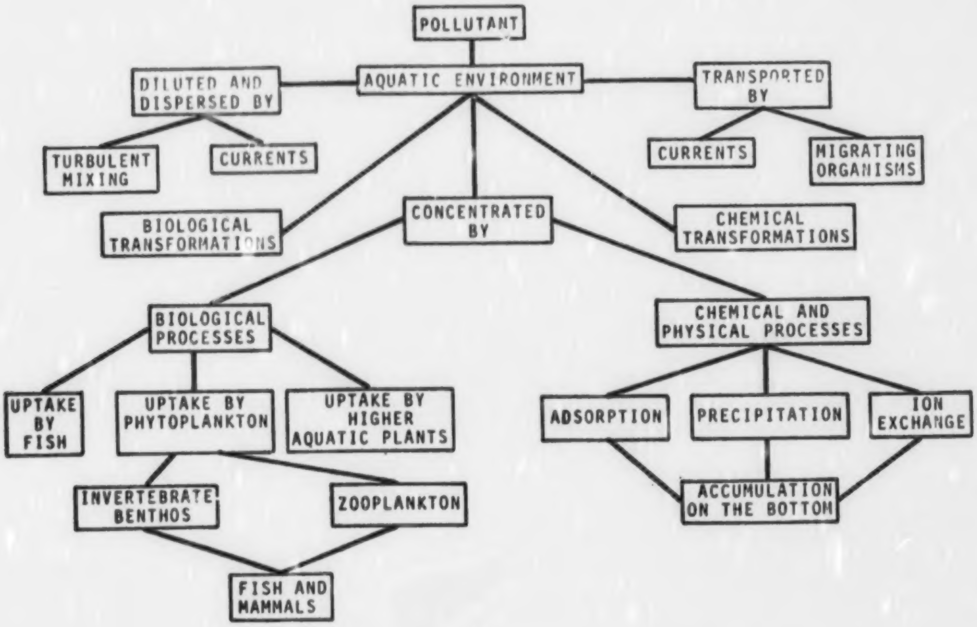
POLLUTANT
DILUTED AND DISPERSED BY
AQUATIC ENVIRONMENT
TRANSPORTED BY
TURBULENT MIXING
CURRENTS
CURRENTS
MIGRATING ORGANISMS
BIOLOGICAL TRANSFORMATIONS
CONCENTRATED BY
CHEMICAL TRANSFORMATIONS
BIOLOGICAL PROCESSES
CHEMICAL AND PHYSICAL PROCESSES
UPTAKE BY FISH
UPTAKE BY PHYTOPLANKTON
UPTAKE BY HIGHER AQUATIC PLANTS
ADSORPTION
PRECIPITATION
ION EXCHANGE
INVERTEBRATE BENTHOS
ZOOPLANKTON
ACCUMULATION ON THE BOTTOM
FISH AND MAMMALS

FIGURE 7. FACTORS AFFECTING THE DISTRIBUTION AND FATE OF TOXIC MATERIALS IN WATER

SECTION V

HYDRAULIC MODEL SELECTION

Three capabilities were required of the hydraulic model to be practicable for routine use: 1) it must be applicable to large scale physical systems (such as entire river basins); 2) it should accommodate as many of the flow regimes as possible which would be present in a river basin (e.g., small streams, large rivers, and tidally influenced regions); and 3) it must utilize an efficient and reliable algorithm.

HYDRAULIC MODELS CONSIDERED

Among the available hydraulic models considered for inclusion in the EXPLORE-I code were the following:

	Author	Description
1.	Amein and Fang	Implicit Flood Routing
2.	Amorocho and Strelkoff	Hydraulic Transients
3.	Garrison	Unsteady Flow Simulation
4.	Pisano	River Basin Simulation
5.	Water Resources Engineers	Storm Water Management

A summary of the hydraulic models reviewed is presented in Appendix A. Few general purpose computer models capable of handling complex river networks and varying hydraulic regimes are available for simulation of open channel flow hydraulics. In fact, general practice has relied upon simple regression relationships for stage and velocity as functions of flow. More sophisticated techniques are required, however, for estuarine hydrodynamics.

The Water Resources Engineers (WRE) Dynamic Estuary Model is to date the only hydrodynamic model capable of handling various hydraulic regimes and complex system geometries. At least three versions of the original program are currently available, including the FWPCA Dynamic Estuary Model,[4] the Columbia River Model,[5] and the Storm Water Management Model.[6] Each version varies in overall generality and in the numerical approximations used.

Preceding page blank

MODEL SELECTION

The hydraulic simulation module of the EXPLORE-I computer model is an adaptation and extension of the receiving water component of the Storm Water Management Model. This model utilizes a pseudo two-dimensional approach to solve momentum and continuity equations on an arbitrary computational mesh consisting of a set of interconnected channels and junctions.

The equations of motion and continuity for open channel flow (Saint-Venant equations) consist of two simultaneous equations:

Momentum

$$\frac{\partial V}{\partial t} + V\frac{\partial V}{\partial x} + g\frac{\partial h}{\partial x} = g\ (S_o - S_f + D_\ell) \qquad (43)$$

Continuity

$$\frac{\partial A}{\partial t} + \frac{\partial Q}{\partial x} = q \qquad (44)$$

where

$V = Q/A$ = average velocity of flow, positive in downstream direction

$A = A[x,h(x,t)]$ = cross-sectional area of flow

Q = discharge across a section

h = depth of flow

q = lateral inflow, negative if outflow

S_o, S_f = bottom slope of channel and resistance slope $\left(S_f = \frac{n^2|v|v}{2.2R^{4/3}}\right)$

R = hydraulic radius

n = Manning's n

D_ℓ = dynamic contribution of lateral discharge

x,t = space and time coordinates, respectively

The dynamic contribution of lateral inflow or outflow is given by

$D_\ell = 0$, for bulk lateral outflow

$D_\ell = \frac{Vq}{2Ag}$, for seepage outflow

$D_\ell = \frac{V-u_\ell}{Ag}q$, for lateral inflow

where

u_ℓ = x-component of the inflow-velocity vector.

The Saint-Venant equations can also be written with discharge instead of velocity as the primary kinetic variable. For flow through a rectangular cross section with negligible bottom slope and dynamic effect (of lateral inflow) these equations reduce to

Momentum

$$\frac{\partial V}{\partial t} + V\frac{\partial V}{\partial x} = -g\frac{\partial h}{\partial x} + gS_o - gS_f + gS_w \qquad (45)$$

Continuity

$$\frac{\partial A}{\partial t} + \frac{\partial Q}{\partial X} = 0 \qquad (46)$$

where

V = vertically averaged channel velocity

h = water depth

Q = volumetric flow rate

A = channel cross-sectional area (A=bh)

b = channel width

h = channel depth

S_w = wind stress term

The wind stress term S_w has been added to the traditional formulation to account for wind effects. In certain cases wind induced currents can be significant to the analysis of the flow patterns.

Most versions of the WRE hydraulic model are formulated in terms of head (potential) instead of water depth, which has created some confusion about the correctness and completeness of the momentum and continuity equations. In previous versions of the hydraulic model, the following substitutions were generally made:

$$\frac{\partial h}{\partial t} = \frac{\partial H}{\partial t} \tag{47}$$

$$\frac{\partial H}{\partial x} = - \frac{\partial h}{\partial x} + S_o \tag{48}$$

$$S_o = - \frac{\partial z}{\partial x} \tag{49}$$

Convenience and convention, rather than computational reasons, dictate the use of these approximations. The bottom slope contribution S_o is generally small in estuarine applications. However, in river systems where changes in elevation drive the motion of water, these contributions can be significant.

The EXPLORE-I hydraulic simulation program uses the modified form of the Saint-Venant equations to model the two-dimensional flow in an estuary or one-dimensional flow in a river system. A system is geometrically represented by a computational grid network. Using a simple routing concept, the flow in the system is prescribed along paths designated by channels connected by junctions. Each junction is characterized by its 1) surface area, 2) water surface elevation, 3) bottom elevation, and 4) the actual (X,Y) coordinates. Surface areas are computed from those polygons formed by the perpendicular bisectors of channels in the network. Flow between these junctions occurs through rectangular channels which connect the junctions. The characteristics of each channel are described by length, width, Manning coefficient, and average bottom elevation at the midpoint. Figure 8 illustrates the channel-junction configuration.

In the numerical solution scheme, the Saint-Venant equations are not solved simultaneously for all points in the water system. Instead, the equation of motion, Equation 50, is solved for each of the channels in the system on the basis of present values of the junction heads.

Momentum

$$\frac{\partial V}{\partial t} = -V\frac{\partial V}{\partial x} - g\frac{\partial H}{\partial X} - gS_f + gS_w \tag{50}$$

where

V = velocity

H = water surface elevation measured from the datum plane

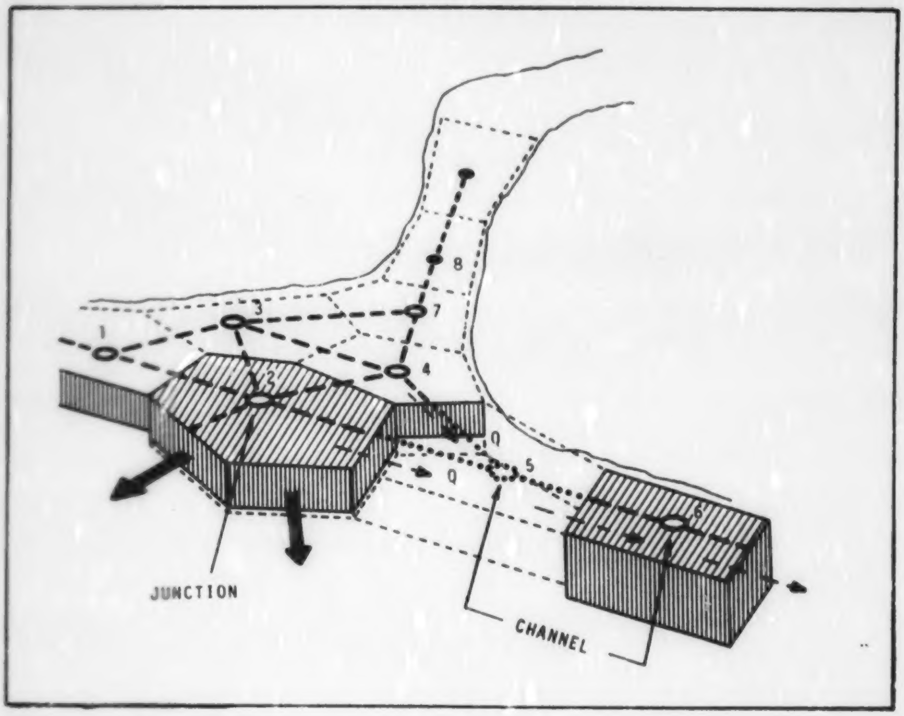

FIGURE 8 CHANNEL-JUNCTION DEFINITION FOR COMPUTATIONAL MESH[30]

$$S_w = \text{wind stress} = \frac{K}{d} \cdot \frac{\rho_a}{g\rho_w} U^2 \cos \psi$$

K = dimensionless coefficient with a value of 0.0026 (Refs. 2 & 3)

d = depth of flow

ρ_a, ρ_w = air and water densities

U = wind velocity

ψ = angle between the wind direction and the axis of the channel

The velocity and flow in each of the channels is thus determined. The equation of continuity, Equation 51, is solved at each of the junctions on the basis of predicted flows in each of the channels.

Continuity

$$A_{sj} \frac{\partial H_j}{\partial t} = \sum_{i=1}^{k} Q_i + Q_j^{im} - Q_j^{ex} - Q_j^{ev} \qquad (51)$$

where

A_{sj} = surface area associated with the junction j

Q_i = flow of a connecting channel

$Q_j^{im}, Q_j^{ex}, Q_j^{ev}$ = water import, export and evaporation rates at the junction

k = number of channels connected to the j^{th} junction

The numerical integration technique employed in the hydraulic model uses a space- and time-staggered scheme based on a simple Runge-Kutta approximation. The finite-difference equation for the momentum equation may be expressed for the i^{th} channel as:

$$\frac{\Delta V_i}{\Delta t} = - V_i \frac{\Delta V_i}{\Delta x_i} - g\frac{\Delta h}{L_i} + gS_o - gK_i|V_i|V_i + gS_w \qquad (52)$$

where

V_i = channel velocity

Δt = time step

$\frac{\Delta V_i}{\Delta x_i}$ = velocity gradient

K_i = frictional resistance coefficient for channel i

g = acceleration of gravity

L_i = channel length

h = average channel depth

$\Delta h = h_j - h_{j+1}$

The velocity gradient term is computed from the continuity equation:

$$- V_i \frac{\Delta V_i}{\Delta x_i} = V_i \left[\frac{b_i}{A_i} \frac{\Delta h_i}{\Delta t} + \frac{V_i}{A_i} \frac{\Delta A_i}{L_i} \right] \tag{53}$$

with

b_i = channel width

A_i = channel cross-sectional area

In addition, the relationships given below

$$\frac{\Delta h_i}{\Delta t} = \frac{\Delta H_i}{\Delta t}, \quad - g\frac{\Delta h}{L_i} + gS_o = - g\frac{\Delta H}{L_i} \tag{54}$$

and

$$\Delta A_i = b_i \Delta h_i \tag{55}$$

are used in intermediate computations of the key variables: V, h, Q, H, A. Since heads (potentials) are designated and computed at junctions the terms $\Delta H_i/\Delta t$ and $\Delta A_i/L_i$ are computed as the average of changes at the junctions at both ends of the channel.

The numerical solution technique proceeds as follows:

Initialization

1. Set initial and boundary flows and stages.
2. Set import and/or export of flows.
3. Set water surface elevations and/or tidal conditions.

Leap Frog Explicit Solution

1. Compute half-interval velocities, $V_i^{t+1/2}$ and quarter-interval channel flow, $Q_i^{t+1/4}$:

$$\begin{aligned} V_i^{t+1/2} = V_i^t + \frac{\Delta t}{2} \Bigg[&- V_i^t \frac{\Delta V_i^t}{\Delta x_i} - g\frac{\Delta h^t}{L_i} + gS_o \\ &- gK_i^t |V_i^t| V_i^t + gS_w \Bigg] \end{aligned} \tag{56}$$

$$Q_i^{t+1/4} = V_i^{t+1/2} A_i^t$$

2. Controlled junction calculations for flow at quarter-interval, Q_i^{t+4}, and head at half-interval, $H_j^{t+1/2}$. Head and/or flow may be specified functions of time or related via a rating curve.

3. Compute head at half-interval, $H_j^{t+1/2}$

$$H_j^{t+1/2} = H_j^t + \frac{\Delta t}{2A_{sj}}\left[\sum_{i=1}^{k} Q_i^{t+1/4} + Q_j^{im} - Q_j^{ex} - Q_j^{ev}\right]$$

4. Compute half-interval flows, $Q_i^{t+1/2}$, and channel areas, $A_i^{t+1/2}$ and full-interval velocities, V_i^{t+1}:

$$A_i^{t+1/2} = A_i^t + b_i\left[\frac{\Delta H_j^{t+1/2} + \Delta H_{j+1}^{t+1/2}}{2}\right]$$

$$V_i^{t+1} = V_i^{t+1/2} + \Delta t\left[-V_i^{t+1/2}\frac{\Delta V_i^{t+1/2}}{\Delta x_i} - g\frac{\Delta h^{t+1/2}}{L_i} + gS_o - gK_i^{t+1/2}\left|V_i^{t+1/2}\right|V_i^{t+1/2}\right]$$

$$Q_i^{t+1/2} = 1/2\left[Q_i^{t+1/4} + V_i^{t+1}A_i^{t+1/2}\right]$$

5. Controlled junction calculations for flows and heads at full time step.

6. Compute full-interval heads, H_j^{t+1}, water depths, h^{t+1} and channel areas, A_i^{t+1}:

$$H_j^{t+1} = H_j^{t+1/2} + \frac{\Delta t}{A_{sj}}\left[\sum_{i=1}^{k} Q_i^{t+1/2} + Q_j^{im} - Q_j^{ex} - Q_j^{ev}\right]$$

$$h_i^{t+1} = 1/2\left[\left(H_j^{t+1} - Z_j\right) + \left(H_{j+1}^{t+1} - Z_{j+1}\right)\right]$$

$$A_i^{t+1} = b_i\, h_i^{t+1}$$

7. Update system parameters and repeat steps 1 through 6 until hydraulic cycle is complete.

8. Average flows and velocities over hydraulic cycle.

This leap-frog scheme introduces a certain degree of accuracy and stability to the explicit numerical solution; however, there are inherent computational limitations. To maintain a stable and accurate solution the following criterion must be approximately satisfied:

$$\Delta t_{max} \leq \frac{L_i}{\left[V_i \left(1 + \frac{gn^2 L_i}{2.2 R^{4/3}} \right) + \sqrt{gR} \right]} \qquad (57)$$

where

Δt_{max} = maximum time step for stable solution.

The expression in the brackets represents the celerity of a shallow water water wave.

SECTION VI

RESERVOIR MODEL SELECTION

The primary requirement of the reservoir model is that it provide realistic representations of the thermal, hydraulic and chemical structure of a deep reservoir or thermal impoundment. The model must be usable in conjunction with current mathematical models of flow and quality in river basin simulations. The specific thermal and hydraulic structure of a reservoir is important not only in determining release temperatures but also in identifying the physical, chemical and biological reactions which produce significant changes in water quality. With these considerations as a basis, three specific requirements for the reservoir model were identified:

- vertical temperature profile predictions;
- description of the hydraulics of stratified flow; and
- prediction of water quality changes.

RESERVOIR MODELS CONSIDERED

Several prominent thermal, hydraulic, and quality models for stratified impoundments were reviewed to select an existing model from which a comprehensive thermal, hydraulic, and quality reservoir model could be synthesized. The quality models developed for the river and estuary models were then adapted to the reservoir model. The four reservoir models listed below were considered

	Author	Description
1.	Water Resources Engineers	Thermal-hydraulic model for reservoirs[7,8]
2.	Clay and Fruh	Impoundment water quality model[9]
3.	Ryan and Harleman	Thermal model for stratified lakes and reservoirs[10]
4.	Markofsky and Harleman	Thermal stratification and water quality model for reservoirs[11]

Preceding page blank

These models are very similar in method and approach, differing mainly in their solution algorithms and treatment of water quality. All four models have been used in field applications and compared with observed data. Calibration and verification of these models have produced very good correlation between observed and predicted temperature patterns; generally, quality predictions, however, have shown very limited success. Other stratified flow models were eliminated from consideration because they were not suitable for general applications, were not available for public use, or did not meet the requirements for the overall model. A summary review of the models considered is presented in Appendix A.

MODEL SELECTION

Water Resources Engineers' multi-segment reservoir model was selected to provide two main components of the overall reservoir model: temperature prediction and interflow patterns. This choice was primarily based on the general merits of the WRE deep reservoir model: (1) extensive field application (e.g., Hungry Horse Reservoir, Lake Roosevelt, Fontana Reservoir, and others); (2) breadth of documentation (References 7,8,12); (3) efficiency of computation; (4) a quasi-two-dimensional description of the temperature patterns; and (5) finer longitudinal discretization of a reservoir. The prime advantage of this model is that it can be used to obtain more detailed descriptions of temperature structures, flow patterns, and quality states.

A transport model compatible with the deep reservoir hydrothermal code was developed to predict the behavior of the water quality parameters in a stratified reservoir. The water quality reactions selected for the river and estuary model were also used in the quality portion of the reservoir model.

DESCRIPTION OF THE RESERVOIR MODEL

Heat Transfer

The mathematical formulation of the WRE multi-segment reservoir model is based on a highly simplified geometric structuring of the problem. A three-dimensional body of water is represented in spatial discretization by a set of segments, each consisting of a set of horizontal layers. Figure 9 presents the idealization of the reservoir geometry used in this model.

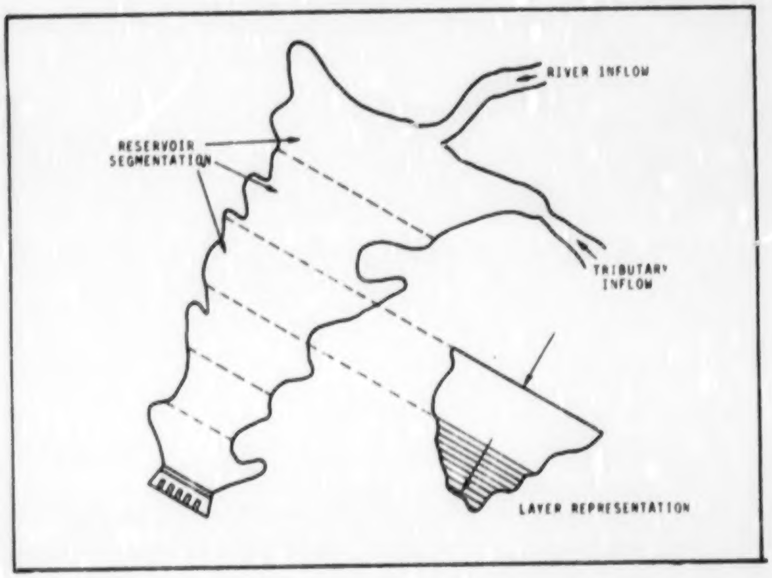
RIVER INFLOW
RESERVOIR SEGMENTATION
TRIBUTARY INFLOW
LAYER REPRESENTATION

FIGURE 9. ILLUSTRATION OF TEMPERATURE-INFLOW RELATIONSHIP FOR THE DEEP RESERVOIR HYDROTHERMAL MODEL

On the basis of this simple conceptualization a water and energy balance is formulated which describes the heat transfer characteristics of each segment and its component subdivisions. The specific water balance expresses continuity for each element in terms of flow rates:

Continuity

$$Q_{vi_j} = \sum_{k=1}^{j-1} (Q_{i_k} - Q_{o_k})$$

and

$$Q_{vo} = Q_i + Q_{vi} - Q_o \qquad (58)$$

where

Q_{vo} = vertical flow rate out of the element

Q_{vi} = vertical flow rate into the element

Q_i = horizontal inflow into the element

Q_o = horizontal outflow from the element

The general equation describing the spatial and temporal temperature variations is expressed as:

Energy

$$\frac{a_j+a_{j+1}}{2}\frac{d\theta_j}{dT} = \frac{a_{j+1}+a_j}{2}\frac{h'_j}{\rho c} + \frac{1}{\Delta z_j}[Q_{i_j}\theta_i - Q_{o_j}\theta_j]$$

$$- \frac{1}{\Delta z_j}[Q_{vo_j}\theta_j - Q_{vi_j}\theta_{j-1}] + \frac{1}{\Delta z_j}[a_{j+1}A_{j+1}\frac{\theta_{j+1}-\theta_j}{1/2(\Delta z_{j+1}+\Delta z_j)}$$

$$- a_jA_j\frac{\theta_j-\theta_{j-1}}{1/2(\Delta z_j+\Delta z_{j-1})}] \qquad (59)$$

where

θ_j = temperature of the jth element

c = heat capacity of water

ρ = density of water

a_{j+1} = area of upper plane bounding the jth element

a_j = area of lower plane bounding the jth element

h'_j = change in external solar heat flux per unit of water depth

A_{j+1} = coefficient of "effective" diffusivity at the upper boundary of the jth element

A_j = coefficient of "effective" diffusivity at the lower boundary of the jth element

Δz_j = thickness of the jth element

Effective mixing processes which occur in the epilimnion are accounted for in the model by a variable effective diffusion coefficient. The diffusion coefficient, which is a function of depth and the location of the thermocline, is calculated by an empirical relationship and is expressed as:

$$A = \begin{cases} A_o e^{-\eta z} & \text{epilimnion} \\ A_1 & \text{hypolimnion} \end{cases} \qquad (60)$$

where

A_o, A_1, η = empirical constants

z = elevation of the j-th element

Specific values for the empirical constant must be determined for each reservoir site.

The external energy source represents the net energy flux passing the air-water interface and is comprised of the algebraic sum of five separate fluxes:

$$h'_j = Q_{sn} + Q_{at} - Q_w - Q_e + Q_c \tag{61}$$

where

Q_{sn} = net short-wave radiation flux across the air-water interface

Q_{at} = net atmospheric (long-wave) radiation flux across the interface to the water body

Q_w = water surface radiation (long-wave) flux from the water body

Q_e = energy loss by evaporation

Q_c = convective energy flux between the water body and the atmosphere

Each component of the external energy term is expressed by algebraic equations derived from heat transfer theory and/or empirical approaches; specific formulae are discussed in detail in Reference 7 and also are presented here.

The net short-wave radiation passing the air-water interface is represented functionally by:

Net Short-Wave Radiation

$$Q_{sn} = Q_o \left[\frac{a'' + 0.5\,(1 - a' - d)}{1 - 0.5\,R_{s_o}\,(1 - a' + d)}\right] (1 - 0.65C^2)\,(1 - R_s) \tag{62}$$

where

Q_{sn} = net short-wave radiation flux, kcal/m^2-hour

Q_o = extraterrestrial radiation flux

a" = mean atmospheric transmission coefficient after scattering and absorption, a function of optical air mass and mean daily precipitable water content

a' = mean atmospheric transmission coefficient after scattering, a function of optical air mass and mean daily precipitable water content

d = total dust attenuation, a function of optical air mass, location, and season ($0.03 \le d \le 0.13$)

C = percent cloud cover (decimal)

R_{s_o} = reflectivity of the water surface to short-wave radiation under a clear sky

R_s = reflectivity of the water surface to short-wave radiation under prevailing sky conditions

$$= A \left[\frac{180\ \alpha}{\pi}\right]^B, \quad 0.35 \le A \le 1.18, \ -0.97 \le B \le -0.45 \qquad (63)$$

where

α = altitude of the sun in radians

$$= \arcsin \left[\sin \frac{\pi\phi}{180} \sin \delta t + \cos \frac{\pi\phi}{180} \cos \delta \cos \frac{\pi t}{12}\right] \qquad (64)$$

The extraterrestrial radiation 'Q_o' is given by:

$$Q_o = \frac{I_o}{r^2} \Big[(\sin\phi \sin\delta)\ (t_e - t_b) + \frac{12}{\pi}(\cos\phi \cos\delta)$$

$$\left(\sin \frac{\pi t_e}{12} - \sin \left(\frac{\pi t_b}{12}\right)\right)\Big] \ \Gamma \qquad (65)$$

with

$$r = 1 + 0.017 \cos \left[\frac{2\pi}{365} (186 - D)\right] \qquad (66)$$

$$\delta = \frac{23.45}{180}\,\pi \quad \cos\left[\frac{2\pi}{365}\,(172-D)\right] \tag{67}$$

$$\dagger_b = ST_b - \Delta\dagger_s + ET - 12 \tag{68}$$

$$\dagger_e = ST_e - \Delta\dagger_s + ET - 12 \tag{69}$$

$$\Delta\dagger_s = \frac{\varepsilon}{15}\,(L_{sm} - L_{1m}) \tag{70}$$

$$ST_r = 12 - \frac{12}{\pi} \quad \arccos\left[\tan\left(\frac{\pi\phi}{180}\right)\right]\, \tan\left(\frac{\pi\delta}{180}\right)\Big] + \Delta\dagger_s + \Delta\dagger_{OR} \tag{71}$$

$$ST_s = 24 - ST_r + 2\,\Delta\dagger + \Delta\dagger_{OR} - \Delta\dagger_{OS} \tag{72}$$

where

1_o = solar constant, 1164 kcal/m^2-hr

r = ratio of the actual and mean distances between the sun and the earth

D = number of the day of the year

ϕ = latitude of the site, degrees

δ = declination of the sun, degrees

$\dagger_b, \dagger_e$ = hours angles corresponding to the beginning and end, respectively, of any time interval between sunrise and sunset

Γ = a correction factor for diurnal exposure to radiation flux ($\Gamma = 0$ when $ST_s \le ST_b$ or $ST_e \le ST_r$, and $\Gamma = 1$ when $ST_r \le ST_b$ or $ST_e \le ST_s$)

ST_b, ST_e = standard times at the beginning and end of the time interval chosen for temperature analysis

ET = equation of time from a solar emphemeris, in hours (may be neglected in approximate computation)

ST_r, ST_s = the standard times of sunrise and sunset, respectively

Δt_s = difference between standard and local civil time in hours

ε = constant ($\varepsilon = -1$ for west longitude, $\varepsilon = +1$ for east longitude)

L_{sm}, L_{lm} = longitude of standard and local meridians, respectively

$\Delta t_{OR}, \Delta t_{OS}$ = hour corrections for obstructions of sunrise and sunset, respectively

In addition, the mean atmospheric transmission coefficient, "a", is given by:

$$a" = \exp\left[-\,(0.465 + 0.134\,w)\,(0.179 + 0.421\exp(-0.721\,m))\,m\right] \tag{73}$$

where m, the optical air mass, and w, the water content, are given by:

$$m = \frac{10^{-Z^*/19,100}}{\sin\alpha + 0.15\left(\frac{180\,\alpha}{\pi} + 3.885\right)^{-1.253}} \tag{74}$$

$$w = 0.86\exp\left[-0.111 + 0.0614\,\bar{\theta}_d\right] \tag{75}$$

in which

Z^* = altitude of the site in meters

α = sun's altitude in radians

$\bar{\theta}_d$ = mean daily dew point (°C)

Similarly, the mean transmission coefficient, a', is expressed by the empirical equation:

$$a' = \exp\left[-(0.465 + 0.134\,w)(0.129 + 0.171\exp(-0.880m))\,m\right] \tag{76}$$

All variables are as previously defined.

The net atmospheric radiation term, Q_{at}, is computed from the equation:

Net Atmospheric Radiation

$$Q_{at} = [0.937 \times 10^{-5}]\, \sigma\, (T_2)^6\, (1 + 0.17C^2)\, (1-R_L) \qquad (77)$$

where

Q_{at} = net atmospheric radiation flux, kcal/m^2-hour

σ = Stefan-Boltzman constant, 4.885×10^{-8} kcal/m^2-hour -°Kelvin^4

T_2 = absolute air temperature at a level of 2 meters above the reservoir surface, °K

R_L = reflectivity of the water surface for atmospheric radiation, ≅ 0.03

Long wave back radiation emitted by the water body is characterized by the Stefan-Boltzman fourth-power radiation law. Thus, back radiation is a function of the absolute temperature of the water at the surface as:

Water Surface Radiation

$$Q_w = 0.97\, \sigma\, T_w^4 \qquad (78)$$

where

Q_w = water surface radiation kcal/m^2-hour

σ = Stefan-Boltzman Constant

T_w = absolute temperature of the water surface, °K

Energy utilized by evaporation is a major component of the heat budget and can often account for 40 to 70 percent of the energy flux from the water body. The general formulation of this term is:

Evaporation Energy Loss

$$Q_e = \rho_w\, (597 - 0.57\, \theta_w)\, [N\, U_2\, (e_o - e_{a2})] \qquad (79)$$

where

Q_e = energy loss by evaporation, kcal/m^2-hour

ρ_w = density of water, kg/m^3

Θ_w = temperature of water surface, ^oC

N = an empirical constant, $millibars^{-1}$

U_2 = wind velocity at a height of two (2) meters, m/hour

e_o = saturation vapor pressure of the air at the temperature of the water surface, millibars

e_{a2} = water vapor pressure at a height of two (2) meters above ground on the upwind shore

and

$$e_{a2} = e_{a2s} - [0.00066(1+0.00115\Theta'_{a2})] (\Theta_{a2}-\Theta'_{a2}) p \qquad (80)$$

in which

e_{a2s} = saturation vapor pressure at the wet bulb temperature of the air millibars

Θ_{a2} = dry bulb air temperature at a height of two (2) meters, ^oC

Θ'_{a2} = wet bulb air temperature at a height of two (2) meters, ^oC

p = local barometric pressure, millibars

The convective heat transfer, Q_c, or sensible heat flux is related to the same variables as the evaporation term. This component is computed from the semi-empirical equation:

Convective Energy Flux

$$Q_c = \frac{p}{0.622} \rho_w c_p N_c U_2 (\Theta_{a2}-\Theta_w) \qquad (81)$$

where

Q_c = convective energy flux, kcal/m^2-hour

c_p = specific heat of the air, kcal/kg-^oC

N_c = an empirical constant, 1.56×10^{-9} $millibars^{-1}$ and

all other terms are as previously defined.

Hydraulics of Stratified Flows

In this model an analytical-empirical approach characterizes both the complex interflows through the reservoir and the withdrawal patterns at the spillway, gates, and other outlets. The thickness of the withdrawal layer, as the interflow thickness, depends functionally on the inflow rates, outflow rates and the degree of stratification. In the case of the withdrawal region, spatial velocity distributions are known functions of the outflow, withdrawal thickness, and width of the reservoir at the outflow; superposition of the horizontal velocity distributions is applied to regions in which withdrawal layers overlap. In the case of reservoir interflows, horizontal velocities are calculated from the horizontal inflow rate and the cross-sectional area at the specific element. Inflows are distributed into a segment according to temperature distributions so that essentially the flow is routed horizontally according to density. Some discussion of the formulations and theoretical basis of this analytical-empirical approach will be found in Reference 8. For completeness, a brief discussion of the fundamental ideas is presented here.

The rationale employed for characterizing the unsteady, thermally stratified flow is best explained by considering the simple example illustrated in Figure 10. Since a pseudo two-dimensional approach (one-dimensional in the vertical) is used, the temperature and flow history of each segment is computed independent of downstream segments. Proceeding from the upstream segment, the outflow history of one segment becomes the inflow history for the next. Horizontal flow between segments is characterized as an interflow (a confined subregion of flow), and the location of the interflow zone is determined on the basis of density compatibility. For example, in segment 1 of Figure 10 the midpoint of the interflow zone is located by scanning the segment temperature profile until the temperature equals the arithmetic mean temperature of the outflow from the upstream segment. The interflow thickness, D, is computed from Debler's criteria:

Interflow Thickness

$$D = 2.88 \left[\frac{Q}{W\sqrt{gE}} \right] \tag{82}$$

where

Q = total flow across the upstream interface

W = segment width

g = acceleration of gravity

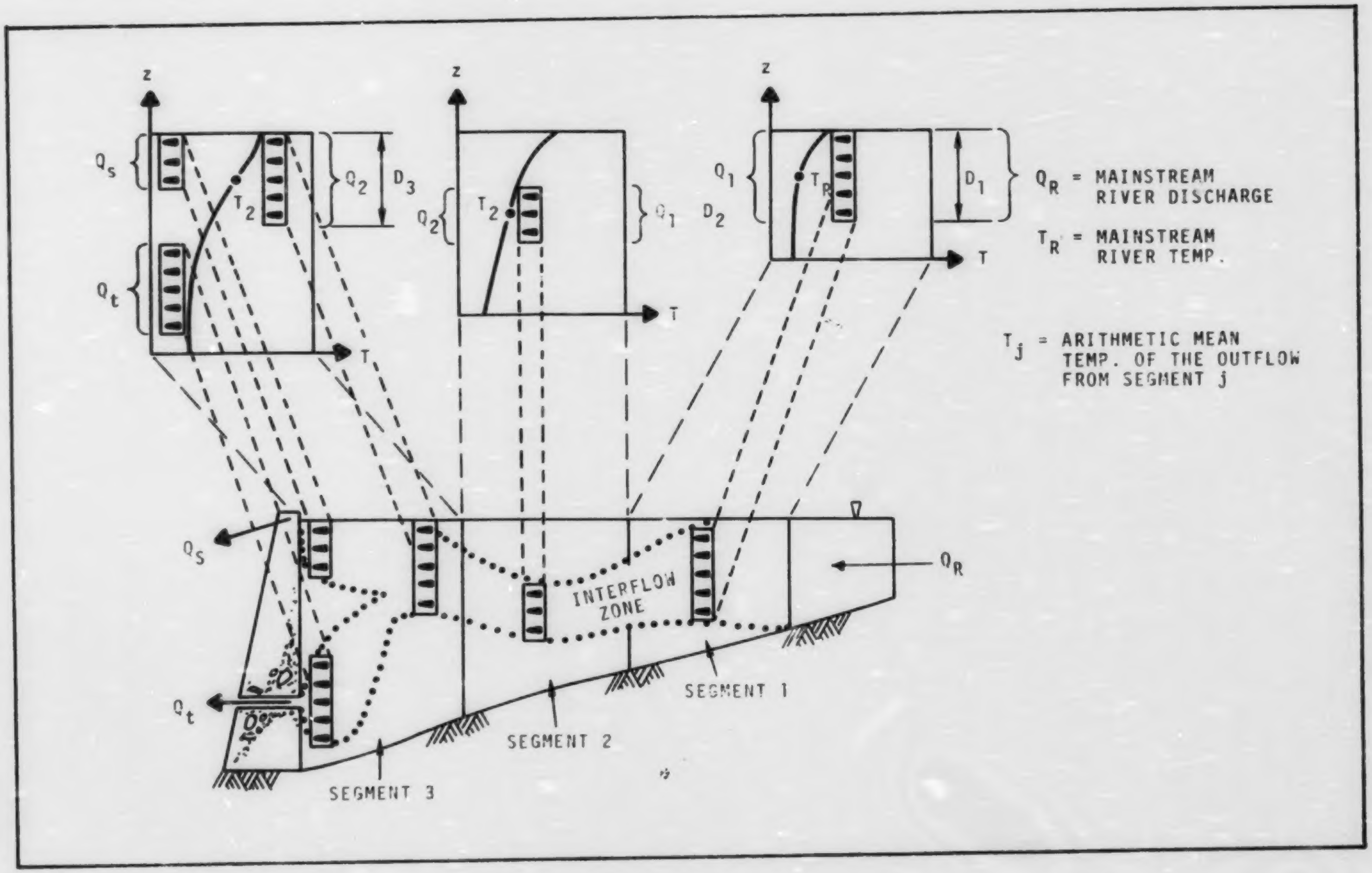
z
Q_s
Q_t
T_2
Q_2
D_3
T
z
Q_2
T_2
Q_1
T
z
Q_1
D_2
T_R
D_1
T
Q_R = MAINSTREAM RIVER DISCHARGE
T_R = MAINSTREAM RIVER TEMP.
T_j = ARITHMETIC MEAN TEMP. OF THE OUTFLOW FROM SEGMENT j
Q_s
Q_t
INTERFLOW ZONE
Q_R
SEGMENT 1
SEGMENT 2
SEGMENT 3

FIGURE 10. DISCRETIZATION OF A RESERVOIR GEOMETRY[8]

E = stability $\left(\frac{\beta}{\rho_o}\right)$

β = density gradient $\left(\frac{-\partial\rho}{\partial Z}\right)$

ρ_o = density at the channel bottom.

Thus the inflow is said to be confined between upper and lower elevation bounds: $Z_c + 1/2D$ and $Z_c - 1/2D$. For cases in which these elevation bounds exceed the physical bounds, the interflow thickness is shifted up or down. The horizontal velocity distribution is assumed to be constant over the interflow zone.

Mass continuity within a reservoir segment is specified by the equation

Continuity

$$\frac{\Delta\overline{V}}{\Delta t}j = Q_{ij} - Q_{oj} \tag{83}$$

with

$\frac{\Delta\overline{V}}{\Delta t}j$ = volume differential (change in storage)

Q_{ij}, Q_{oj} = total horizontal inflow and outflow for segment j.

Since the total inflow and water surface elevations for segment j are known functions of time, the total horizontal outflow is computed directly from Equation 83. Next, the flow ratio, Q_r, is computed from

$$Q_r = \frac{Q_{oj}}{Q_{ij}} \tag{84}$$

Once the distribution of horizontal inflows is determined (see Equations 88 through 91) the horizontal outflow of each layer (element) is computed from

$$Q_{oj}^{(k)} = Q_r Q_{ij}^{(k)} \qquad k = 1,2,3,\ldots m \text{ layers} \tag{85}$$

Vertical flows into and out of each layer are computed from flow balance equations (58a. and 58b.).

The vertical temperature profile will generally differ from segment to segment; consequently, the thickness of interflow D will also vary. To maintain energy continuity of horizontally advected heat across adjacent segments it is required that

$$\sum_{n}^{m} \rho c Q_{i,j}^{(k)} T_j^{(k)} = \sum_{n'}^{m'} \rho c Q_{o,j-1}^{(k)} T_{j-1}^{(k)} \qquad (86)$$

where

ρ = density of water

c = heat capacity of water

$Q_{i,j}^{(k)}$ = horizontal inflow to layer k of segment j

$Q_{o,j-1}^{(k)}$ = horizontal outflow from layer k of segment j-1 (upstream segment)

$T_j^{(k)}, T_{j-1}^{(k)}$ = temperature of the layer k for segment j and j-1

n,n' = layer indices of lower interflow bound

m,m' = layer indices of upper interflow bound

j,k = segment and layer indices, respectively.

For computational convenience, the temperature profile within the interflow zone is approximated by a linear function of elevation, namely:

$$T_k = m(Z_k - Z_o) + b \qquad (87)$$

where

$b = T_o$

$Z_o = Z_c - 1/2D$

and

T_k = temperature of the kth layer

Z_k = elevation of the kth layer

m = slope.

The slope term, m, is computed from the relationships between flow and velocity within the interflow zone. If Q is the total flow across the interface of adjacent segments, the velocity, u, within the interflow zone is constant and defined by

$$U_{j-1} = \frac{Q}{A_{j-1}} = \frac{QL_{j-1}}{\overline{V}_{j-1}} = \frac{Q_{o,j-1}^{(k)} L_{j-1}}{\overline{V}_{j-1}^{(k)}} \qquad (88)$$

$$U_j = \frac{Q}{A_j} = \frac{QL_j}{\overline{V}_j} = \frac{Q_{i,j}^{(k)} L_j}{\overline{V}_j^{(k)}} \qquad (89)$$

and in turn

$$Q_{o,j-1}^{(k)} = \frac{Q\overline{V}_{j-1}^{(k)}}{\overline{V}_{j-1}} \qquad (90)$$

$$Q_{i,j}^{(k)} = \frac{Q\overline{V}_j^{(k)}}{\overline{V}_j} \qquad (91)$$

where

A_j = mean cross-sectional area of interflow zone

L_j = length of the segment j

$\overline{V}_j$ = total volume of segment j

$\overline{V}_j^{(k)}$ = volume of element k

j = segment index

With the above relationships, the slope term, m, is defined as

$$m = \frac{\overline{V}_{j-1} \sum_{k=n'}^{m'} \overline{V}_{j-1}^{(k)} T_{j-1}^{(k)} - T_o}{\overline{V}_j \sum_{k=n}^{m} \overline{V}_j^{(k)} Z_{j,k} - Z_{j,o}} \qquad (92)$$

The interfacing of adjacent segments is carried out automatically in the Deep Reservoir Hydrothermal Model for all segments except the final one, upstream of the dam.

Treatment of the downstream segment is based on similar analytical concepts of selective withdrawal. The withdrawal depth, d, as illustrated in Figure 11 is defined as

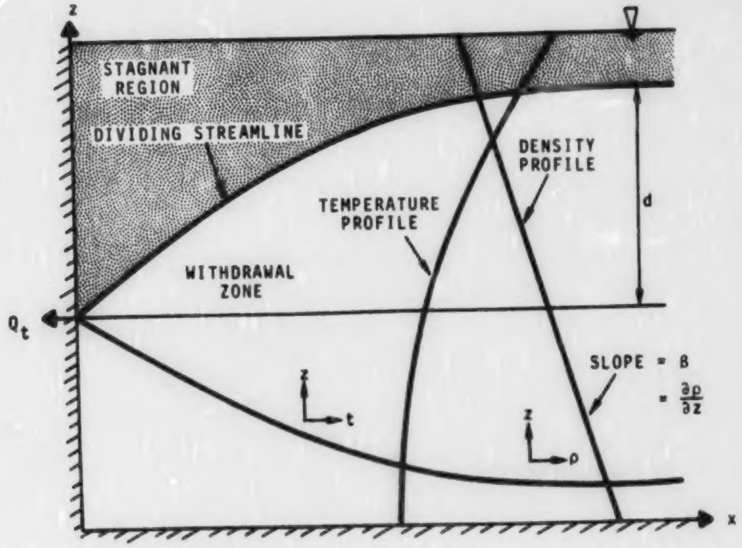
z
STAGNANT REGION
DIVIDING STREAMLINE
DENSITY PROFILE
TEMPERATURE PROFILE
d
WITHDRAWAL ZONE
Q_t
SLOPE = β
$= \frac{\partial\rho}{\partial z}$
z
t
z
ρ
x

FIGURE 11. CONCEPTUALIZATION OF A WITHDRAWAL ZONE[8]

$$d = 2.0 \left[q \sqrt{\frac{\rho_o}{g\beta}} \right]^{1/2} \qquad (93)$$

where

q = volumetric discharge per unit width

ρ_o = density centerline of outlet

g = gravitational constant

$\beta = \frac{-\partial\rho}{\partial Z}$ along centerline of outlet.

The discharge, q, is computed as

$$q = \frac{Q_s}{w_s} \quad \text{surface outlet} \qquad (94)$$

and

$$q = \frac{Q_t}{2w_t} \quad \text{submerged outlets} \qquad (95)$$

with

Q_s, Q_t = spillway

w_s, w_t = widths

For regions in which the assumed flow fields overlap, the profiles are simply superimposed. Velocity is assumed constant within the withdrawal layers and is computed by dividing the discharge by the cross sectional area of the withdrawal zone:

$$u(Z) = \frac{Q}{w(2d)} \tag{96}$$

If the bounds of the submerged withdrawal layer exceeds the physical bounds, the velocity field is revised and distributed uniformly over the revised withdrawal depth. Similarly, if the submerged withdrawal zone overlaps the water layers above the thermocline the withdrawal depth is adjusted below the thermocline. Both of these situations are illustrated in Figure 12.

In cases where natural convective mixing is dominant in the epilimetric region (see Figure 13) the theory of Craya is used in determining the distribution of flows. In this approach, the density profile is represented by a step function with

$$\rho(Z) = \begin{cases} \rho & Z > Z_t \\ \rho + \Delta\rho & Z < Z_t \end{cases} \tag{97}$$

where Z_t is the elevation of the thermocline. A critical epilimnetic discharge at which water will begin to be withdrawn from the hypolimnion is defined as

Surface Outlets

$$q_c = \frac{Q_s}{w_s} = \sqrt{0.75 \quad g \; d_r^3 \; \frac{\Delta\rho}{\rho}} \tag{98}$$

Submerged Outlets

$$q_c = \frac{Q_t}{w_t} = \sqrt{1.52 \quad g \; h^3 \; \frac{\Delta\rho}{\rho}} \quad , \quad 2\,h \le d_r \tag{99}$$

where d_r and h are defined in Figure 13. If the flow q is greater than q_c for any outlet or combination of outlets, Debler's criterion is used to compute the withdrawal depth from the hypolimnion using for the discharge $q-q_c$ and stability E evaluated below the thermocline. The velocity profile in epilimnion and withdrawal zone are assumed constant.

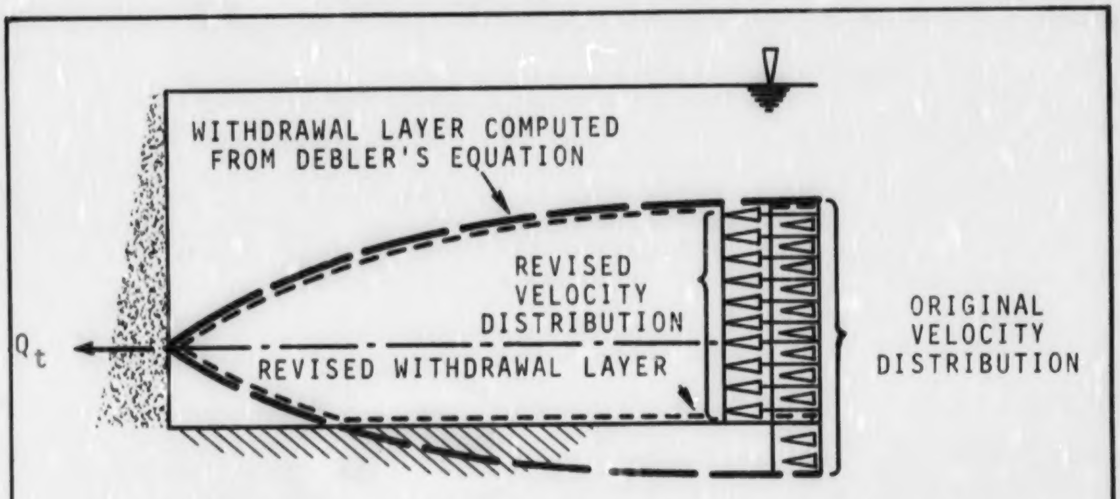
WITHDRAWAL LAYER COMPUTED FROM DEBLER'S EQUATION
REVISED VELOCITY DISTRIBUTION
ORIGINAL VELOCITY DISTRIBUTION
Q_t
REVISED WITHDRAWAL LAYER

A. WITHDRAWAL REGION WITH DIVIDING STREAMLINE CROSSING THE PHYSICAL BOUNDARY

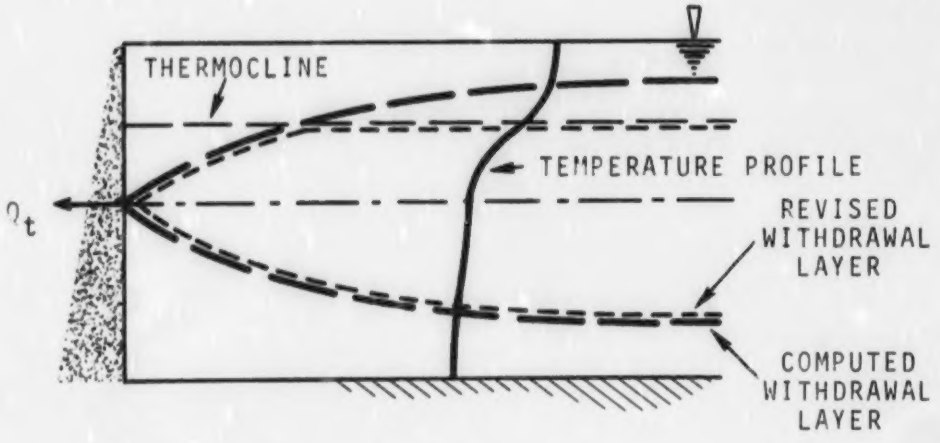
THERMOCLINE
TEMPERATURE PROFILE
Q_t
REVISED WITHDRAWAL LAYER
COMPUTED WITHDRAWAL LAYER

B. WITHDRAWAL REGION WITH DIVIDING STREAMLINE OVERLAPPING THE THERMOCLINE

FIGURE 12. ILLUSTRATION OF WITHDRAWAL LAYER CONFIGURATIONS[8]

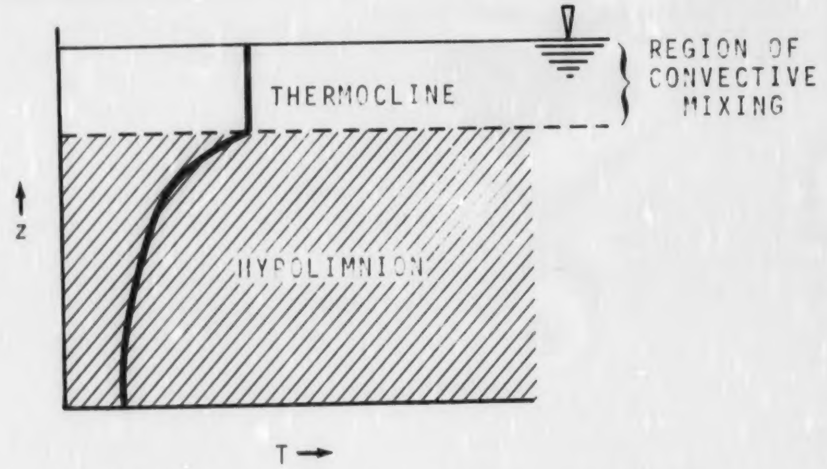
REGION OF CONVECTIVE MIXING
THERMOCLINE
z
HYPOLIMNION
T →

A. REPRESENTATION OF CONVECTIVE MIXING IN EPILIMNION

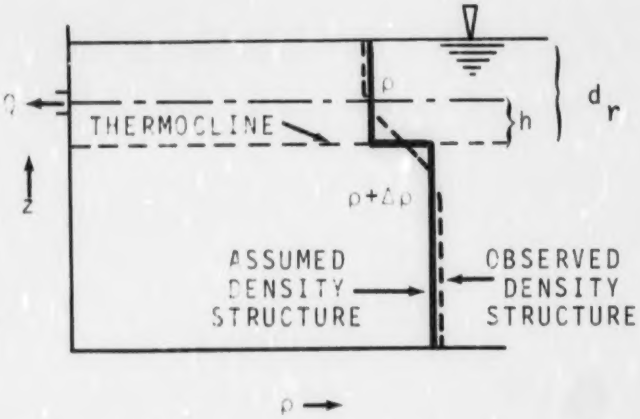
Q
THERMOCLINE
ρ
h
d_r
z
ρ+Δρ
ASSUMED DENSITY STRUCTURE
OBSERVED DENSITY STRUCTURE
ρ →

B. DENSITY PROFILES

FIGURE 13. TEMPERATURE AND DENSITY STRUCTURE FOR APPLICATION OF CRAYA'S CRITERIA[8]

Water Quality

To describe the spatial and temporal variations in water quality other than temperature and density (i.e., dissolved oxygen, biochemical oxygen demand, algal populations, and nutrient materials) a reservoir water quality submodel is required. The reservoir quality submodel developed in this work is based on a scientific rationale which has been successfully applied to solute transport problems with simultaneous chemical reactions. Basically this approach approximates the formulation of the overall quality problem by partitioning the mechanisms of change into mass transport and chemical reactions. Utilizing the segment-element discretization the mass transport equations are derived for the finite layer (element) as:

Solute Transport

$$\frac{\partial C^{(k)}}{\partial t} = D_z \frac{\partial^2 C^{(k)}}{\partial z^2} - \frac{Q^v}{A} \frac{\partial C^{(k)}}{\partial z} + \frac{1}{A\Delta z} (Q_i^h C_i^{(k)} - Q_o^h C^{(k)}) + S^{(k)} \tag{100}$$

where

$C^{(k)}$ = concentration of kth constituent, k = 1,2,...,n

$C_i^{(k)}$ = concentration of upstream flow

D_z = effective diffusion coefficient

A = horizontal surface area of water plane for element

Q^v = vertical flow through element (layer)

Q_i^h, Q_o^h = horizontal inflow and outflow to element

Δz = element thickness

$S^{(k)}$ = source of kth constituent

This formulation of advective-diffusive transport for the layer discretization is somewhat simplified in that small vertical gradients in area and diffusion coefficients are neglected. These approximations are justified by the following facts:

1. for fine vertical discretizations, $\partial A/\partial z$ contributions are small;
2. knowledge of the effective diffusion is limited and specific coefficient values are subject to various empiricisms, so that consideration of $\partial D_z/\partial z$ term might produce computational difficulties; and
3. reservoirs with quality problems have flows characterized by low Froude numbers.

A standard implicit finite-difference approximation(13) of the mass transport equation:

$$\frac{C_{j,n+1}^{(k)} - C_{j,n}^{(k)}}{\Delta t} = \frac{D_z}{\Delta z^2}\left(C_{j-1,n+1}^{(k)} - 2C_{j,n+1}^{(k)} + C_{j+1,n+1}^{(k)}\right) - \frac{Q^v}{A\Delta z}\left(C_{j,n+1}^{(k)} - C_{j-1,n+1}^{(k)}\right) + \frac{1}{A\Delta z}\left(Q_i^h C_i^{(k)} - Q_o^h C_{j,n+1}^{(k)}\right) + S_{j,n+1}^{(k)} \qquad (101)$$

where

j = node index

n = time plane index

$\Delta z, \Delta t$ = space and time increments, respectively

reduces the mathematical problem to a simple matrix equation:

$$[A]\left\{C^{(k)}\right\} = \left\{B^{(k)}\right\} \qquad (102)$$

The coefficient matrix A exhibits some very convenient computational properties (tridiagonal, diagonally dominant, etc.) and is readily solved by Gaussian elimination. This numerical formulation is unconditionally stable, highly accurate, and computationally efficient. Effects of "numerical dispersion" may cause difficulties if the vertical advection term dominates the diffusion term.

However, the model should normally be applied to reservoirs with low discharge-to-volume ratios and low Froude numbers where quality dynamics are usually of interest, and thus "numerical dispersion" should not be significant. If "numerical dispersion" becomes a major problem, it is recommended that numerical techniques such as those recently developed by Price, et. al.[14] be used. These new numerical schemes employ Galerkin principles to formulate finite-element equations of high order accuracy, while minimizing the effects of pseudo dispersion.

Boundary conditions for the transport equations are presently assumed to be reflective according to the method of images (e.g., $\partial C^{(k)}/\partial n = 0$) at the bottom and air-water interface. Further testing of the model may indicate mixed boundary conditions (e.g., $\alpha C^{(k)} + \beta \partial C^{(k)}/\partial n + \gamma^{(k)} = 0$) or a combination of reflective and specified boundary conditions to be a better alternative.

Mechanisms of chemical change in water quality are accounted for in the reservoir model by solving the set of ordinary differentail equations describing the interrelationships between dissolved oxygen, biochemical oxygen demand, algal populations, and the principal nutrient materials:nitrogen and phosphorus. Specific models included in the reservoir model are discussed in section IV of this report. Two simple modifications to the quality models have been included for proper adaptation to reservoirs. Reaeration is presently confined to the uppermost layer (element) and the reaeration coefficient is reformulated as a linear function of wind speed:

$$K = a + bw \tag{102}$$

where

K = reaeration coefficient

a,b = empirical constants

w = wind speed

Secondly, benthic biochemical oxygen demand and sedimentary phosphorus are defined for the bottom element only. The system of ordinary differential equations representing the complete quality dynamics is solved by a fourth order Runge-Kutta technique with Runge coefficients. "Equilibrated" quality states are defined at the end of a simulation time step and obtained by superimposing the chemical change in quality (over the time step) onto the changes due to transport.

PROBLEMS ENCOUNTERED

The orginally planned overall reservoir model was completed but not verified against field data. Insurmountable difficulties with the selected thermal-hydraulic model (the EPA version of the WRE multi-segment reservoir model) were encountered in the calibration and verification at Detroit Reservoir (Figure 39). Intensive efforts to correct the inoperative components of the thermal-hydraulic code failed repeatedly. Eventually the nature and sources of difficulty were determined; the final section of this report summarizes the specific details of the problems. Time and funding constraints prevented selection and application of an alternate thermal-hydraulic model.

The quality component of the reservoir model, which was written to interface with other single segment thermal-hydraulic models with little modification, was completed. The quality submodel was not verified with field observations at Detroit Reservoir since the WRE thermal-hydraulic code was not operational. Minor modifications in the present program may later prove necessary as it is applied to prototype simulations. These modifications may include: (1) reformulation of boundary conditions, (2) use of variable element thickness, (3) inclusion of variable diffusion coefficients, and/or (4) extension of the current model to a multi-segment version.

SECTION VII

VERIFICATION OF EXPLORE-I RIVER BASIN CODE ON THE WILLAMETTE RIVER BASIN

Testing and verification of the EXPLORE-I river basin model was conducted on the Willamette River Basin in Oregon. This basin was chosen for several reasons:

- The Willamette is a large river with a tidally influenced reach, several major tributaries, and considerable flow regulation, thereby encompassing a wide range of hydraulic conditions.
- A considerable number of municipal and industrial developments discharge wastes into the river system.
- Measurements of hydraulic and water quality data have been made in reasonable detail throughout the basin.

Because of the availability of historical hydrologic and water quality data, the summer of 1967 was selected for verification.

The purpose of a river basin model of this type is not to describe in great detail what is occurring at each location but rather to give the environmental engineer, biologist, or ecologist using the model a reliable estimate of the hydraulic characteristics and water quality parameters, thus allowing the proper assessment of alternate resource management schemes.

Modeling of a system as large and complex as the Willamette River Basin required that a number of simplifying assumptions be made. In addition, because of a lack of measured values some of the input data had to be estimated. Care was taken not to oversimplify the system or extrapolate so much input data that the model no longer represented the real river system.

In general three criteria determined the extent to which the rivers in the basin were modeled:

- nonexistence upstream of significant municipal or industrial waste load
- lack of width or depth data
- absence of flow-time records

Preceding page blank

Verification on the Willamette took part in two phases. In the first phase, the region from Salem to Portland was considered in detail and calculations were made to calibrate and verify the model for this region. In the second phase, the entire river basin was set up and functionally tested to demonstrate the model's ability to handle large regions. The verification of the model in the region from Salem to Portland is discussed in this report.

The physical layout of the river basin from Salem to Portland is shown in Figure 14. The 63 node positions were placed an average of two miles apart. However, the locations of existing water quality stations, USGS stream gauging stations, and other physical characteristics were considered in the placement of the nodes. The node furthest downstream is located at the Morrison Street Bridge (river mile 12.1), Portland, where a stage-time recorder provides the necessary water levels for use in the model. The tributary end points were chosen according to the criteria discussed above.

VERIFICATION OF HYDRAULIC CODE

Verification of the hydraulic code required the gathering of data about the river basin from a number of diverse sources. Data were, in general, available for most of the mainstem of the Willamette. However, on the tributaries the water depths and the Manning friction factors were not known. The methods used in estimating these values and in gathering and correlating data on the Willamette River Basin are discussed. A summary of the references used in gathering these data is presented in the table below.

TABLE 2

SUMMARY OF THE DATA SOURCES USED IN MODEL CALIBRATION ON WILLAMETTE RIVER BASIN

Physical Data Sources

- U.S. Geological Survey 15 minute and 7 1/2 minute quardrangle topographic maps.
- "River Mile Index, Willamette River and Tributaries," prepared by the Hydrology Subcommittee of the Columbia Basin Inter-Agency Committee.
- Oregon State Water Resources Board Map No. 2.6 of the Willamette Drainage Basin (1964).

TABLE 2 (continued)

- Water Surface Profile Charts WR-05-10, WR-05-17, WR-05-18, WR-05-19 prepared by the U.S. Corps of Engineers, Portland District.
- Velocity, Average Depth and Cross-sectional Area versus Willamette River Mile from Willamette Falls to the Middle Fork of the Willamette.

Flow Data Sources

- "1967 Water Resources Data for Oregon, Part 1." Surface Water Records, United States Department of the Interior Geological Survey - Water Resources Division.
- "1967 Water Resources Data for Washington, Part 1." Surface Water Records, United States Department of the Interior Geological Survey - Water Resources Division.
- Willamette River Basin, State Water Resources Board, Salem, Oregon, June 1967.
- Lower Willamette River Basin, State Water Resources Board, Salem, Oregon, June 1965.
- Middle Willamette River Basin, State Water Resources Board, Salem, Oregon, June 1963.
- "Appraisal of Streamflow in the Tualatin River Basin, Washington County, Oregon," C. H. Swift III, United States Department of the Interior Geological Survey - Water Resources Division, 1971.

Controlled Node Data Sources

- "Water Discharge Determinations for the Tidal Reach of the Willamette River from Ross Island Bridge to Mile 10.3," Portland, Oregon, G. R. Dempster, Jr., and Gale A. Lutz; United States Department of the Interior, Portland, Oregon, 1967.
- "Tide Tables, High and Low Water Predictions, West Coast of North and South America Including the Hawaiian Islands," U.S. Department of Commerce Coast and Geodetic Survey, 1964.
- State of Oregon Fish Commission Horseshoe Plot Plan, Cul-de-Sac Plot Plan and Site Plan for the Willamette Falls Fishway, May 14, 1965.

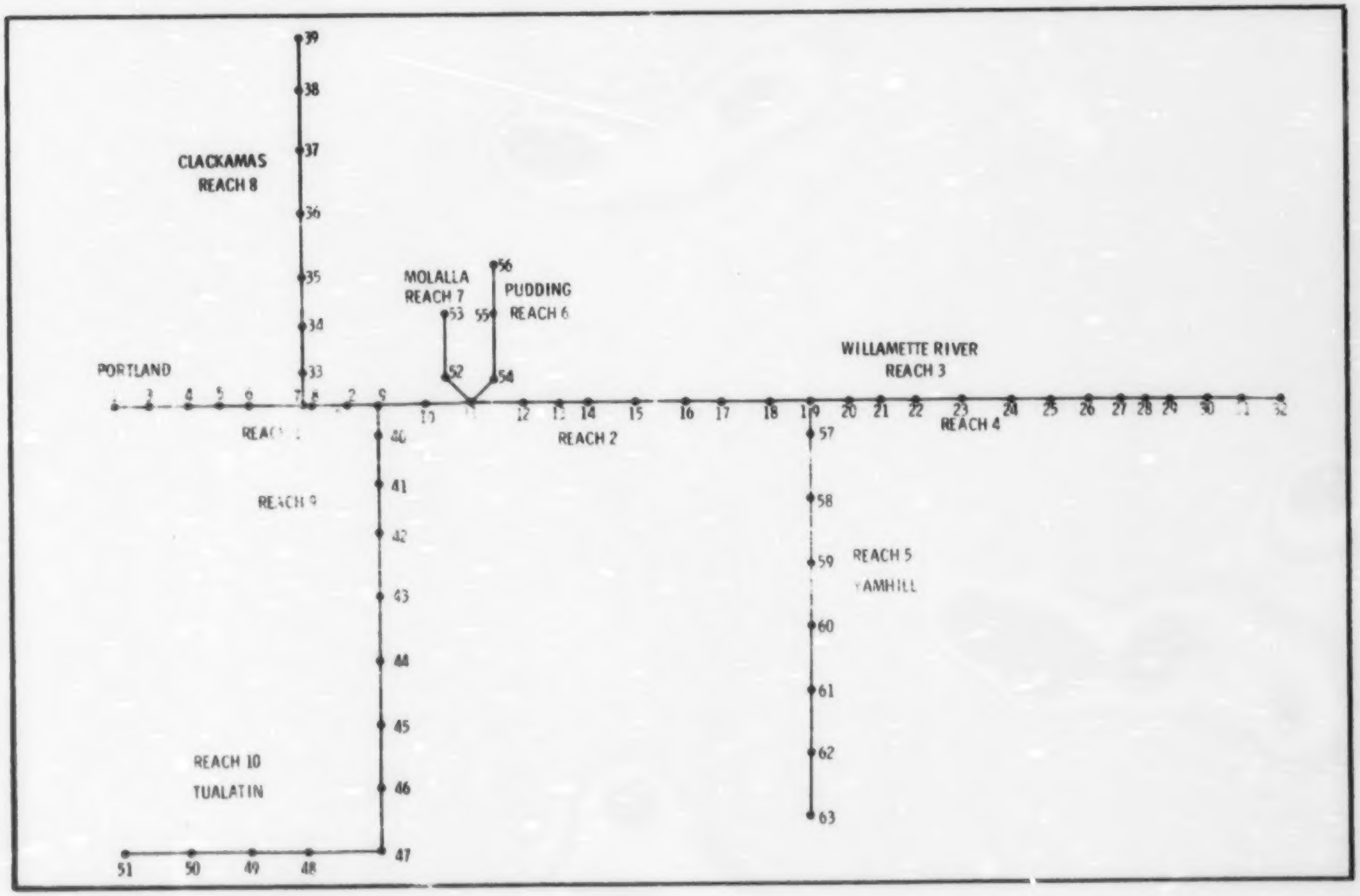
CLACKAMAS
REACH 8
MOLALLA
REACH 7
PUDDING
REACH 6
WILLAMETTE RIVER
REACH 3
PORTLAND
REACH 1
REACH 2
REACH 4
REACH 9
REACH 5
YAMHILL
REACH 10
TUALATIN
1
3
4
5
6
7
8
2
9
10
11
12
13
14
15
16
17
18
19
20
21
22
23
24
25
26
27
28
29
30
31
32
33
34
35
36
37
38
39
40
41
42
43
44
45
46
47
48
49
50
51
52
53
54
55
56
57
58
59
60
61
62
63

FIGURE 14. WILLAMETTE RIVER BASIN SIMULATION FROM SALEM TO PORTLAND

Junction Data

Five sets of data had to be collected for each junction (node). These are explained below.

Surface Areas. All nodal surface areas were obtained from USGS 7 1/2 and 15 minute topographic maps. The locations of the junctions were marked on the maps with the help of dividers and the Willamette River Mile Index[15]. The surface area of each node was measured in square inches with a self-compensating polar planimeter. These values were then converted to millions of square feet according to the maps' scales.

X-Y Coordinates. The (X,Y) coordinates of each junction point were obtained by marking the position of each node point on a 1964 State Water Resources Board Map No. 2.6 and then digitizing the points (X,Y) coordinates with a computer driven graphics digitizer table.

Initial Values of Water Heads. On the mainstem of the Willamette River values for initial water surface elevations for each node were obtained from Water Surface Profile charts compiled by the U.S. Army Corps of Engineers. The data used were taken on August 11, 1965, and the elevations are referenced to mean sea level. On all Willamette tributaries modeled the initial water surface elevations were obtained as follows:

- The river miles were marked for each tributary to be simulated on the USGS topographic maps.
- A table was made containing the elevation of each contour line which crossed the tributary as well as the position in tributary miles where the crossing occurred.
- Graphs were then made from these tables for each tributary being simulated and the positions of the nodal points were marked. The estimate of the water surface head was taken from these graphs.

Inflow and Withdrawals. Data on the flows at the upstream end of each river were obtained from USGS stream gauging stations where available. Flow data were taken from References 16 and 17. Two steady flow conditions were simulated, June 3-9 and September 1-7. The flows used were the averaged values for the 7 day time period. The June flows were the high flows for the summer 1967 period and the September flows corresponded to the lowest flows recorded in that summer. Table 3 shows the average flow values obtained from USGS records for each of these time periods. Inflow data were not available for some cases, for example on the Pudding River; in other cases, the inflows between two

TABLE 3

TABULATION OF THE USGS FLOW DATA USED IN THE VERIFICATION RUNS

	USGS gauge number	Position in stream or river miles	Approximate Simulation nodal position	Average flow Sept 1967 (cfs)	Average flow June 1967 (cfs)	
Willamette (Salem)	14-1910	84.16	32	6570	11114	*
Willamette (Newberg)	14-1980	38.5	13	6757	10929	
Mill Creek	14-1920	2.11	31	65.6	66.1	
South Yamhill	14-1940	16.71	63	9.9	207.6	
North Yamhill	14-1970	20.5	59	6.4	43.9	
Molalla	14-2000	6.01	53	33.9	499.4	
Tualatin	14-2075	1.8	40	11.4	307.4	
Clackamas	14-2100	23.1	39	662.	2043.	
Clackamas	14-2110	4.8	34	678.	2546.	

*Note the discrepancy here. It was assumed that the Salem gauge data were correct and the Newberg values were ignored.

gauging stations could come from a number of streams. The methods used to calculate and distribute these inflows are discussed for the September verification period; the same methods were used for the June flow data.

- Clackamas River Inflows. Three major streams (Clear Creek, Deep Creek and Eagle Creek) enter the Clackamas between gauges 2100 and 2110. References 18, 19, and 20 give estimates of the average annual yields for the drainage areas of these streams. From these average yield estimates a ratio was formed so that flow estimates for these creeks could be made. The ratio for each creek is simply the annual yield of that creek divided by the total annual yield of the creeks for which the flow is being calculated. The flow difference between gauge

2100 and gauge 2110 is multiplied by the calculated ratio for each creek to give the predicted inflow. This number is then added to the Clackamas node nearest that creek's mouth. Table 4 shows a tabulation of the flow data for these creeks.

TABLE 4

TABULATION OF CLACKAMAS RIVER INFLOW DATA

Inflow description	Simulation node where inflow is added	Average annual yield (acre ft)	Ratio	Sept. 1967 flow (cfs)	June 1967 flow (cfs)
Clackamas Flow at Estacada	39	--	--	662	2043
Clear Creek	35	93520	.304	4.7	150
Deep Creek	36	73630	.239	3.8	121
Eagle Creek	37	140900	.457	7.5	239

- Molalla and Yamhill Inflows. The Molalla and Yamhill inflows are shown in Table 3.

- Pudding Inflow Estimation. Because the only flow data on the Pudding was many miles upstream from the simulation end point, the inflow for this river was estimated by the ratio method described for the Clackamas. The Pudding flow was calculated from the Molalla flow according to the formula:

$$\text{Pudding flow} = \text{Molalla flow} \times \frac{\text{Pudding annual yield}}{\text{Molalla annual yield}}$$

For September 1967, a value of 36.7 cfs was calculated and for June 1967, a value of 543 cfs was calculated.

- Tualatin Inflow Data. The inflows to each Tualatin node were determined from a set of ratios (as described above) along with the data from USGS gauge 14-2075. These inflows were calculated according to Reference 20, an in-depth study of streamflow in the Tualatin basin. Table 5 lists the

Tualatin River nodes and the ratio for each node which, when multiplied by the Tualatin mouth flow, yields the inflow value for that node.

TABLE 5

TUALATIN RIVER FLOW RATIOS AND THE FLOW VALUES USED TO SIMULATE THE SEPTEMBER 1967 FLOW PERIOD AND THE JUNE 1967 FLOW PERIOD

Simulation node	Ratio	Calculated Sept 1967 inflow (mouth flow 11.4 cfs)	Calculated June 1967 inflow (mouth flow 307.4 cfs)
40	0.005	0.05	1.34
41	0.042	0.48	12.89
42	0.035	0.40	10.7
43	0.038	0.44	11.8
44	0.0	0.0	0.0
45	0.008	0.09	2.4
46	0.008	0.09	2.4
47	0.073	0.84	22.56
48	0.008	0.09	2.4
49	0.039	0.45	12.0
50	0.016	0.18	4.8
51	0.728	8.32	223.0

- Willamette Inflows. During the September flow period the flow rate at Salem plus all measured and calculated tributary inflows combined are less than the measured flow rate at Newberg. It was assumed that this increase between Salem and Newberg was due to unmeasured tributary flows or groundwater infiltration; therefore 5.0 cfs was added at each node between Salem and Newberg to account for this runoff. These additions accounted for less than 1.5% of the total flow at Newberg. Later experience revealed that small differences of this type are the rule rather than the exception.

  During the June flow period the flow at Newberg was about 400 cfs less than the sum of the Salem and tributary flows. Since no significant withdrawals could be identified, it was assumed that the Salem and tributary flows were correct.

Junction Bottom Elevations. The junction bottom elevations used in the verification problem were obtained via two separate procedures. In the first, data on the average water depth at each river mile were acquired from Reference 22 for the mainstem Willamette above Willamette Falls (river mile 27). Below Willamette Falls, USGS maps having depth contours and specific sounding values were used to make river cross-section plots at 1/2 river mile increments for the estuary portion of the Willamette mainstem. From these cross-section plots the average depth, river cross-sectional area and width were calculated and a graph of average river depth versus river mile was made for the mainstem of the Willamette. The positions of the Willamette node boundaries were marked on the graph and the average depth for each node was calculated from the areas under the curve. Bottom elevations were then determined from the difference between the water surface elevation and the average water depth.

No data existed for average river depth on the Willamette tributaries nor did the USGS maps have tributary depth contours or sounding data. A second procedure was therefore adopted for estimating the depth of these tributaries.

The bottom surface slope in the channels was assumed to be equal to the water surface slope and the water depth in the tributary channels was estimated with the equation

$$\begin{pmatrix}\text{water depth}\\ \text{in a channel}\end{pmatrix} = \left[\frac{\begin{pmatrix}\text{Estimated flow}\\ \text{in the channel}\end{pmatrix} * \begin{pmatrix}\text{Manning}\\ \text{coefficient chosen}\\ \text{for the channel}\end{pmatrix}}{1.49 \begin{pmatrix}\text{Channel}\\ \text{width}\end{pmatrix} \sqrt{\dfrac{\begin{matrix}\text{Head at} & & \text{Head at}\\ \text{upper} & - & \text{lower}\\ \text{junction} & & \text{junction}\end{matrix}}{\text{channel length}}}}\right]^{3/5} \qquad (103)$$

From these estimates of channel depth the average water depths for the junctions were estimated. The bottom elevations were obtained by taking the difference between the junction head and these estimates of water depth.

Channel Data

Certain physical data were required as input for each channel. The channel lengths were simply the distances in feet along the river between the two adjacent nodes. The depth for each channel was taken as the average of the depths of the adjacent nodes. The width of the channel was taken as the channel flow cross-sectional area divided by the depth.

For the tributaries the width was computed from the surface area and channel length. An initial estimate of water depth in the channels was then determined by Equation 103. From these initial depth estimates junction bottom elevations were estimated and the channel bottom elevations were simply determined from the average of the bottom elevations of the junction at the channel end points.

Along the mainstem of the Willamette and most of the tributaries a Manning coefficient of 0.035 was used. This was varied during the verification procedure when necessary. Initial velocity estimates were not made along the mainstem Willamette but in the tributaries initial velocity estimates were made with Equation 103 and the channel cross-sectional area. This was done to increase the rate of convergence of the solution along the tributaries where the high velocities and small depths tend to slow convergence.

Controlled Node Data

Two hydraulic controlled nodes were used in simulating the Willamette River Basin. The downstream end of the Willamette River is a tidally controlled node. Tidal variation data were taken from Reference 23 which presents the stage versus time data at the Morrison Bridge in Portland. The second controlled node was at Willamette Falls which was treated as a wier with an elevation of 52 feet, a width of 2029 feet, and a coefficient of 2.5.

Results

A listing of the input data deck for the September 1967 low flow hydraulic verification case and the summary of the hydraulic input can be found in the User's Manual. Verification was also conducted for the June 1967 medium flow case. The model performed well for the June flow problem but was near instability in the tributary channels for the extremely low September flow case. Figure 15 shows a plot of water surface and bottom elevation versus river mile for the mainstem of the Willamette during the September flow case. Figure 16 is a comparison between the water depths predicted by the model and the actual water depths measured for approximately the same flow conditions. The calculated and measured data agree rather closely, considering that the model predicts the river condition averaged over a junction whereas values are measured for traverses at specific locations.

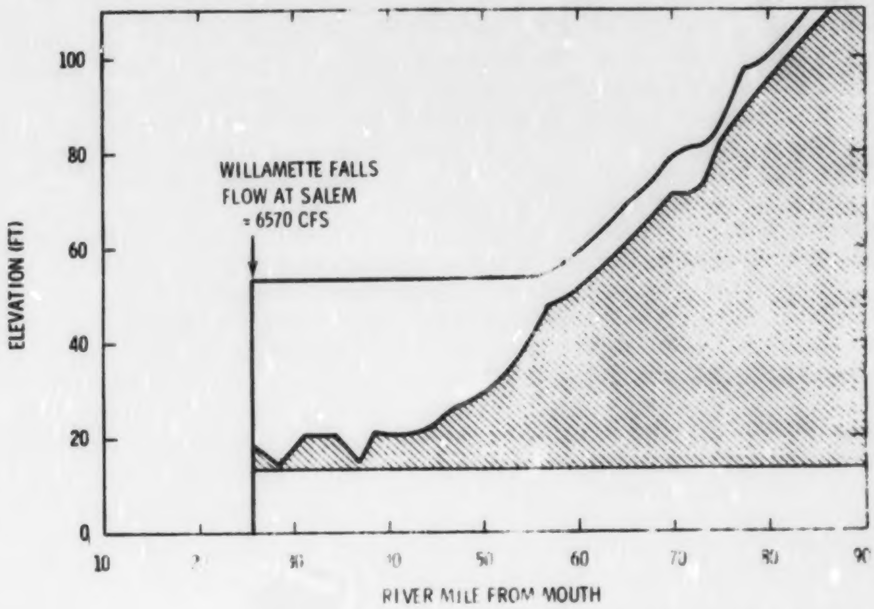

FIGURE 15. PREDICTED WATER SURFACE ELEVATION FROM WILLAMETTE FALLS TO SALEM

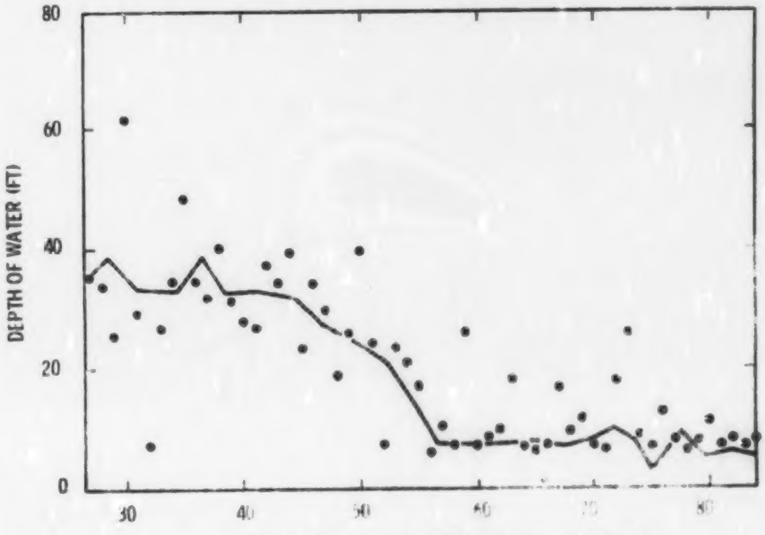

FIGURE 16. WATER DEPTH VERSUS RIVER MILE FROM SALEM TO PORTLAND

Figure 17 is a plot of velocities (September flow case) predicted by the model for the Willamette mainstem compared with the measured velocity data from Reference 22 for approximately the same flow conditions. As with the depth data, the match between calculated and measured data is generally good considering that the measured velocities are at specific traverse points and the model is predicting the average river properties over the channel width. The variations in head for the tidally controlled node (node 1) and the node below Willamette Falls (node 8) are shown in the User's Manual for the September 1967 flow case. This flow case exhibited steady water heads above the Falls on the mainstem Willamette and its tributaries. However, some of the tributary heads, velocities and flows for the September 1967 flow case exhibited oscillations as large as ±15 percent from the mean value. The largest variations occurred on the Clackamas. Variations on the Tualatin and Yamhill were less; on the Molalla and Pudding they were almost nonexistent. These tributary oscillations do not greatly influence the accuracy of the quality code since, in the case of the Clackamas, the travel time from Estacada to the Willamette is short and the flow oscillation is small (15 percent or less). The smaller oscillations, ∿10 percent on the Tualatin and Yamhill, did not affect the quality simulation.

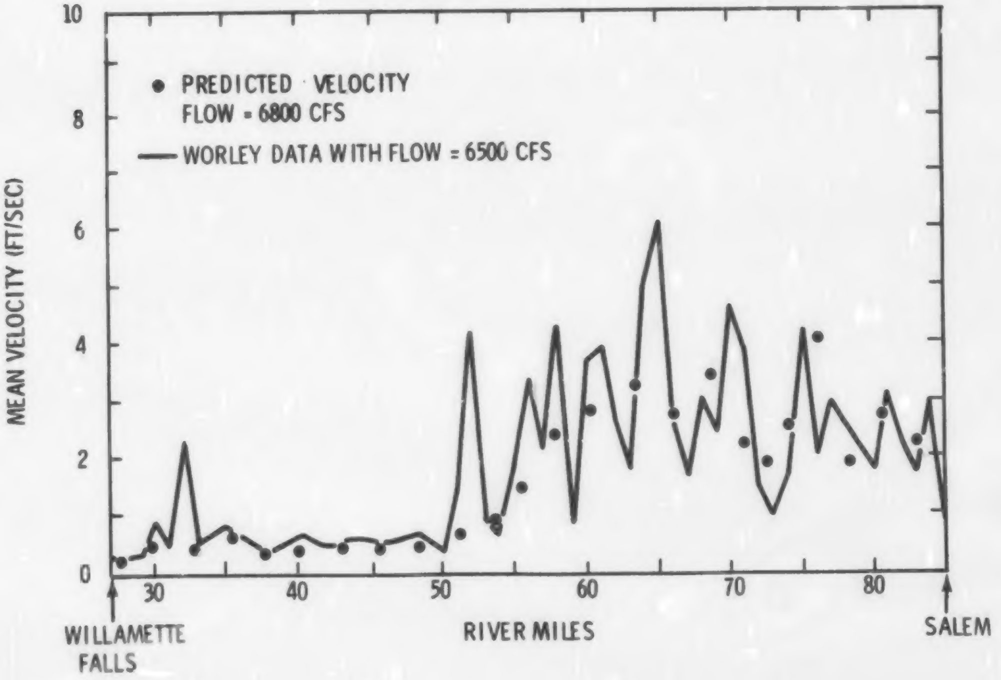

FIGURE 17. VELOCITY PROFILE FROM SALEM TO PORTLAND

The application of the WRE hydraulic code to the Willamette system revealed some limitations in the code which had not been previously defined. The first problem appeared in channels connecting the mainstem with its tributaries. The WRE code did not define small tributary channels or any channel between a bay and a river; rivers and tributaries were treated as channels. Application of the WRE code to the Willamette River immediately pointed out the necessity of considering "small tributary channels." At every junction between the Willamette and a tributary, the first upstream tributary node and the connecting channel dried up. The depth in a channel is computed by the WRE code from the heads at the ends of the channel. As long as the tributary inflow and/or bottom slopes were similar to the mainstem, no problem occurred; however, when the bottom slope of a tributary channel was appreciably greater than that of the river or embayment, the channel became dry. Figure 18 shows a channel cross-sectional diagram of a small tributary connecting to a larger river. Note that the depth calculated by the original WRE code is too large, causing too high a flow in the channel. In the revised code, small tributary channels are treated as any other channels when backflow occurs. However, for normal downstream flow cases, estimate of hydraulic radius for the small tributary channels is made from the value of water depth at the first upstream junction on the tributary.

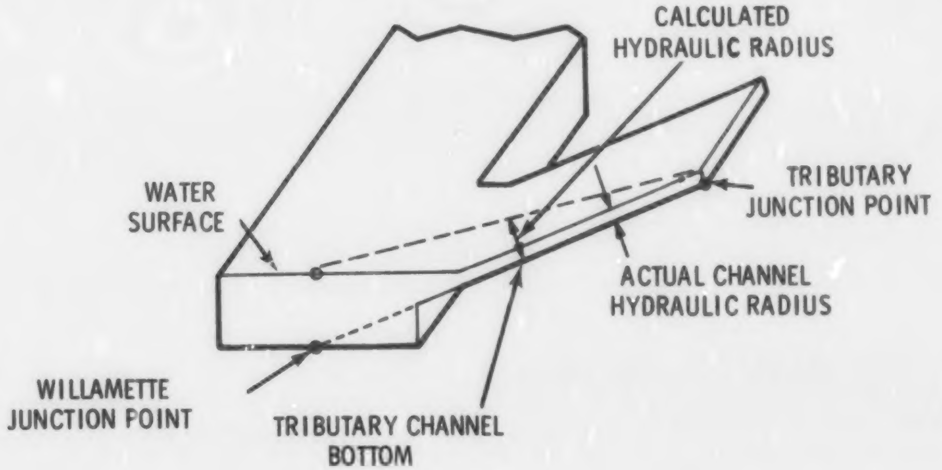

FIGURE 18. DIAGRAM ILLUSTRATING SMALL TRIBUTARY CHANNEL CONFIGURATION

Another problem in the original WRE code was evident for the September 1967 case. The Willamette tributaries for these extremely low flows began to exhibit instability problems which could not be remedied by greater node spacing, change in the Manning coefficient, or by any other means. An exhaustive set of studies was performed on the Clackamas and it was found that the only way to decrease the instability was to increase the tributary flow rate. Equation 104 is the stability equation programmed in the WRE code.

$$\Delta t \le \frac{0.75\ (\text{channel length})}{\sqrt{g \left(\begin{array}{l}\text{channel}\\ \text{hydraulic} + 2\\ \text{radius (ft)}\end{array}\right)}} \qquad (104)$$

Table 6 is a stability chart based on this criterion for various values of hydraulic radius and channel length. Examination of this table and data on the tributaries being simulated indicates there is no reason to suspect a stability problem. When the stability criterion published in the Storm Water Management document is applied (Equation 105), a much different picture develops. Tables 7 , 8 , and 9 are stability charts formed by using Equation 105 for velocity estimates of 0, 1, and 2 ft/sec and a Manning coefficient of 0.035.

$$\Delta t \le \frac{\Delta X}{\left[V\left(1 + \frac{n^2\ \Delta X\ g}{2.21\ R{*}{*}4/3}\right) + \sqrt{gR}\right]} \qquad (105)$$

where V = mean velocity

g = gravitational constant

n = Manning's resistance coefficient, R = hydraulic radius of the channel

ΔX = length of the channel (i.e., distance between nodes)

In developing Equation 104, WRE assumed the velocity term in the denominator of 105 to be negligible. This is a valid assumption for embayments and large rivers where velocities are low and channel hydraulic radii are relatively large, as a comparison between stability Tables 6 and 7 will verify. On the Willamette tributaries with the September 1967 flow conditions, the V term and the $\sqrt{gR}$ term in Equation 105 are negligible and the ΔX or channel length term in the numerator

TABLE 6

STABILITY CHART CALCULATED BY USING THE WRE STABILITY CRITERION (EQUATION 105)

CHANNEL LENGTH (IN THOUSANDS OF FEET)

TIME (IN HUNDREDS OF SECONDS)

HYD RAD (FT)	.5	1.0	1.5	2.0	2.5	3.0	3.5	4.0	4.5	5.0	5.5	6.0	6.5	7.0	7.5	8.0	8.5	9.0	9.5	10.0
.5	.5	.8	1.3	1.7	2.1	2.5	2.9	3.3	3.8	4.2	4.6	5.0	5.4	5.9	6.3	6.7	7.1	7.5	7.9	8.4
1.0	.5	.8	1.1	1.5	1.9	2.3	2.7	3.1	3.4	3.8	4.2	4.6	5.0	5.3	5.7	6.1	6.5	6.9	7.2	7.6
1.5	.5	.7	1.1	1.4	1.8	2.1	2.5	2.8	3.2	3.5	3.9	4.2	4.6	4.9	5.3	5.7	6.0	6.4	6.7	7.1
2.0	.5	.7	1.0	1.3	1.7	2.0	2.3	2.6	3.0	3.3	3.6	4.0	4.3	4.6	5.0	5.3	5.6	5.9	6.3	6.6
2.5	.5	.6	.9	1.2	1.6	1.9	2.2	2.5	2.8	3.1	3.4	3.7	4.0	4.4	4.7	5.0	5.3	5.6	5.9	6.2
3.0	.5	.6	.9	1.2	1.5	1.8	2.1	2.4	2.7	3.0	3.3	3.5	3.8	4.1	4.4	4.7	5.0	5.3	5.6	5.9
3.5	.5	.6	.8	1.1	1.4	1.7	2.0	2.3	2.5	2.8	3.1	3.4	3.7	3.9	4.2	4.5	4.8	5.1	5.4	5.6
4.0	.5	.5	.8	1.1	1.3	1.6	1.9	2.2	2.4	2.7	3.0	3.2	3.5	3.8	4.0	4.3	4.6	4.9	5.1	5.4
4.5	.5	.5	.8	1.0	1.3	1.6	1.8	2.1	2.3	2.6	2.9	3.1	3.4	3.6	3.9	4.1	4.4	4.7	4.9	5.2
5.0	.5	.5	.7	1.0	1.2	1.5	1.7	2.0	2.2	2.5	2.7	3.0	3.2	3.5	3.7	4.0	4.2	4.5	4.7	5.0
5.5	.5	.5	.7	1.0	1.2	1.4	1.7	1.9	2.2	2.4	2.7	2.9	3.1	3.4	3.6	3.9	4.1	4.3	4.6	4.8
6.0	.5	.5	.7	.9	1.2	1.4	1.6	1.9	2.1	2.3	2.6	2.8	3.0	3.3	3.5	3.7	4.0	4.2	4.4	4.7
6.5	.5	.5	.7	.9	1.1	1.4	1.6	1.8	2.0	2.3	2.5	2.7	2.9	3.2	3.4	3.6	3.9	4.1	4.3	4.5
7.0	.5	.5	.7	.9	1.1	1.3	1.5	1.8	2.0	2.2	2.4	2.6	2.9	3.1	3.3	3.5	3.7	4.0	4.2	4.4
7.5	.5	.5	.6	.9	1.1	1.3	1.5	1.7	1.9	2.1	2.4	2.6	2.8	3.0	3.2	3.4	3.6	3.9	4.1	4.3
8.0	.5	.5	.6	.8	1.0	1.3	1.5	1.7	1.9	2.1	2.3	2.5	2.7	2.9	3.1	3.3	3.6	3.8	4.0	4.2
8.5	.5	.5	.6	.8	1.0	1.2	1.4	1.6	1.8	2.0	2.2	2.4	2.7	2.9	3.1	3.3	3.5	3.7	3.9	4.1
9.0	.5	.5	.6	.8	1.0	1.2	1.4	1.6	1.8	2.0	2.2	2.4	2.6	2.8	3.0	3.2	3.4	3.6	3.8	4.0
9.5	.5	.5	.6	.8	1.0	1.2	1.4	1.6	1.8	1.9	2.1	2.3	2.5	2.7	2.9	3.1	3.3	3.5	3.7	3.9
10.0	.5	.5	.6	.8	1.0	1.1	1.3	1.5	1.7	1.9	2.1	2.3	2.5	2.7	2.9	3.1	3.2	3.4	3.6	3.8
10.5	.5	.5	.6	.7	.9	1.1	1.3	1.5	1.7	1.9	2.1	2.2	2.4	2.6	2.8	3.0	3.2	3.4	3.6	3.7
11.0	.5	.5	.5	.7	.9	1.1	1.3	1.5	1.6	1.8	2.0	2.2	2.4	2.6	2.7	2.9	3.1	3.3	3.5	3.7
11.5	.5	.5	.5	.7	.9	1.1	1.3	1.4	1.6	1.8	2.0	2.2	2.3	2.5	2.7	2.9	3.1	3.2	3.4	3.6
12.0	.5	.5	.5	.7	.9	1.1	1.2	1.4	1.6	1.8	1.9	2.1	2.3	2.5	2.6	2.8	3.0	3.2	3.4	3.5
12.5	.5	.5	.5	.7	.9	1.0	1.2	1.4	1.6	1.7	1.9	2.1	2.3	2.4	2.6	2.8	3.0	3.1	3.3	3.5
13.0	.5	.5	.5	.7	.9	1.0	1.2	1.4	1.5	1.7	1.9	2.0	2.2	2.4	2.6	2.7	2.9	3.1	3.2	3.4
13.5	.5	.5	.5	.7	.8	1.0	1.2	1.3	1.5	1.7	1.8	2.0	2.2	2.3	2.5	2.7	2.9	3.0	3.2	3.4
14.0	.5	.5	.5	.7	.8	1.0	1.2	1.3	1.5	1.7	1.8	2.0	2.1	2.3	2.5	2.6	2.8	3.0	3.1	3.3
14.5	.5	.5	.5	.7	.8	1.0	1.1	1.3	1.5	1.6	1.8	2.0	2.1	2.3	2.4	2.6	2.8	2.9	3.1	3.3
15.0	.5	.5	.5	.6	.8	1.0	1.1	1.3	1.4	1.6	1.8	1.9	2.1	2.2	2.4	2.6	2.7	2.9	3.0	3.2
15.5	.5	.5	.5	.6	.8	.9	1.1	1.3	1.4	1.6	1.7	1.9	2.1	2.2	2.4	2.5	2.7	2.8	3.0	3.2
16.0	.5	.5	.5	.6	.8	.9	1.1	1.2	1.4	1.6	1.7	1.9	2.0	2.2	2.3	2.5	2.6	2.8	3.0	3.1
16.5	.5	.5	.5	.6	.8	.9	1.1	1.2	1.4	1.5	1.7	1.8	2.0	2.2	2.3	2.5	2.6	2.8	2.9	3.1
17.0	.5	.5	.5	.6	.8	.9	1.1	1.2	1.4	1.5	1.7	1.8	2.0	2.1	2.3	2.4	2.6	2.7	2.9	3.0
17.5	.5	.5	.5	.6	.7	.9	1.0	1.2	1.3	1.5	1.6	1.8	1.9	2.1	2.2	2.4	2.5	2.7	2.8	3.0
18.0	.5	.5	.5	.6	.7	.9	1.0	1.2	1.3	1.5	1.6	1.8	1.9	2.1	2.2	2.4	2.5	2.7	2.8	3.0
18.5	.5	.5	.5	.6	.7	.9	1.0	1.2	1.3	1.5	1.6	1.8	1.9	2.0	2.2	2.3	2.5	2.6	2.8	2.9
19.0	.5	.5	.5	.6	.7	.9	1.0	1.2	1.3	1.4	1.6	1.7	1.9	2.0	2.2	2.3	2.5	2.6	2.7	2.9
19.5	.5	.5	.5	.6	.7	.9	1.0	1.1	1.3	1.4	1.6	1.7	1.9	2.0	2.1	2.3	2.4	2.6	2.7	2.9
20.0	.5	.5	.5	.6	.7	.8	1.0	1.1	1.3	1.4	1.5	1.7	1.8	2.0	2.1	2.3	2.4	2.5	2.7	2.8
20.5	.5	.5	.5	.6	.7	.8	1.0	1.1	1.3	1.4	1.5	1.7	1.8	2.0	2.1	2.2	2.4	2.5	2.6	2.8
21.0	.5	.5	.5	.6	.7	.8	1.0	1.1	1.2	1.4	1.5	1.7	1.8	1.9	2.1	2.2	2.3	2.5	2.6	2.8
21.5	.5	.5	.5	.5	.7	.8	1.0	1.1	1.2	1.4	1.5	1.6	1.8	1.9	2.0	2.2	2.3	2.5	2.6	2.7
22.0	.5	.5	.5	.5	.7	.8	.9	1.1	1.2	1.3	1.5	1.6	1.8	1.9	2.0	2.2	2.3	2.4	2.6	2.7
22.5	.5	.5	.5	.5	.7	.8	.9	1.1	1.2	1.3	1.5	1.6	1.7	1.9	2.0	2.1	2.3	2.4	2.5	2.7
23.0	.5	.5	.5	.5	.7	.8	.9	1.1	1.2	1.3	1.5	1.6	1.7	1.9	2.0	2.1	2.2	2.4	2.5	2.6
23.5	.5	.5	.5	.5	.7	.8	.9	1.0	1.2	1.3	1.4	1.5	1.7	1.8	2.0	2.1	2.2	2.4	2.5	2.6
24.0	.5	.5	.5	.5	.6	.8	.9	1.0	1.2	1.3	1.4	1.6	1.7	1.8	1.9	2.1	2.2	2.3	2.5	2.6

TABLE 7

STABILITY CHART CALCULATED FROM EQUATION 105 (n = 0.035)

VELOCITY= .0(FT/SEC)

HYDRAULIC RADIUS (FT)

TIME (IN HUNDREDS OF SECONDS)

CHANNEL LENGTH (THOUSANDS OF FEET)	1.0	2.0	4.0	6.0	8.0	10.0	14.0	18.0	22.0	26.0	30.0	34.0	38.0	42.0	48.0	52.0	56.0	60.0	64.0	68.0
.5	.9	.6	.4	.4	.3	.3	.2	.2	.2	.2	.2	.2	.1	.1	.1	.1	.1	.1	.1	.1
1.0	1.8	1.2	.9	.7	.6	.6	.5	.4	.4	.3	.3	.3	.3	.3	.3	.2	.2	.2	.2	.2
1.5	2.6	1.9	1.3	1.1	.9	.8	.7	.6	.5	.5	.5	.5	.4	.4	.4	.4	.4	.3	.3	.3
2.0	3.5	2.5	1.8	1.4	1.2	1.1	.9	.8	.8	.7	.6	.6	.6	.5	.5	.5	.5	.5	.4	.4
2.5	4.4	3.1	2.2	1.8	1.6	1.4	1.2	1.0	.9	.9	.8	.8	.7	.7	.6	.6	.6	.6	.6	.5
3.0	5.3	3.7	2.6	2.2	1.9	1.7	1.4	1.2	1.1	1.0	1.0	.9	.9	.8	.8	.7	.7	.7	.7	.6
3.5	6.2	4.4	3.1	2.5	2.2	2.0	1.6	1.5	1.3	1.2	1.1	1.1	1.0	1.0	.9	.9	.8	.8	.8	.7
4.0	7.1	5.0	3.5	2.9	2.5	2.2	1.9	1.7	1.5	1.4	1.3	1.2	1.1	1.1	1.0	1.0	.9	.9	.9	.9
4.5	7.9	5.6	4.0	3.2	2.8	2.5	2.1	1.9	1.7	1.6	1.4	1.4	1.3	1.2	1.1	1.1	1.1	1.0	1.0	1.0
5.0	8.8	6.2	4.4	3.6	3.1	2.8	2.4	2.1	1.9	1.7	1.6	1.5	1.4	1.4	1.3	1.2	1.2	1.1	1.1	1.1
5.5	9.7	6.9	4.8	4.0	3.4	3.1	2.6	2.3	2.1	1.9	1.8	1.7	1.6	1.5	1.4	1.3	1.3	1.3	1.2	1.2
6.0	10.6	7.5	5.3	4.3	3.7	3.3	2.8	2.5	2.3	2.1	1.9	1.8	1.7	1.6	1.5	1.5	1.4	1.4	1.3	1.3
6.5	11.5	8.1	5.7	4.7	4.1	3.6	3.1	2.7	2.4	2.2	2.1	2.0	1.9	1.8	1.7	1.6	1.5	1.5	1.4	1.4
7.0	12.3	8.7	6.2	5.0	4.4	3.9	3.3	2.9	2.6	2.4	2.3	2.1	2.0	1.9	1.8	1.7	1.6	1.6	1.5	1.5
7.5	13.2	9.4	6.6	5.4	4.7	4.2	3.5	3.1	2.9	2.6	2.4	2.3	2.1	2.0	1.9	1.8	1.8	1.7	1.7	1.6
8.0	14.1	10.0	7.1	5.8	5.0	4.5	3.8	3.3	3.0	2.8	2.6	2.4	2.3	2.2	2.0	2.0	1.9	1.8	1.8	1.7
8.5	15.0	10.6	7.5	6.1	5.3	4.7	4.0	3.5	3.2	2.9	2.7	2.6	2.4	2.3	2.2	2.1	2.0	1.9	1.9	1.8
9.0	15.9	11.2	7.9	6.5	5.6	5.0	4.2	3.7	3.4	3.1	2.9	2.7	2.6	2.4	2.3	2.2	2.1	2.0	2.0	1.9
9.5	16.8	11.8	8.4	6.8	5.9	5.3	4.5	3.9	3.5	3.3	3.1	2.9	2.7	2.6	2.4	2.3	2.2	2.2	2.1	2.0
10.0	17.6	12.5	8.8	7.2	6.2	5.6	4.7	4.2	3.8	3.5	3.2	3.0	2.9	2.7	2.5	2.4	2.4	2.3	2.2	2.1
10.5	18.5	13.1	9.3	7.6	6.5	5.9	4.9	4.4	3.9	3.6	3.4	3.2	3.0	2.9	2.7	2.6	2.5	2.4	2.3	2.2
11.0	19.4	13.7	9.7	7.9	6.9	6.1	5.2	4.6	4.1	3.8	3.5	3.3	3.1	3.0	2.8	2.7	2.6	2.5	2.4	2.4
11.5	20.3	14.3	10.1	8.3	7.2	6.4	5.4	4.8	4.3	4.0	3.7	3.5	3.3	3.1	2.9	2.8	2.7	2.6	2.5	2.5
12.0	21.2	15.0	10.6	8.6	7.5	6.7	5.7	5.0	4.5	4.1	3.9	3.6	3.4	3.3	3.1	2.9	2.8	2.7	2.6	2.6
12.5	22.0	15.6	11.0	9.0	7.8	7.0	5.9	5.2	4.7	4.3	4.0	3.8	3.6	3.4	3.2	3.1	2.9	2.8	2.8	2.7
13.0	22.9	16.2	11.5	9.4	8.1	7.2	6.1	5.4	4.9	4.5	4.2	3.9	3.7	3.5	3.3	3.2	3.1	3.0	2.9	2.8
13.5	23.8	16.8	11.9	9.7	8.4	7.5	6.4	5.6	5.1	4.7	4.3	4.1	3.9	3.7	3.4	3.3	3.2	3.1	3.0	2.9
14.0	24.7	17.5	12.3	10.1	8.7	7.8	6.6	5.8	5.3	4.8	4.5	4.2	4.0	3.8	3.6	3.4	3.3	3.2	3.1	3.0
14.5	25.6	18.1	12.8	10.4	9.0	8.1	6.8	6.0	5.5	5.0	4.7	4.4	4.1	3.9	3.7	3.5	3.4	3.3	3.2	3.1
15.0	26.5	18.7	13.2	10.8	9.4	8.4	7.1	6.2	5.5	5.2	4.8	4.5	4.3	4.1	3.8	3.7	3.5	3.4	3.3	3.2
15.5	27.3	19.3	13.7	11.2	9.7	8.6	7.3	6.4	5.8	5.4	5.0	4.7	4.4	4.2	3.9	3.8	3.7	3.5	3.4	3.3
16.0	28.2	20.0	14.1	11.5	10.0	8.9	7.5	6.7	6.0	5.5	5.2	4.8	4.6	4.4	4.1	3.9	3.8	3.6	3.5	3.4
16.5	29.1	20.6	14.5	11.9	10.3	9.2	7.8	6.9	6.2	5.7	5.3	5.0	4.7	4.5	4.2	4.0	3.9	3.8	3.6	3.5
17.0	30.0	21.2	15.0	12.2	10.6	9.5	8.0	7.1	6.4	5.9	5.5	5.1	4.9	4.6	4.3	4.2	4.0	3.9	3.7	3.6
17.5	30.9	21.8	15.4	12.6	10.9	9.8	8.2	7.3	6.6	6.1	5.6	5.3	5.0	4.8	4.5	4.3	4.1	4.0	3.9	3.7
18.0	31.7	22.4	15.9	13.0	11.2	10.0	8.5	7.5	6.8	6.2	5.8	5.4	5.1	4.9	4.6	4.4	4.2	4.1	4.0	3.8
18.5	32.6	23.1	16.3	13.3	11.5	10.3	8.7	7.7	7.0	6.4	6.0	5.6	5.3	5.0	4.7	4.5	4.4	4.2	4.1	4.0
19.0	33.5	23.7	16.8	13.7	11.8	10.6	9.0	7.9	7.1	6.6	6.1	5.7	5.4	5.2	4.8	4.6	4.5	4.3	4.2	4.1
19.5	34.4	24.3	17.2	14.0	12.2	10.9	9.2	8.1	7.3	6.7	6.3	5.9	5.6	5.3	5.0	4.8	4.6	4.4	4.3	4.2
20.0	35.3	24.9	17.6	14.4	12.5	11.2	9.4	8.3	7.5	6.9	6.4	6.0	5.7	5.4	5.1	4.9	4.7	4.6	4.4	4.3

TABLE 8

STABILITY CHART CALCULATED FROM EQUATION 105 (n = 0.035)

```
  CHANNEL*
   LENGTH*                                                  VELOCITY=  1.0(FT/SEC)
(THOUSANDS*
 OF FEET)*                                                  HYDRAULIC RADIUS (FT)
         *  1.0  2.0  4.0  6.0  8.0 10.0 14.0 18.0 22.0 26.0 30.0 34.0 38.0 42.0 48.0 52.0 56.0 60.0 64.0 68.0
         *************************************************************************************************
         *                                                   TIME (IN HUNDREDS OF SECONDS)
     .5  *   .3   .4   .4   .3   .3   .3   .2   .2   .2   .2   .2   .1   .1   .1   .1   .1   .1   .1   .1   .1
    1.0  *   .4   .6   .7   .6   .6   .5   .4   .4   .4   .3   .3   .3   .3   .3   .2   .2   .2   .2   .2   .2
    1.5  *   .4   .8   .9   .9   .8   .7   .7   .6   .5   .5   .5   .4   .4   .4   .4   .4   .3   .3   .3   .3
    2.0  *   .5   .9  1.1  1.1  1.0  1.0   .9   .8   .7   .7   .6   .6   .6   .5   .5   .5   .5   .4   .4   .4
    2.5  *   .5   .9  1.3  1.3  1.3  1.2  1.1  1.0   .9   .8   .8   .7   .7   .7   .6   .6   .6   .6   .5   .5
    3.0  *   .5  1.0  1.4  1.5  1.5  1.4  1.3  1.1  1.1  1.0   .9   .9   .8   .8   .7   .7   .7   .7   .6   .6
    3.5  *   .5  1.0  1.6  1.7  1.7  1.6  1.5  1.3  1.2  1.1  1.1  1.0  1.0   .9   .9   .8   .8   .8   .8   .7
    4.0  *   .5  1.1  1.7  1.9  1.9  1.8  1.6  1.5  1.4  1.3  1.2  1.2  1.1  1.0  1.0   .9   .9   .9   .9   .8
    4.5  *   .5  1.1  1.8  2.0  2.0  2.0  1.8  1.7  1.6  1.5  1.4  1.3  1.2  1.2  1.1  1.1  1.0  1.0  1.0   .9
    5.0  *   .5  1.1  1.9  2.2  2.2  2.2  2.0  1.9  1.7  1.6  1.5  1.4  1.4  1.3  1.2  1.2  1.1  1.1  1.1  1.0
    5.5  *   .5  1.1  2.0  2.3  2.4  2.3  2.2  2.0  1.9  1.8  1.7  1.6  1.5  1.4  1.3  1.3  1.3  1.2  1.2  1.1
    6.0  *   .5  1.2  2.1  2.4  2.5  2.5  2.4  2.2  2.0  1.9  1.8  1.7  1.6  1.6  1.5  1.4  1.4  1.3  1.3  1.2
    6.5  *   .5  1.2  2.1  2.5  2.7  2.7  2.5  2.4  2.2  2.1  2.0  1.9  1.8  1.7  1.6  1.5  1.5  1.4  1.4  1.3
    7.0  *   .5  1.2  2.2  2.7  2.9  2.8  2.7  2.5  2.4  2.2  2.1  2.0  1.9  1.8  1.7  1.6  1.6  1.5  1.5  1.5
    7.5  *   .5  1.2  2.2  2.8  3.0  3.0  2.9  2.7  2.5  2.4  2.2  2.1  2.0  1.9  1.8  1.8  1.7  1.6  1.6  1.6
    8.0  *   .5  1.2  2.3  2.9  3.1  3.1  3.0  2.8  2.7  2.5  2.4  2.3  2.2  2.1  1.9  1.9  1.8  1.8  1.7  1.7
    8.5  *   .5  1.2  2.3  3.0  3.2  3.3  3.2  3.0  2.8  2.7  2.5  2.4  2.3  2.2  2.1  2.0  1.9  1.9  1.8  1.8
    9.0  *   .5  1.2  2.4  3.0  3.3  3.4  3.3  3.2  3.0  2.8  2.7  2.5  2.4  2.3  2.2  2.1  2.0  2.0  1.9  1.9
    9.5  *   .5  1.2  2.4  3.1  3.4  3.5  3.5  3.3  3.1  3.0  2.8  2.7  2.5  2.4  2.3  2.2  2.1  2.1  2.0  2.0
   10.0  *   .5  1.3  2.5  3.2  3.5  3.7  3.6  3.5  3.3  3.1  2.9  2.8  2.7  2.6  2.4  2.3  2.3  2.2  2.1  2.1
   10.5  *   .5  1.3  2.5  3.3  3.7  3.8  3.8  3.6  3.4  3.2  3.1  2.9  2.8  2.7  2.5  2.4  2.4  2.3  2.2  2.2
   11.0  *   .5  1.3  2.5  3.3  3.8  3.9  3.9  3.8  3.6  3.4  3.2  3.1  2.9  2.8  2.7  2.6  2.5  2.4  2.3  2.3
   11.5  *   .5  1.3  2.6  3.4  3.9  4.0  4.1  3.9  3.7  3.5  3.4  3.2  3.1  2.9  2.8  2.7  2.6  2.5  2.4  2.4
   12.0  *.  .5  1.3  2.6  3.5  3.9  4.2  4.2  4.1  3.9  3.7  3.5  3.3  3.2  3.1  2.9  2.8  2.7  2.6  2.5  2.5
   12.5  *   .5  1.3  2.6  3.5  4.0  4.3  4.3  4.2  4.0  3.8  3.6  3.5  3.3  3.2  3.0  2.9  2.8  2.7  2.6  2.6
   13.0  *   .5  1.3  2.7  3.6  4.1  4.4  4.5  4.3  4.1  3.9  3.8  3.6  3.4  3.3  3.1  3.0  2.9  2.8  2.7  2.7
   13.5  *   .5  1.3  2.7  3.7  4.2  4.5  4.6  4.5  4.3  4.1  3.9  3.7  3.6  3.4  3.2  3.1  3.0  2.9  2.9  2.8
   14.0  *   .5  1.3  2.7  3.7  4.3  4.6  4.7  4.6  4.4  4.2  4.0  3.9  3.7  3.5  3.4  3.2  3.1  3.0  3.0  2.9
   14.5  *   .5  1.3  2.7  3.8  4.4  4.7  4.9  4.7  4.6  4.4  4.2  4.0  3.8  3.7  3.5  3.4  3.2  3.2  3.1  3.0
   15.0  *   .5  1.3  2.8  3.8  4.4  4.8  5.0  4.9  4.7  4.5  4.3  4.1  3.9  3.8  3.6  3.5  3.4  3.3  3.2  3.1
   15.5  *   .5  1.3  2.8  3.9  4.5  4.9  5.1  5.0  4.8  4.6  4.4  4.2  4.1  3.9  3.7  3.6  3.5  3.4  3.3  3.2
   16.0  *   .5  1.3  2.8  3.9  4.6  5.0  5.2  5.1  5.0  4.8  4.6  4.4  4.2  4.0  3.8  3.7  3.6  3.5  3.4  3.3
   16.5  *   .5  1.3  2.8  3.9  4.7  5.1  5.3  5.3  5.1  4.9  4.7  4.5  4.3  4.1  3.9  3.8  3.7  3.6  3.5  3.4
   17.0  *   .5  1.3  2.8  4.0  4.7  5.2  5.4  5.4  5.2  5.0  4.8  4.6  4.4  4.3  4.0  3.9  3.8  3.7  3.6  3.5
   17.5  *   .5  1.3  2.8  4.0  4.8  5.2  5.6  5.5  5.4  5.2  4.9  4.7  4.6  4.4  4.2  4.0  3.9  3.8  3.7  3.6
   18.0  *   .5  1.3  2.9  4.1  4.9  5.3  5.7  5.6  5.5  5.3  5.1  4.9  4.7  4.5  4.3  4.1  4.0  3.9  3.8  3.7
   18.5  *   .5  1.3  2.9  4.1  4.9  5.4  5.8  5.8  5.6  5.4  5.2  5.0  4.8  4.6  4.4  4.2  4.1  4.0  3.9  3.8
   19.0  *   .6  1.3  2.9  4.1  5.0  5.5  5.9  5.9  5.7  5.5  5.3  5.1  4.9  4.7  4.5  4.4  4.2  4.1  4.0  3.9
   19.5  *   .6  1.3  2.9  4.2  5.0  5.6  6.0  6.0  5.9  5.7  5.4  5.2  5.0  4.9  4.6  4.5  4.3  4.2  4.1  4.0
   20.0  *   .6  1.3  2.9  4.2  5.1  5.6  6.1  6.1  6.0  5.8  5.6  5.4  5.2  5.0  4.7  4.6  4.4  4.3  4.2  4.1
```

TABLE 9

STABILITY CHART CALCULATED FROM EQUATION 105 n = 0.035)

VELOCITY= 2.0(FT/SEC)

HYDRAULIC RADIUS (FT)

TIME (IN HUNDREDS OF SECONDS)

CHANNEL LENGTH (THOUSANDS OF FEET)	1.0	2.0	4.0	6.0	8.0	10.0	14.0	18.0	22.0	26.0	30.0	34.0	38.0	42.0	48.0	52.0	56.0	60.0	64.0	68.0
.5	.2	.3	.3	.3	.3	.2	.2	.2	.2	.2	.2	.1	.1	.1	.1	.1	.1	.1	.1	.1
1.0	.2	.4	.5	.5	.5	.5	.4	.4	.3	.3	.3	.3	.3	.3	.2	.2	.2	.2	.2	.2
1.5	.2	.5	.7	.7	.7	.7	.6	.6	.5	.5	.4	.4	.4	.4	.4	.3	.3	.3	.3	.3
2.0	.3	.5	.8	.9	.9	.9	.8	.7	.7	.6	.6	.6	.5	.5	.5	.5	.4	.4	.4	.4
2.5	.3	.6	.9	1.0	1.1	1.0	1.0	.9	.8	.8	.7	.7	.7	.6	.6	.6	.6	.5	.5	.5
3.0	.3	.6	1.0	1.2	1.2	1.2	1.1	1.1	1.0	.9	.9	.8	.8	.8	.7	.7	.7	.6	.6	.6
3.5	.3	.6	1.1	1.3	1.4	1.4	1.3	1.2	1.1	1.1	1.0	1.0	.9	.9	.8	.8	.8	.8	.7	.7
4.0	.3	.6	1.1	1.4	1.5	1.5	1.5	1.4	1.3	1.2	1.2	1.1	1.1	1.0	.9	.9	.9	.9	.8	.8
4.5	.3	.6	1.2	1.5	1.6	1.6	1.6	1.5	1.4	1.4	1.3	1.2	1.2	1.1	1.1	1.0	1.0	1.0	.9	.9
5.0	.3	.6	1.2	1.6	1.7	1.8	1.8	1.7	1.6	1.5	1.4	1.4	1.3	1.3	1.2	1.1	1.1	1.1	1.0	1.0
5.5	.3	.6	1.2	1.6	1.8	1.9	1.9	1.8	1.7	1.6	1.6	1.5	1.4	1.4	1.3	1.3	1.2	1.2	1.1	1.1
6.0	.3	.6	1.3	1.7	1.9	2.0	2.0	2.0	1.9	1.8	1.7	1.6	1.6	1.5	1.4	1.4	1.3	1.3	1.2	1.2
6.5	.3	.6	1.3	1.7	2.0	2.1	2.2	2.1	2.0	1.9	1.8	1.7	1.7	1.6	1.5	1.5	1.4	1.4	1.3	1.3
7.0	.3	.6	1.3	1.8	2.1	2.2	2.3	2.2	2.1	2.0	2.0	1.9	1.8	1.7	1.6	1.6	1.5	1.5	1.4	1.4
7.5	.3	.6	1.4	1.9	2.2	2.3	2.4	2.4	2.3	2.2	2.1	2.0	1.9	1.8	1.8	1.7	1.6	1.6	1.5	1.5
8.0	.3	.6	1.4	1.9	2.2	2.4	2.5	2.5	2.4	2.3	2.2	2.1	2.0	2.0	1.9	1.8	1.7	1.7	1.7	1.6
8.5	.3	.7	1.4	1.9	2.3	2.5	2.6	2.6	2.5	2.4	2.3	2.2	2.2	2.1	2.0	1.9	1.9	1.8	1.8	1.7
9.0	.3	.7	1.4	2.0	2.4	2.6	2.7	2.7	2.7	2.6	2.5	2.4	2.3	2.2	2.1	2.0	2.0	1.9	1.9	1.8
9.5	.3	.7	1.4	2.0	2.4	2.7	2.9	2.9	2.8	2.7	2.6	2.5	2.4	2.3	2.2	2.1	2.1	2.0	2.0	1.9
10.0	.3	.7	1.4	2.1	2.5	2.7	3.0	3.0	2.9	2.8	2.7	2.6	2.5	2.4	2.3	2.2	2.2	2.1	2.1	2.0
10.5	.3	.7	1.5	2.1	2.5	2.8	3.1	3.1	3.0	2.9	2.8	2.7	2.6	2.5	2.4	2.3	2.3	2.2	2.2	2.1
11.0	.3	.7	1.5	2.1	2.6	2.9	3.2	3.2	3.1	3.1	3.0	2.8	2.7	2.7	2.5	2.4	2.4	2.3	2.2	2.2
11.5	.3	.7	1.5	2.1	2.6	3.0	3.3	3.3	3.3	3.2	3.1	3.0	2.9	2.8	2.6	2.6	2.5	2.4	2.3	2.3
12.0	.3	.7	1.5	2.2	2.7	3.0	3.3	3.4	3.4	3.3	3.2	3.1	3.0	2.9	2.7	2.7	2.6	2.5	2.4	2.4
12.5	.3	.7	1.5	2.2	2.7	3.1	3.4	3.5	3.5	3.4	3.3	3.2	3.1	3.0	2.9	2.8	2.7	2.6	2.5	2.5
13.0	.3	.7	1.5	2.2	2.8	3.1	3.5	3.6	3.6	3.5	3.4	3.3	3.2	3.1	3.0	2.9	2.8	2.7	2.6	2.6
13.5	.3	.7	1.5	2.2	2.8	3.2	3.6	3.7	3.7	3.6	3.5	3.4	3.3	3.2	3.1	3.0	2.9	2.8	2.7	2.7
14.0	.3	.7	1.5	2.3	2.8	3.2	3.7	3.8	3.8	3.7	3.6	3.5	3.4	3.3	3.2	3.1	3.0	2.9	2.8	2.8
14.5	.3	.7	1.5	2.3	2.9	3.3	3.8	3.9	3.9	3.9	3.8	3.6	3.5	3.4	3.3	3.2	3.1	3.0	2.9	2.9
15.0	.3	.7	1.5	2.3	2.9	3.4	3.8	4.0	4.0	4.0	3.9	3.8	3.6	3.5	3.4	3.3	3.2	3.1	3.0	3.0
15.5	.3	.7	1.5	2.3	2.9	3.4	3.9	4.1	4.1	4.1	4.0	3.9	3.8	3.6	3.5	3.4	3.3	3.2	3.1	3.1
16.0	.3	.7	1.6	2.3	3.0	3.4	4.0	4.2	4.2	4.2	4.1	4.0	3.9	3.8	3.6	3.5	3.4	3.3	3.2	3.1
16.5	.3	.7	1.6	2.4	3.0	3.5	4.1	4.3	4.3	4.3	4.2	4.1	4.0	3.9	3.7	3.6	3.5	3.4	3.3	3.2
17.0	.3	.7	1.6	2.4	3.0	3.5	4.1	4.4	4.4	4.4	4.3	4.2	4.1	4.0	3.8	3.7	3.6	3.5	3.4	3.3
17.5	.3	.7	1.6	2.4	3.1	3.6	4.2	4.5	4.5	4.5	4.4	4.3	4.2	4.1	3.9	3.8	3.7	3.6	3.5	3.4
18.0	.3	.7	1.6	2.4	3.1	3.6	4.3	4.5	4.6	4.6	4.5	4.4	4.3	4.2	4.0	3.9	3.8	3.7	3.6	3.5
18.5	.3	.7	1.6	2.4	3.1	3.7	4.3	4.6	4.7	4.7	4.6	4.5	4.4	4.3	4.1	4.0	3.9	3.8	3.7	3.6
19.0	.3	.7	1.6	2.4	3.1	3.7	4.4	4.7	4.8	4.8	4.7	4.6	4.5	4.4	4.2	4.1	4.0	3.9	3.8	3.7
19.5	.3	.7	1.6	2.4	3.2	3.7	4.4	4.8	4.9	4.9	4.8	4.7	4.6	4.5	4.3	4.2	4.1	4.0	3.9	3.8
20.0	.3	.7	1.6	2.5	3.2	3.8	4.5	4.9	5.0	5.0	4.9	4.8	4.7	4.6	4.4	4.3	4.2	4.1	4.0	3.9

and denominator cancel leaving the Δt essentially a function of (hydraulic radius)$^{4/3}$/velocity (Manning coef.)^2. It would appear from this relationship that increasing the Manning coefficient would help. Studies on the Clackamas and other Willamette tributaries indicate it does not since the increase in the Manning coefficient results in reduced velocity and increased hydraulic radius, leaving Δt estimates from Equation 105 somewhat smaller than before. Decreases in the Manning coefficient also do not cause any appreciable increase in the value of Δt. The only parameter which affected the stability problem was an increase in tributary flow rate.

In summary, experience with the WRE hydraulic model indicates that it is a good river basin model, especially for estuary modeling. Certain limitations originally present in the WRE code have been removed, such as allowing the use of a number of controlled nodes and allowing the user to mark "small tributary channels." Experience with the September low flow stability problem has identified the range of flow regimes for which the code can be successfully applied.

VERIFICATION OF WATER QUALITY MODEL

The calibration and verification phase was conducted on the Willamette River Basin between Salem and Portland, Oregon to demonstrate the efficacy of the integrated quality models. The first twelve days in September 1967, during which the lowest flows of the summer were experienced in the basin, were chosen as the quality calibration period. A twelve day calibration period was selected since this represented approximately twice the total travel time in the Willamette River from Salem to Portland. Verification was then conducted for the first week in June 1967 and the first week in August 1967. The August flows were quite similar to those occurring in September while the June flows were considerably higher. The September flow data were used for the August verification.

In general all of the quality parameter reaction constants were chosen to match the data available in September. These values were then used to predict the quality concentrations along the Willamette River for the verification periods. No attempt was made to calibrate the model on each of the major tributaries to the Willamette River for two reasons. First, measured water quality data were insufficient to allow meaningful calibration on all the tributaries except the Tualatin. In addition, many waste sources and water withdrawal and addition policies were not identified in the available data. An effort was made to match the water quality concentrations measured at the mouth of each tributary to insure that the calibration on the Willamette River would be meaningful.

It should be noted that the submodel constants chosen in this study represent values which predict the parameter concentration and the trends in concentration changes reasonably well. However, these constants are not a unique set. Further correlation between predicted and measured values, including some statistical analysis of the results, should be performed before constants applicable over a wide range of conditions are determined.

Water Quality Data

Measurements of water quality parameter concentrations in the Willamette River Basin were obtained from the Environmental Protection Agency STORET System. On the mainstem of the Willamette River from Salem to Portland the measurements consisted of approximately daily dissolved oxygen (DO) readings, weekly 5-day biochemical oxygen demand (BOD) readings and monthly ammonia (NH_3), nitrate (NO_3) and orthophosphate (PO_4) readings. Less frequent measurements of these concentrations were also taken on all of the major tributaries. The values of all of the measured data used in this report are summarized in Table 10.

BOD waste discharges for pulp mills located in Newberg (at approximately river mile 50) and at Willamette Falls (approximately river mile 26.6) were used. Discharge of treated municipal sewage from two plants at West Linn and one at Oregon City were considered. However, the BOD output of these plants was negligible compared to that of the pulp mills, hence their discharges were not identified in sufficient detail to be included in the model. The pulp mills account for the majority of the BOD discharged to the Willamette River between Portland and Salem and neglecting the other minor sources did not prevent model calibration and verification. The discharge data are shown in Table 11.

Results of Model Calibration and Verification of Biochemical Oxygen Demand (BOD). The effect of varying the deoxygenation coefficient, k_1, on the predicted values of BOD are shown in Figure 19 for the river stretch between Willamette Falls and Salem. It is apparent from this graph that a single value for the deoxygenation coefficient does not describe the BOD behavior. The values of the deoxygenation and sedimentation rate constants chosen for the calibrated model are shown in Figure 20. Settling of the BOD as the river slows its velocity and enters the slack water of the Newberg pool was accounted for in Reach 3. Although no measurements of benthic BOD demands were available, the selected sedimentation constant for this reach was considered reasonable.

TABLE 10

DATA USED FOR CALIBRATION AND VERIFICATION OF EXPLORE-I WATER QUALITY MODEL

Willamette River Data - Summer 1967

Date	R.M.	Temp	DO	BOD	NH_3	NO_3	PO_4
6/6	12.1	17.0	6.1	1.5			
	16.6	16.0	6.6	1.7			
	25.5	18.0	6.8	3.2			
	27.8	18.0	6.6	0.7			
	34.4	18.0	6.5	1.0			
	48.6	18.0	6.4	1.3			
	50.0	18.0	6.5	0.9			
	51.8	19.0	6.8	1.1			
	71.9	19.0	7.4	2.1			
	83.9	18.0	7.6	4.8			
6/20	7.0				.33	.07	.12
	34.4				.43	.05	.17
	71.9				.50	.10	.18
8/1	12.1	22.0	4.2	0.4			
	16.6	23.0	4.4	1.2			
	25.5	22.0	6.1	2.2			
	27.8	22.0	6.2	0.9			
	34.4	22.5	6.2	0.6			
	48.6	23.0	6.4	0.7			
	50.0	23.0	6.5	1.1			
	51.8	23.0	6.4	0.6			
	71.9	23.0	7.2	1.1			
	83.9	22.0	6.6	1.7			
8/15	7.0				.03	.15	.11
	34.4				.03	.31	.09
	71.9				.03	.27	.09
8/29	83.9	21.0	6.8	2.3			
8/31	12.1	21.5	4.3				
	16.6	21.5	4.6				
	25.5	21.0	6.0				
	27.8	21.0	5.7				
	34.4	21.5	6.0				
	48.6	21.0	6.9				
	50.0	21.5	6.4				
	51.8	22.0	6.4				
	71.9	21.0	6.6				

Table 10 (continued)

Date	R.M.	Temp	DO	BOD	NH_3	NO_3	PO_4
9/1	16.6	21.0	4.4				
	34.4	21.5	6.1				
	71.9	21.5	6.6				
9/4	16.6	22.0	4.3				
	34.4	22.5	6.2				
	71.9	21.5	7.0				
9/5	12.1	21.0	4.2	1.0			
	16.6	21.0	4.6	1.1			
	25.5	21.0	8.4	1.2			
	27.8	21.0	6.1	0.8			
	34.4	21.0	6.4	1.1			
	48.6	21.0	6.9	1.1			
	50.0	21.0	6.7	1.1			
	51.8	22.0	6.6	0.9			
	71.9	21.0	7.2	2.0			
	83.9	21.0	7.3	1.8			
9/6	16.6	21.5	7.2				
	34.4	21.0	6.4				
	71.9	20.5	7.1				
9/7	16.6	21.0	6.4				
	34.4	21.0	6.8				
	71.9	20.0	7.0				
9/8	16.6	21.0	5.5				
	34.4	21.0	6.9				
	71.9	20.0	6.9				
9/9	16.6	21.0	7.3				
	34.4	21.0	6.7				
	71.9	20.0	7.4				
9/10	16.6	19.5	5.8				
	34.4	19.5	6.6				
	71.9	18.5	7.1				
9/11	16.6	21.0	6.8				
	34.4	19.5	8.3				
	71.9	18.5	7.2				
9/12	12.1	19.5	6.1	0.9			
	16.6	19.5	6.9	1.4			
	25.5	19.5	8.1	1.8			
	27.8	19.0	6.3	0.8			

Table 10 (continued)

Date	R.M.	Temp	DO	BOD	NH_3	NO_3	PO_4
	34.4	19.0	6.5	0.8			
	48.6	18.0	7.0	1.1			
	50.0	18.0	7.2	1.4			
	51.8	18.5	7.0	1.0			
	71.9	18.0	7.5	1.8			
	83.9	17.5	7.2	2.0			
9/19	7.0				.31	.32	.02
	34.4				.28	.43	.05
	71.9				.37	.36	.06
Tualatin River Data - Summer 1967							
6/6	0.2	19.0	10.1	4.4	.43	.09	.42
	5.5	20.0	16.1	7.6			
	8.5	18.0	9.6	3.0			
	11.5	18.0	9.1	2.6			
	16.0	18.0	7.0	1.2	.44	.05	.45
	27.1	19.0	5.8	0.9			
	33.5	18.0	6.0	1.3			
	38.7	18.0	6.3	1.0			
	45.0	18.0	7.6	0.8	.610	.10	.25
8/1	5.5	28.0	12.9	3.2	.36	.01	.30
9/5	0.2	20.0	7.2	5.0	.58	.02	.44
	5.5	19.0	0.2	15.0	1.6	.02	.48
	8.5	19.0	6.4	6.0	4.6	.17	6.5
	11.5	21.0	8.5	3.3	.50	.04	.21
	16.0	21.0	8.8	2.2	.36	.06	.19
	27.1	21.0	2.8	2.8	.41	.01	.24
	33.5	20.0	4.2	2.7	.55	.21	4.1
	38.7	20.0	7.4	5.3	.39	.04	.34
	45.0	19.0	5.2	2.1	.47	.05	.23
Clackamas River Data - Summer 1967							
8/1	0.2	21.0	9.5	0.5	.3	.01	.16
	8.1	21.0	9.3	0.4	.23	.01	.13
Molalla River Data - Summer 1967							
8/1	3.5	25.0	9.2	0.9	.37	.01	.14
Pudding River Data - Summer 1967							
8/1	5.3	26.0	15.6	4.1	.35	.01	.41
Yamhill River Data - Summer 1967							
8/2	5.0	23.0	9.9	3.4	.18	.01	.23

TABLE 11

DISCHARGE DATA FOR EXPLORE-I VERIFICATION ON WILLAMETTE RIVER BASIN

Description	Date	BOD, lbs/day
Pulp Mill, Newberg River Mile 50.0	6-1	35,247
	6-9	8,029*
	7-28	13,843
	8-4	9,629
	9-1	12,160
	9-8	14,600
	9-15	14,700
Pulp Mill, Oregon City River Mile 26.6	6-3	48,273
	6-9	41,220
	7-28	41,460
	8-4	40,840
	9-1	29,920
	9-8	22,660
	9-15	28,170
Pulp Mill, West Linn River Mile 26.6	6-1	101,463
	6-9	64,385
	7-28	19,703
	8-4	20,588
	9-1	19,504
	9-8	17,966
	9-15	18,887
Oaklodge STP	6-7	380
	8-3	312
	9-6	406
	9-8	122
	9-18	156
West Linn STP	6-5	25
	8-3	23
	9-4	19.5
	9-7	14.2
	9-11	26.4
Oregon City STP	6-5	133
	8-8	1,586
	9-4	566
	9-8	448
	9-12	378

*Denoted as "POOR DATA" in records

Table 11 (continued)

Description	Date	BOD,lbs/day
Milwaukie STP	6-5	125
	8-3	130
	9-5	67
	9-8	105
	9-12	100

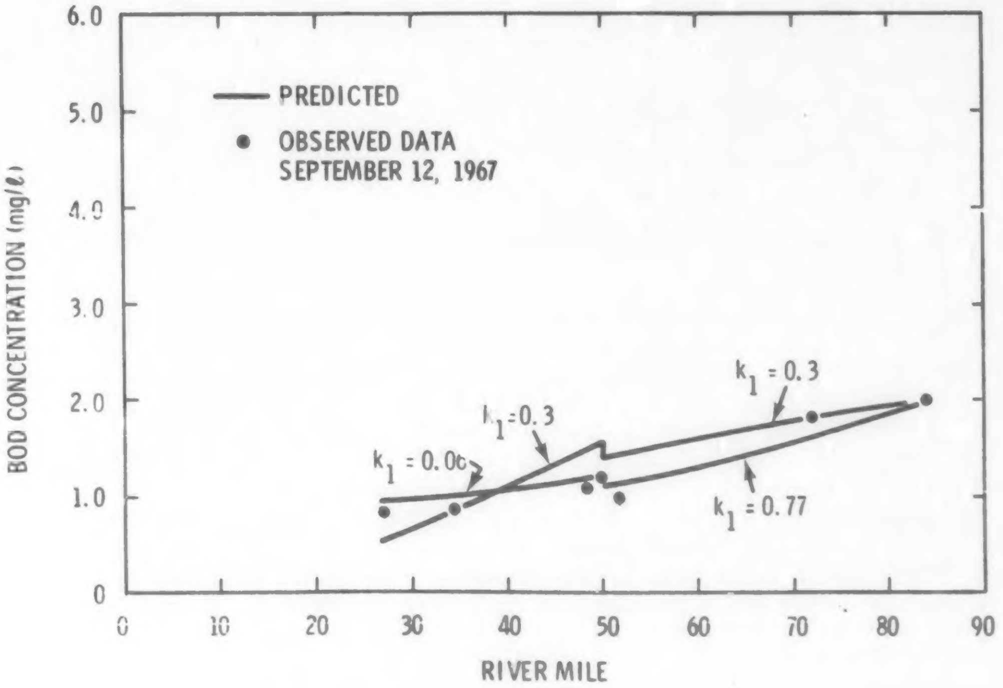

FIGURE 19. EFFECT OF DEOXYGENATION COEFFICENT, k_1, ON PREDICTED BOD VALUES

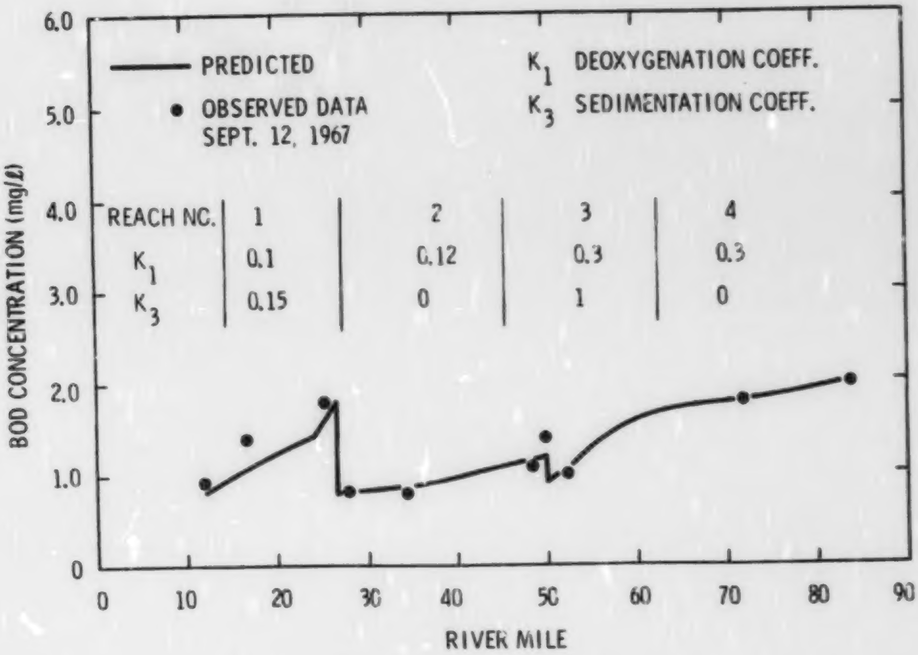

FIGURE 20. CALIBRATED BOD MODEL

Verification of the reaction constants are shown in Figure 21 for the August 1967 data and in Figure 22 for the June 1967 data. For the August period, the agreement between predicted and measured data is quite good. For the June data, the agreement is poor if measured value of 4.8 mg/ℓ is used as the initial condition at the upstream boundary condition at Salem (solid line in Figure 22). Another calculation was performed by arbitrarily assigning the initial condition a value of 2.5 mg/ℓ (dotted line in Figure 22). In this case the BOD data are predicted more accurately. There are two possible reasons why the high value at Salem and much lower values around river miles 72 and 50 are not matched by the calibrated model. It could be that the data point is not representative of the average BOD in the river as a result of experimental error or sampling of local concentrations. Other physical phenomena, such as large scale settling of BOD directly below Salem, might not be represented properly in the model.

The variation of BOD with time for the 12 day September calibration period at three particular locations along the river at river miles 71.9, 34.4, and 16.6 are shown in Figures 23, 24, and 25 respectively. The graphs show reasonable correlation at each location.

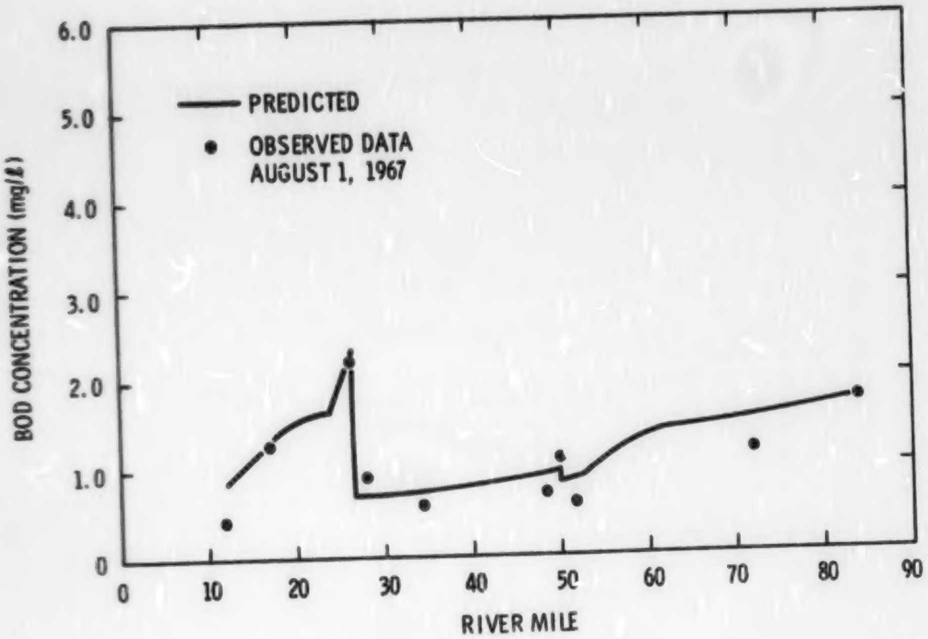

FIGURE 21. VERIFICATION OF BOD MODEL WITH AUGUST 1967 DATA

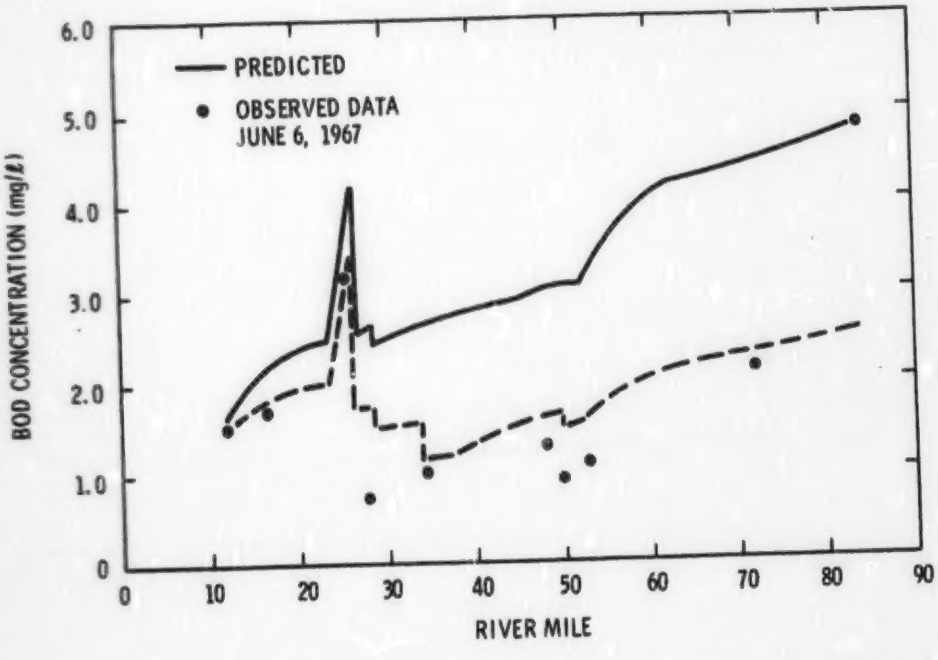

FIGURE 22. VERIFICATION OF BOD MODEL WITH JUNE 1967 DATA

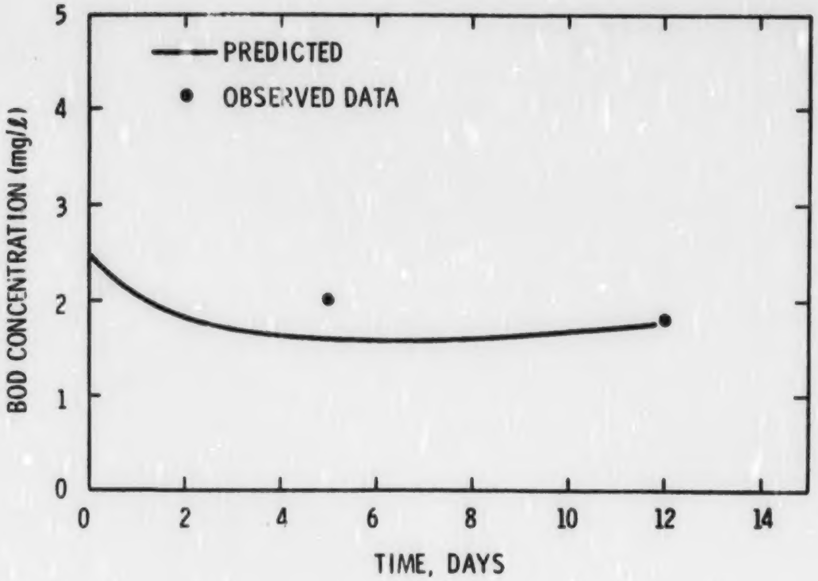

FIGURE 23. PREDICTED AND OBSERVED DATA FOR BOD AT RIVER MILE 71.9 FOR PERIOD 1-12 SEPT. 1967

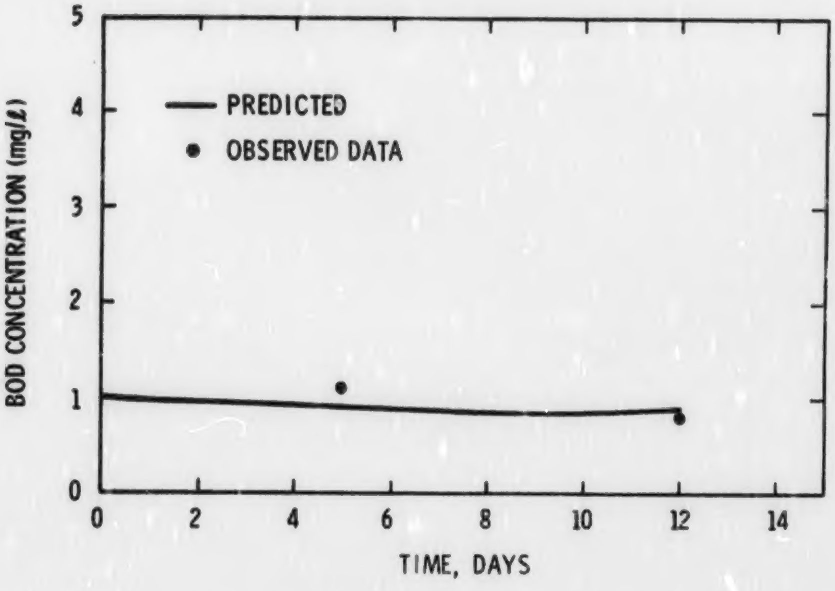

FIGURE 24. PREDICTED AND OBSERVED DATA FOR BOD AT RIVER MILE 34.4 FOR PERIOD 1-12 SEPT. 1967

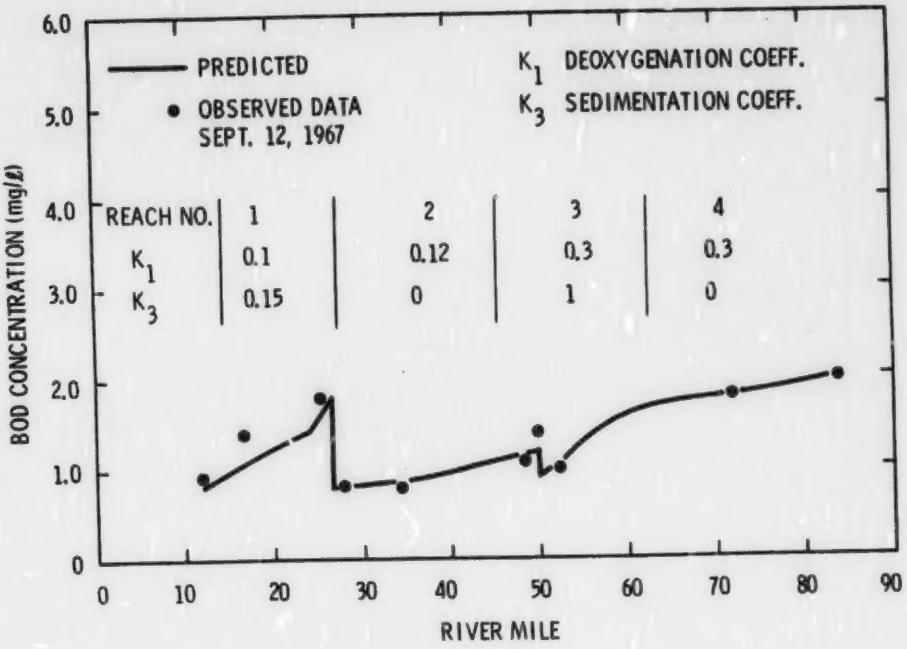

FIGURE 25. PREDICTED AND OBSERVED DATA FOR BOD AT RIVER MILE 16.6 FOR PERIOD 1-12 SEPT. 1967

Dissolved Oxygen (DO). The dissolved oxygen levels in the Willamette are affected by many phenomena. In this study three effects were considered:

- 5-day BOD
- ammonia-nitrate oxidation taken from nitrogen data
- reaeration

Given the 5-day BOD and nitrogenous BOD loadings for September 1-12, the effect of the reaeration coefficient, k_2, on the DO level between Salem and Willamette Falls is shown in Figure 26. In general the reaeration predictions of Churchill and of Thackston and Krenkel are high all along this stretch of river. A good correlation was found using Equation 29.

$$k_2 = 9.24 \frac{\nu^{0.8}}{h^{1.67}} \qquad (29)$$

The DO profile for the calibrated stretch of river is shown in Figure 27. The measured DO concentration below Willamette

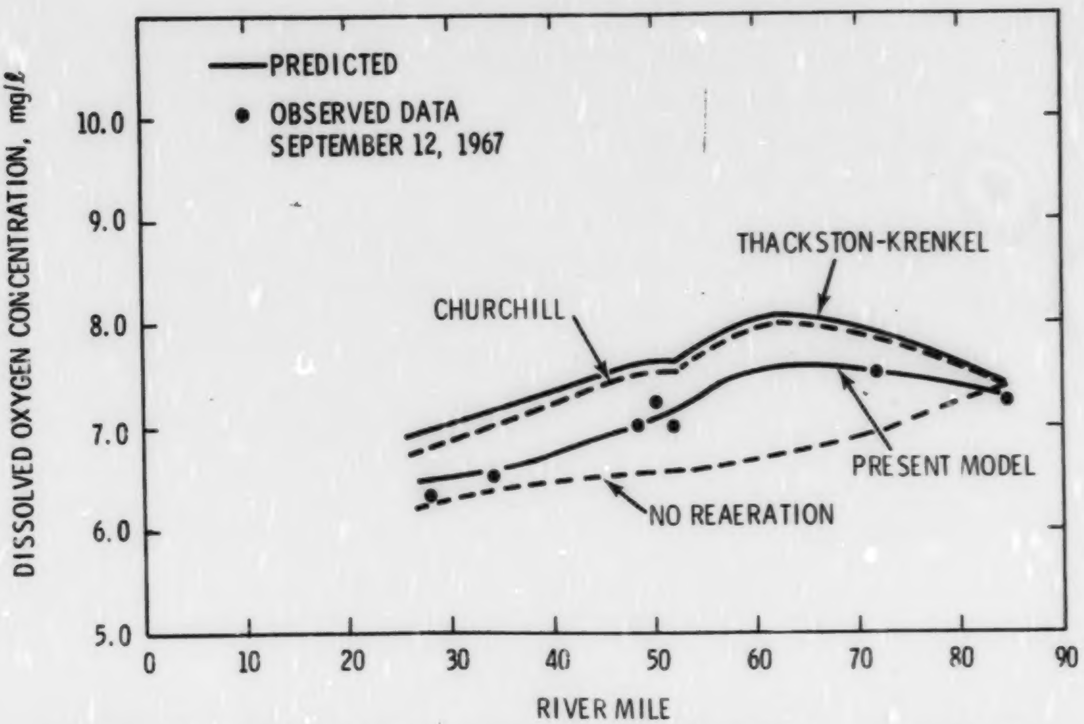

FIGURE 26. EFFECT OF REAERATION COEFFICIENT k_2 ON PREDICTED DISSOLVED OXYGEN LEVELS

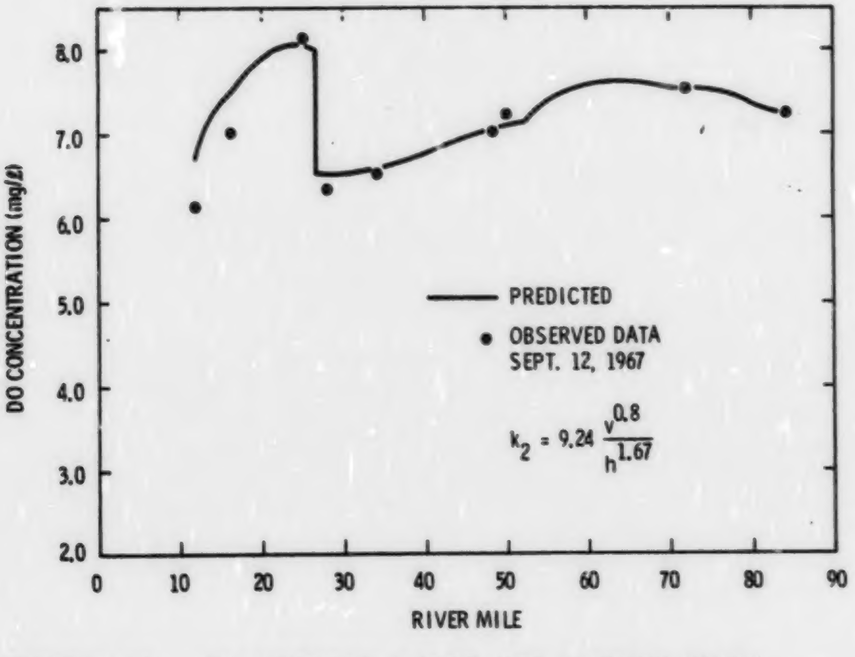

FIGURE 27. CALIBRATED DISSOLVED OXYGEN MODEL

Falls required the specification of DO at about 88 percent of the saturation value to account for the reaeration present in the regulated flow of the water over Willamette Falls. The DO levels predicted in the estuary section are slightly higher than those measured. The small reaeration coefficient in the estuary is a result of the low velocities and relatively great depths. Hence, this discrepancy is most likely due to DO utilization which has not been accounted for rather than to improper reaeration correlation.

The DO profiles predicted for the August and June data are shown in Figures 28 and 29 respectively. In both cases the DO levels at Willamette Falls were calculated by the code and not specified as in the calibration calculations. The prediction is quite good except in the estuary, where it is again high.

The June predictions deviate considerably from the data below river mile 34.4. One reason for this is the very high DO level used in the Pudding River (in excess of 15 mg/ℓ). This high DO level was measured in August when the flow of the Pudding was considerably less than in June. If a saturated value for DO (about 9-10 mg/ℓ) were assumed for the Pudding, the large increase in DO at river mile 34.4 would not be present and the predicted values would be very close to the observed data.

The variations with time for the 12-day September calibration period at river miles 71.9, 34.4 and 16.6 are shown in Figures 30, 31, and 32. Good correlation is apparent except for the first part of the time period at river mile 16.6 (Figure 31). Here the large difference in measured DO levels between the 5th and 6th indicates some drastic change in discharge not simulated in the calibration.

Nitrogen. The calibrated results of the nitrogen model are shown in Figure 33. Because of the lack of information on nitrogen sources and nitrogen concentrations in the tributaries for the period of calibration, it was felt that a more detailed calibration was not justified. Examination of the calibration data indicates that the oxidation of ammonia to nitrate is properly accounted for in the model. The August and June verification periods are shown in Figures 34 and 35 respectively. The agreement for the August period is very good, but the low ammonia concentration precludes any real dynamic simulation. For the June period, the model does not account for the nitrate decrease between river mile 72 and 35. The calculated ammonia levels also dip considerably at river mile 24 due to dilution by the Clackamas River. The

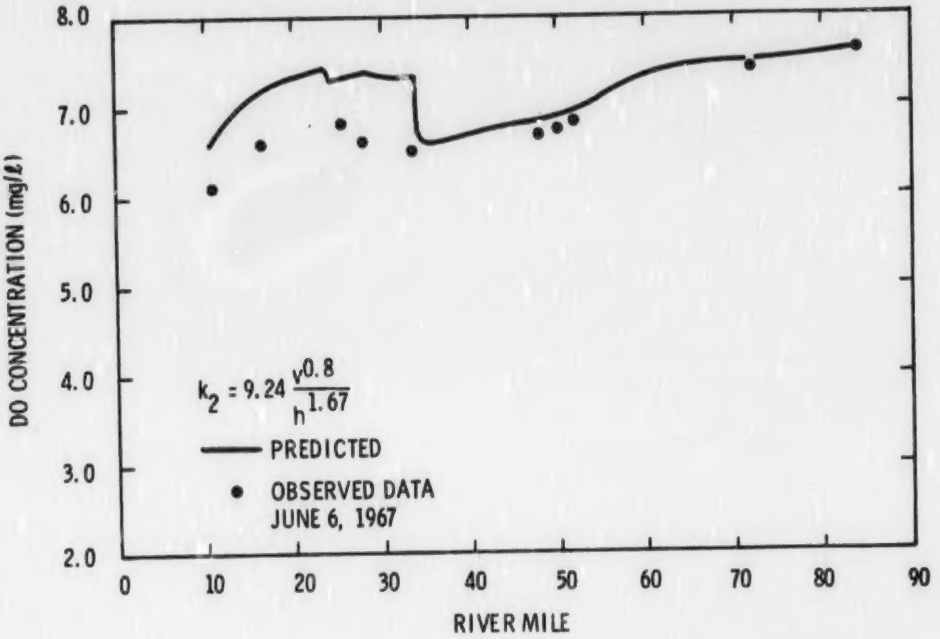

FIGURE 28. VERIFICATION OF DISSOLVED OXYGEN MODEL WITH AUGUST 1967 DATA

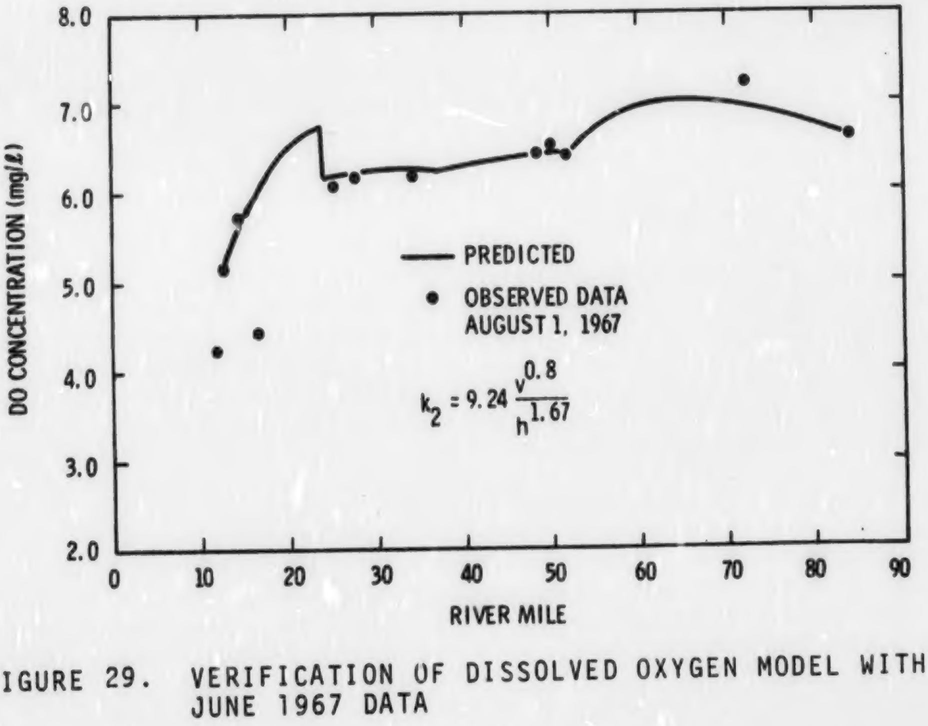

FIGURE 29. VERIFICATION OF DISSOLVED OXYGEN MODEL WITH JUNE 1967 DATA

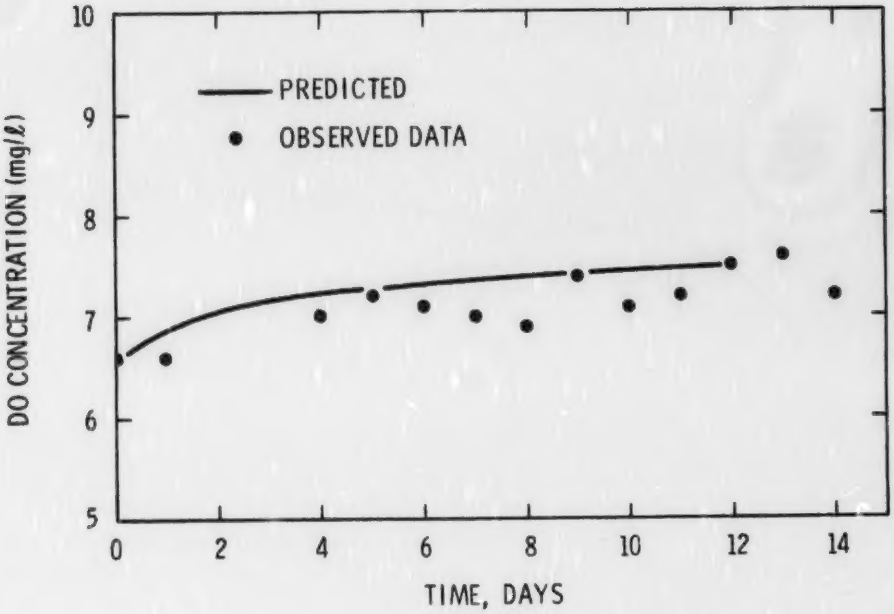

FIGURE 30. PREDICTED AND OBSERVED DATA FOR DISSOLVED OXYGEN AT RIVER MILE 71.9 FOR PERIOD 1-12 SEPT. 1967

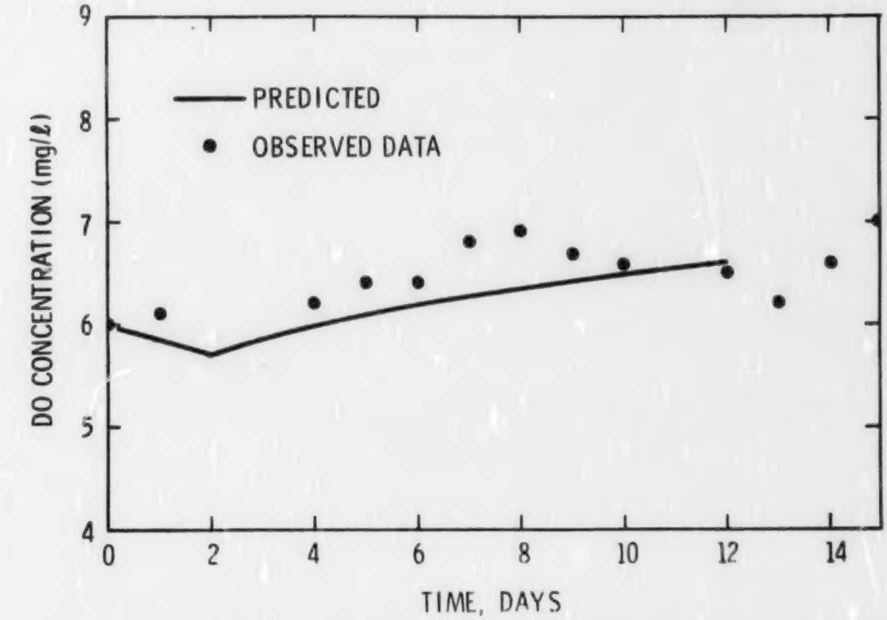

FIGURE 31. PREDICTED AND OBSERVED DATA FOR DISSOLVED OXYGEN AT RIVER MILE 34.4 FOR PERIOD 1-12 SEPT. 1967

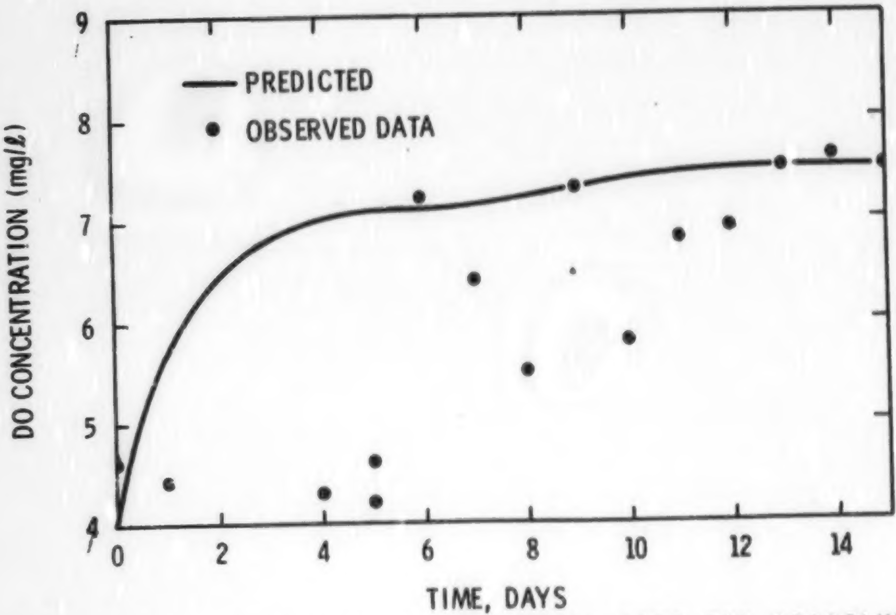

FIGURE 32. PREDICTED AND OBSERVED DATA FOR DISSOLVED OXYGEN AT RIVER MILE 16.6 FOR PERIOD 1-12 SEPT. 1967

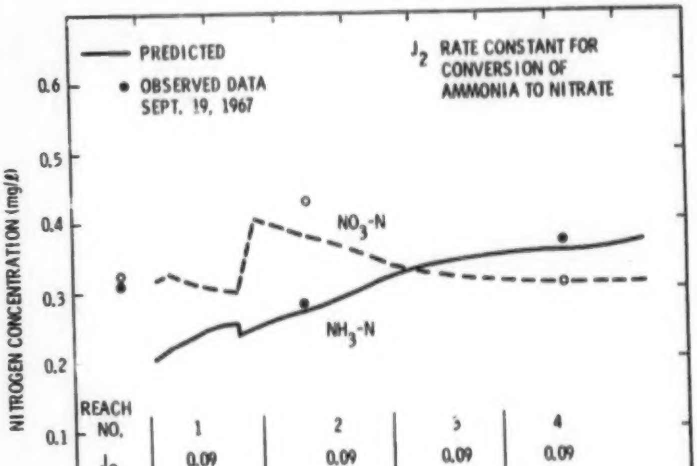

FIGURE 33. CALIBRATED NITROGEN MODEL

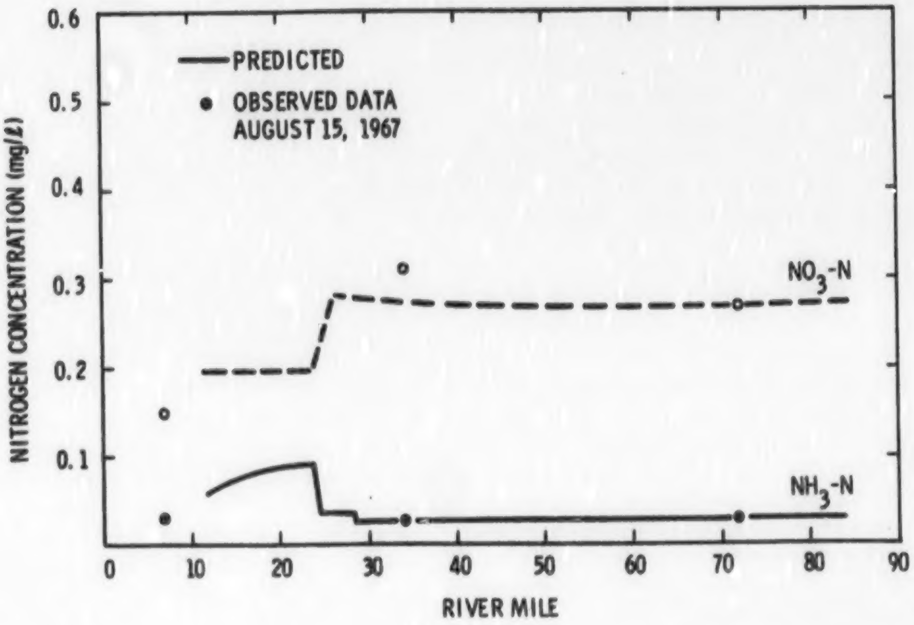

FIGURE 34. VERIFICATION OF NITROGEN MODEL WITH AUGUST 1967 DATA

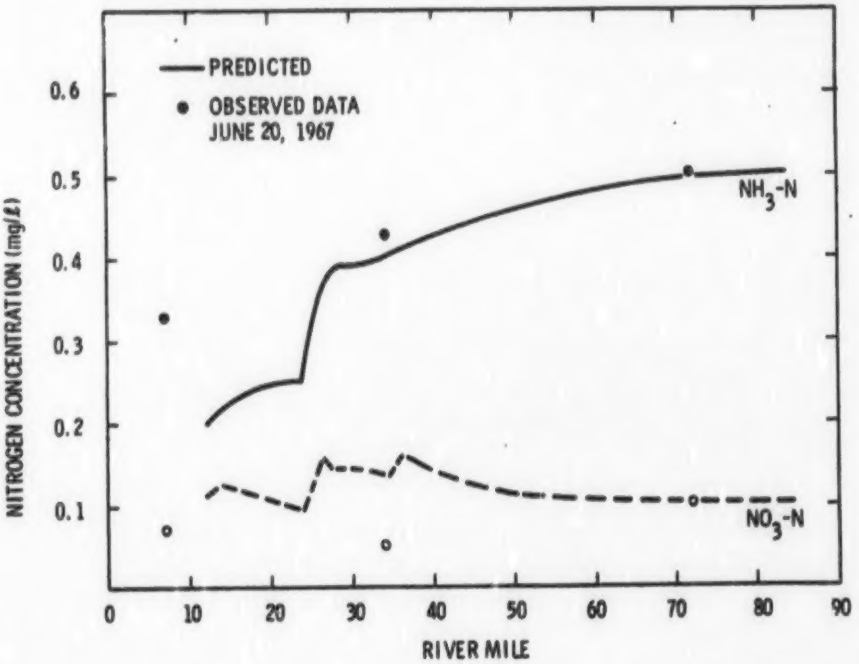

FIGURE 35. VERIFICATION OF NITROGEN MODEL WITH JUNE 1967 DATA

ammonia mass in the Clackamas for the June verification period was assumed to be that measured in August. Since the June flows were considerably greater than the August flows, a very low ammonia concentration was obtained in the Clackamas River in the June calculations. There are many plausible reasons for the variation in ammonia concentrations; however, data were not available to determine the exact cause.

Phosphorus. The calibrated model of orthophosphate is shown in Figure 36. As was the case in modeling nitrogen, a lack of information on phosphorus sources and concentrations in the tributaries precluded a more detailed calibration. The August and June verifications are shown in Figures 37 and 38. The August data indicate that, if the tributary concentrations are approximately correct, the decay constant of 0.09 is too high and the treatment of phosphorus as a conservative substance may result in closer agreement. The predictions during the June verification are considerably better; however, once again the tributary concentrations are not well known for this time period.

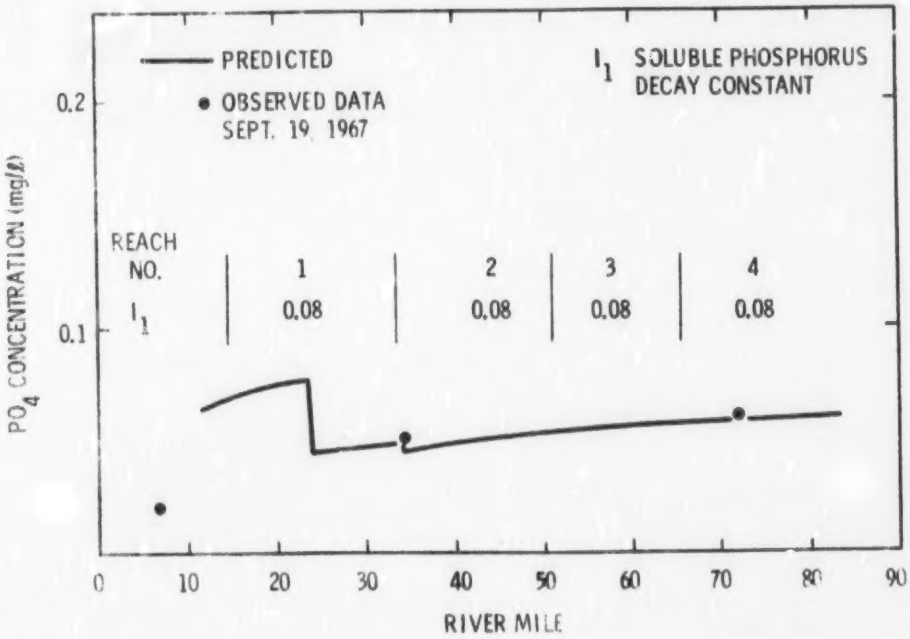

FIGURE 36. CALIBRATION OF PHOSPHORUS MODEL

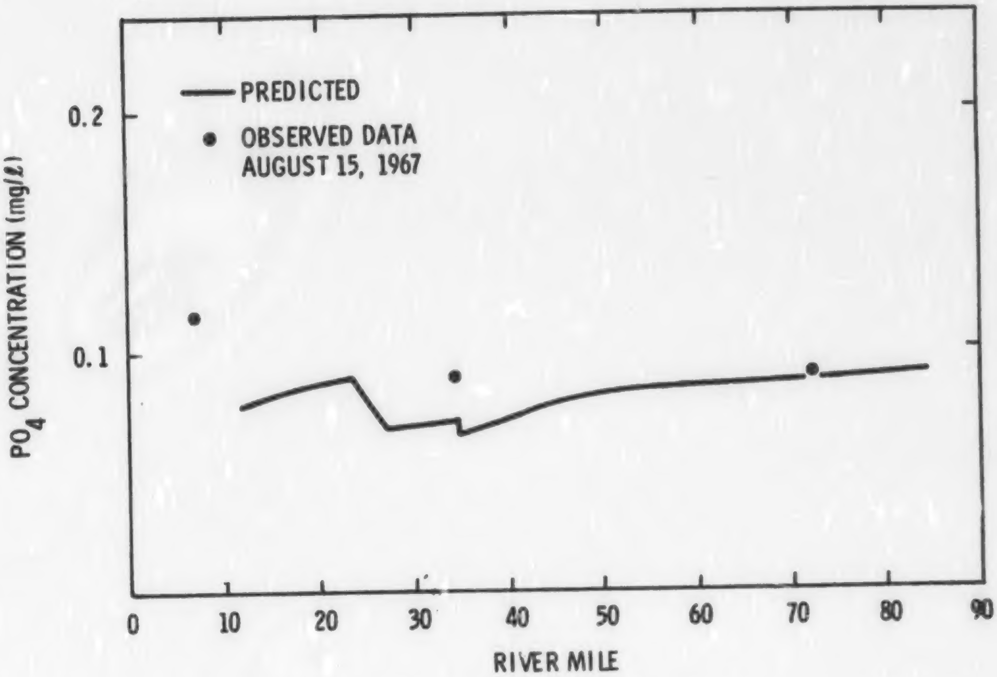

FIBURE 37. VERIFICATION OF PHOSPHORUS MODEL WITH AUGUST 1967 DATA

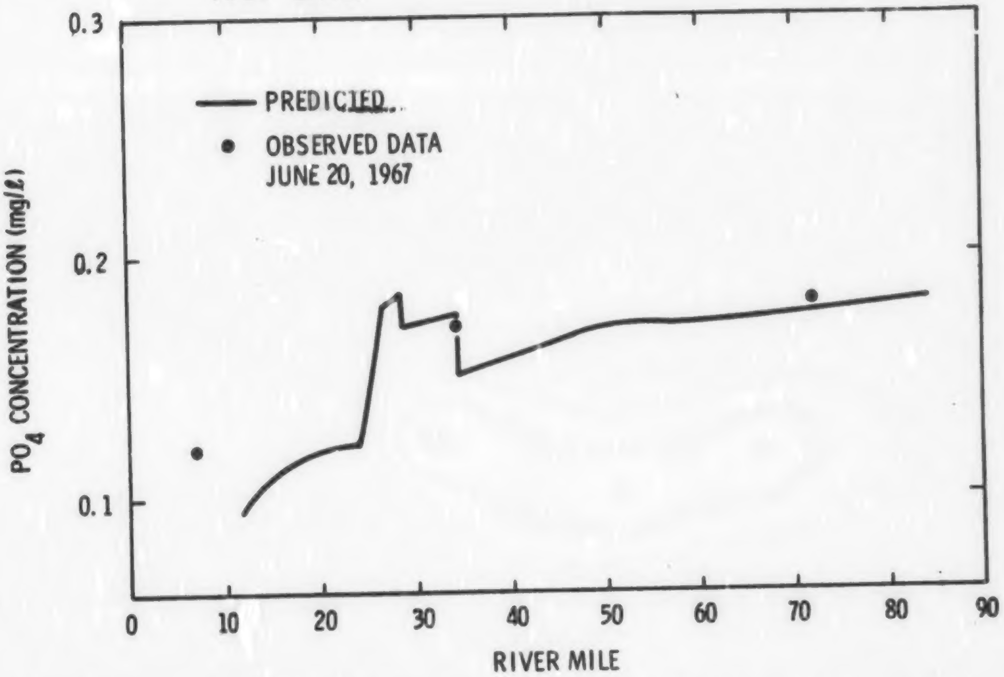

FIGURE 38. VERIFICATION OF PHOSPHORUS MODEL WITH JUNE 1967 DATA

SECTION VIII

MODEL VERIFICATION ON DETROIT RESERVOIR

Detroit Reservoir, shown in Figures 39 and 40, was selected for calibration and verification of the overall reservoir model. This choice was based on the general availability of meteorologic, hydraulic, hydrologic, and quality data. Although Detroit Reservoir does not possess any significant quality dynamics or eutrophication, extensive measurements of dissolved oxygen, nutrient materials, and temperatures have been compiled and documented[24] by the Corps of Engineers. For other potential reservoir sites in the Willamette River Basin where water quality problems do exist, adequate data for calibration and verification of the reservoir model were not available.

PROBLEMS ENCOUNTERED IN CALIBRATION

Numerous difficulties were encountered in the calibration of the thermal-hydraulic component of the model. Although initial functional tests appeared to be valid, the multisegment simulations on Detroit Reservoir were unsuccessful because the computer model became inoperative. Eight-segment and four-segment simulations were attempted but the program consistently terminated during simulation. A single segment run was also attempted but meaningful results were not obtained.

During concentrated efforts to debug the original program coding, several errors were detected and corrected. Typical coding errors were:

1. multiple definitions of variable names;
2. omission of variables from common blocks;
3. improper programming of the interpolation algorithm; and
4. coding logic faults.

Although the detected coding errors were corrected, the overall workability of the code was not improved. A detailed parametric and sensitivity analysis was conducted to establish the "unique set" of parameters: (1) diffusivities, (2) maximum and minimum temperature gradients, (3) stabilities, (4) time steps, (5) element sizes, and (6) initial time rates of temperature changes. These efforts, using 1966 data, for the most part failed to provide reasonable results in the single segment stimulation of Detroit Reservoir. Other

Preceding page blank

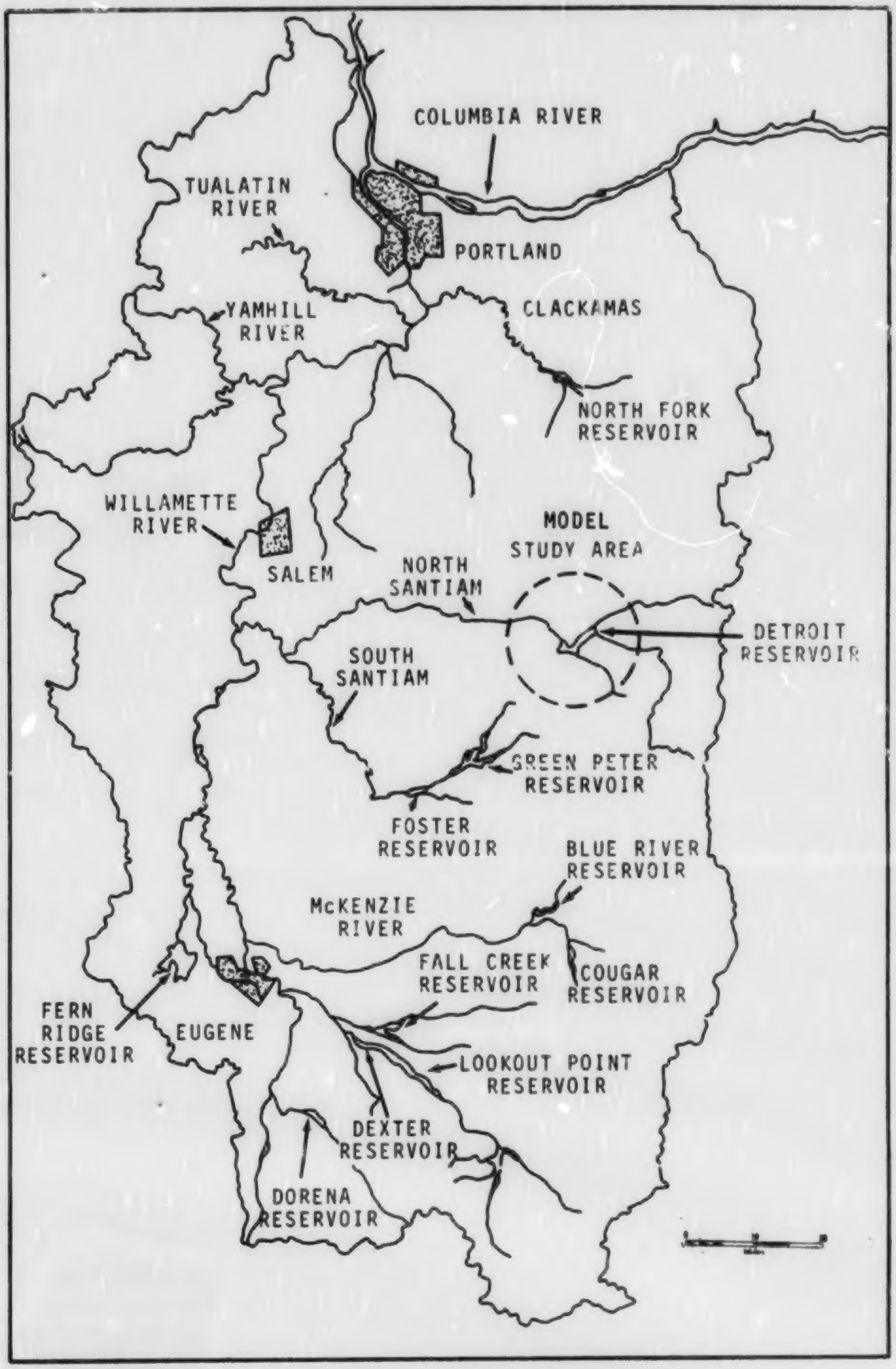
COLUMBIA RIVER
TUALATIN RIVER
PORTLAND
CLACKAMAS
YAMHILL RIVER
NORTH FORK RESERVOIR
WILLAMETTE RIVER
SALEM
MODEL STUDY AREA
NORTH SANTIAM
DETROIT RESERVOIR
SOUTH SANTIAM
GREEN PETER RESERVOIR
FOSTER RESERVOIR
BLUE RIVER RESERVOIR
McKENZIE RIVER
FALL CREEK RESERVOIR
COUGAR RESERVOIR
FERN RIDGE RESERVOIR
EUGENE
LOOKOUT POINT RESERVOIR
DEXTER RESERVOIR
DORENA RESERVOIR

FIGURE 39. DETROIT RESERVOIR: MODEL STUDY AREA

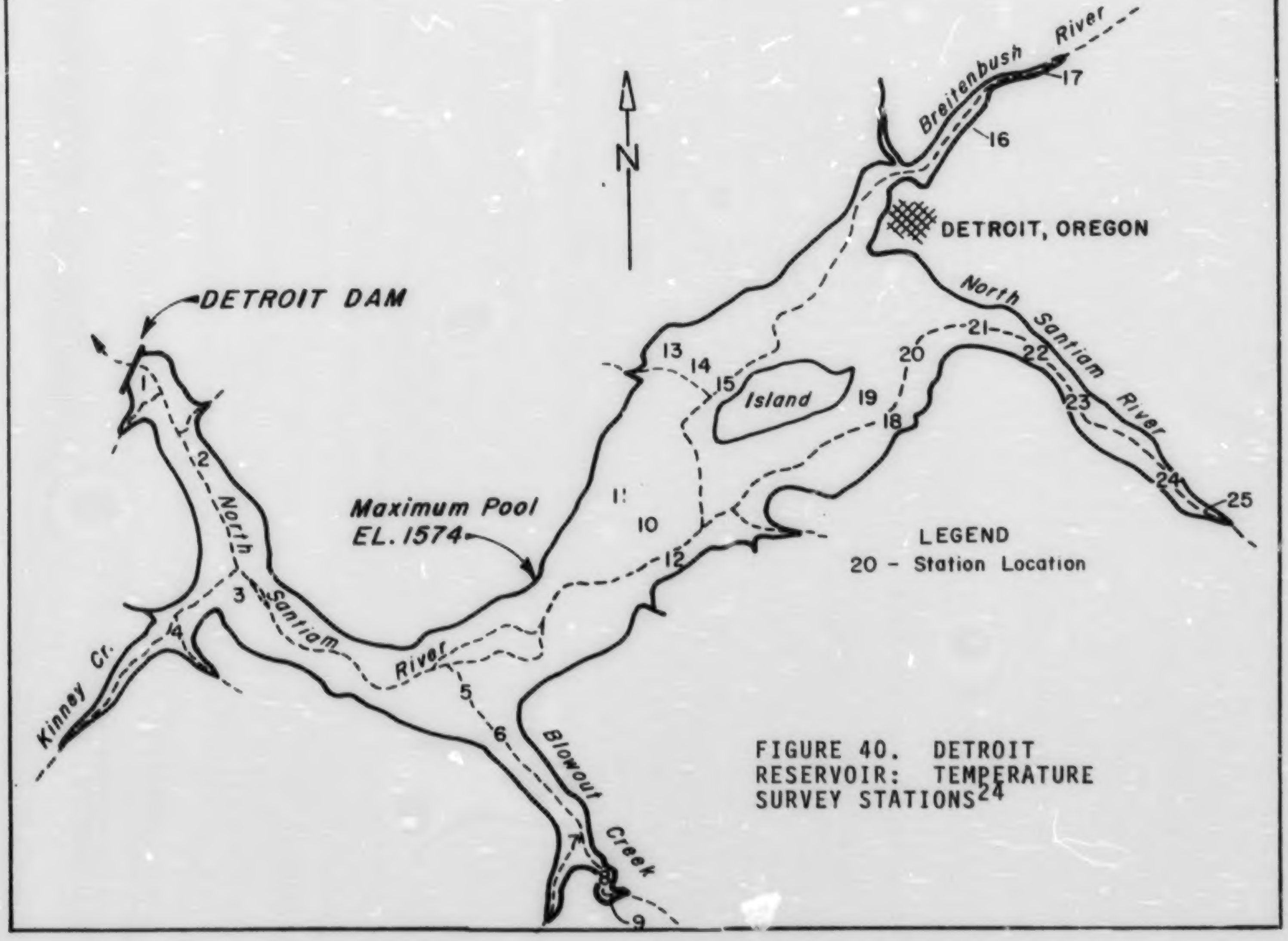
DETROIT DAM
Maximum Pool
EL. 1574
N
Breitenbush River
DETROIT, OREGON
North Santiam River
Island
Kinney Cr.
Blowout Creek
1
2
3
4
5
6
7
8
9
10
11
12
13
14
15
16
17
18
19
20
21
22
23
24
25
LEGEND
20 - Station Location

FIGURE 40. DETROIT RESERVOIR: TEMPERATURE SURVEY STATIONS[24]

efforts to resolve the difficulties consisted of making term by term comparisons between the coded equations and the documented model formulation[7,8]. Final debugging runs eventually identified the source of difficulty to be the flow distribution subroutine, SUBH. It became apparent that the program logic for vertical distribution of flows had been designed to produce "forced" results which would create the effect of tilted isotherms. However, the scheme worked only when the original (initial) temperature profile was inclined. Test runs with uniform (i.e., fully mixed) initial conditions consistently produced spurious results in the distribution of flows and thus created an improper water balance including flows upstream. The subprogram SUBH has been modified and reprogrammed to be consistent with documented theory[12]. Test runs with the corrected version have been satisfactory.

Other investigators[25,26,27,28] who have attempted to apply the original EPA version of WRE reservoir models have reported similar difficulties and program coding errors. Larry Rosener,[29] program co-author of the WRE model, has indicated that the application of the multi-segment model often requires "quite a bit of subjective use," and has further suggested that the code is not applicable to Detroit Reservoir because the temperature profile "lacks inclination," i.e., has no tilted isotherms. Recent comparative studies at Vanderbilt University indicated problems with the EPA version of the WRE reservoir code; program coding errors similar to those detected in this work were reported. Numerous difficulties have led investigators at The Bureau of Reclamation in Colorado to abandon the EPA version in favor of the latest WRE single segment reservoir program. This single revised segment version has apparently been successfully applied to Detroit Reservoir by the Corps of Engineers.

The concentrated effort required to debug the WRE Deep Reservoir Temperature Model severely penalized full development of the quality component of the reservoir model. Although the quality submodel has been formulated and programmed, verification of the model was not completed.

PROGRAM TESTING

Functional tests of the quality submodel have assured its workability. Simple reservoir geometries with steady flow and constant temperature were studied. A simple test simulation was conducted on Detroit Reservoir using hypothetical flow, meteorologic, temperature quality data; initial and upstream inflow conditions for this simulation are summarized in Figures 41 and 42. A listing of the specific card input deck prepared for this test is presented in the User's Manual. Sample results of a 30 day simulation are summarized in Figures 43 through 48. All simulation runs conducted in this trial phase were successful.

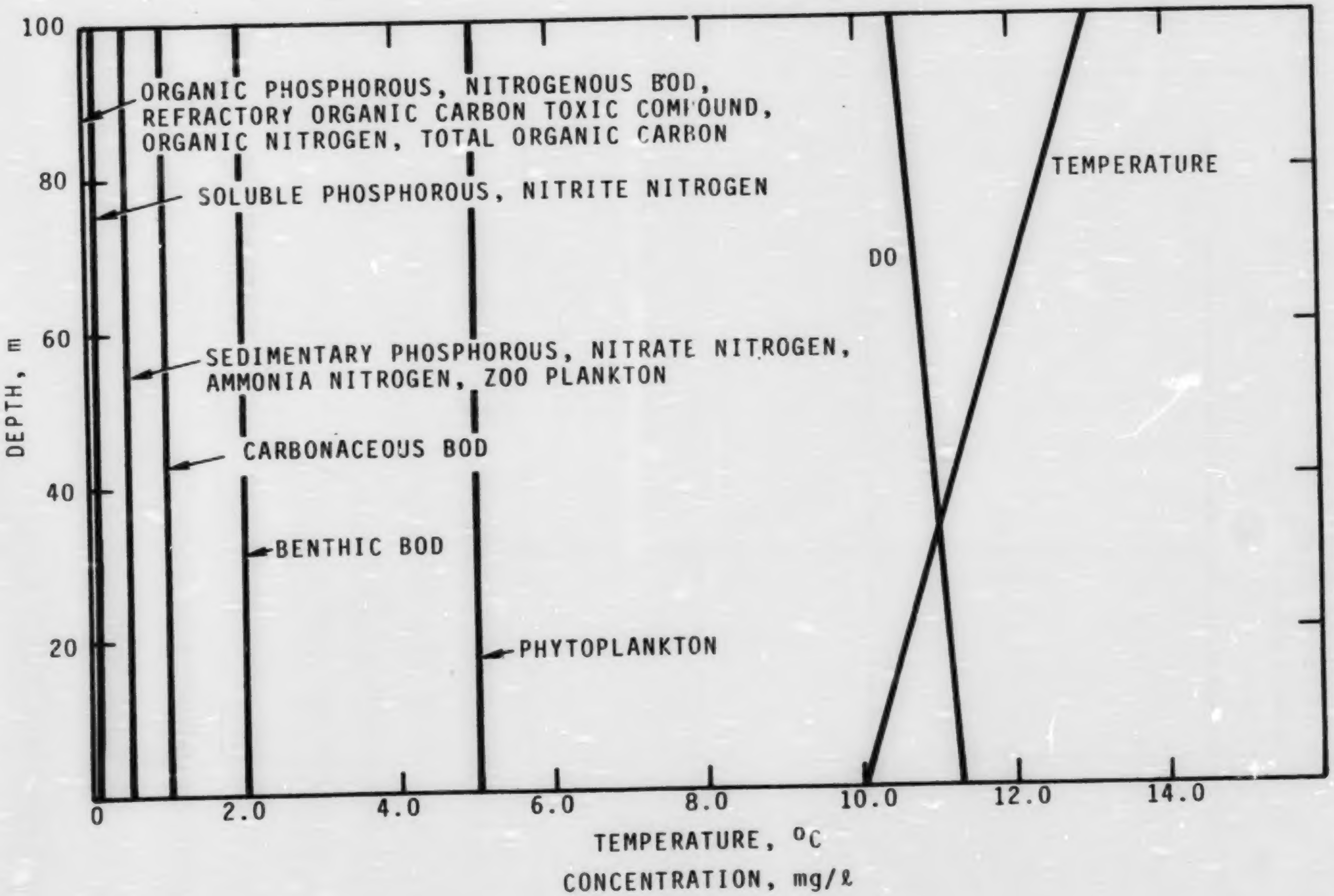

FIGURE 41. INITIAL CONDITIONS

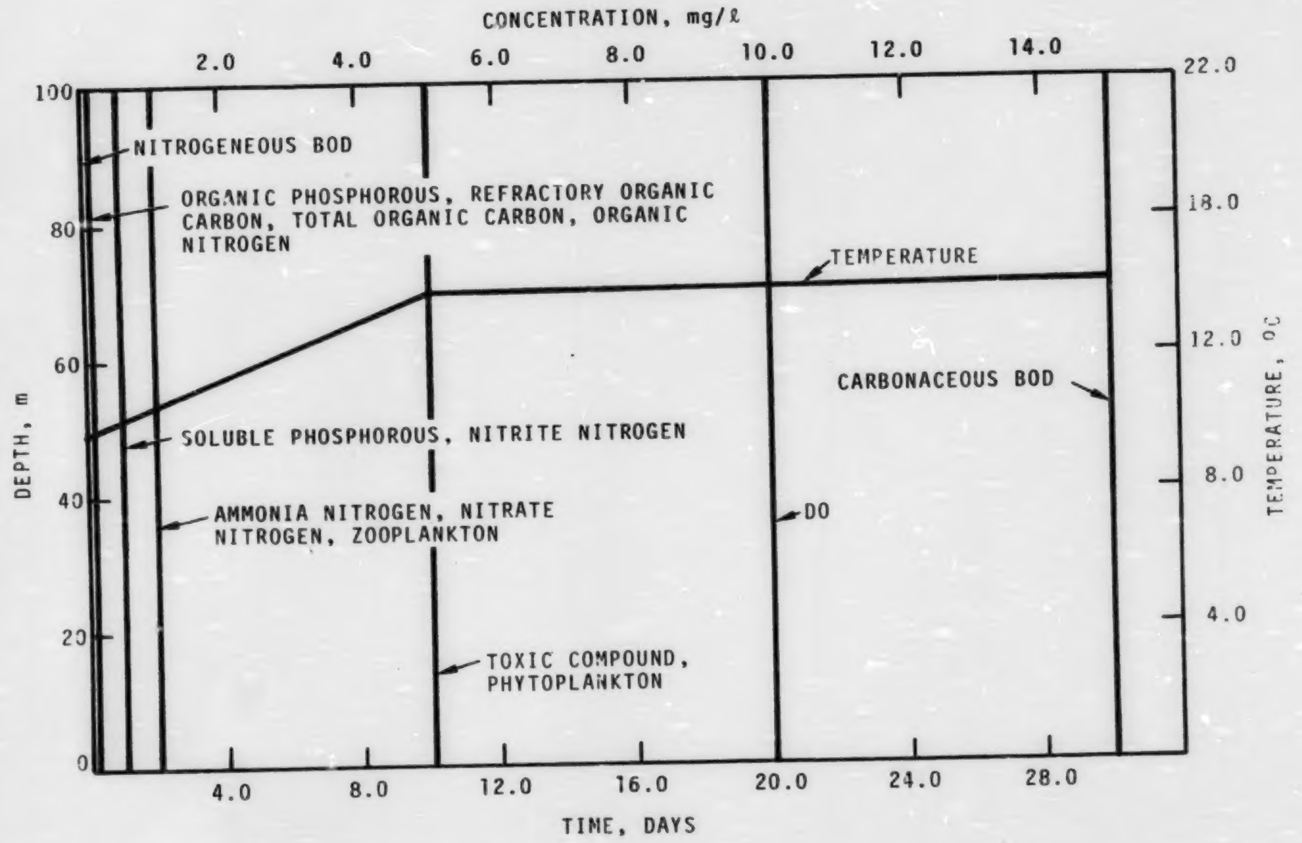

FIGURE 42. UPSTREAM INFLOW (BOUNDARY CONDITIONS)

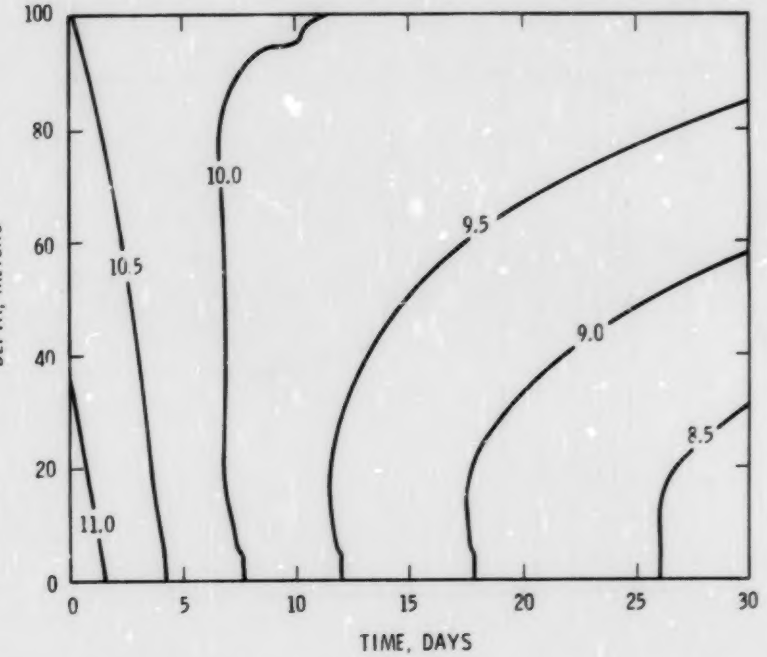

FIGURE 43. RESERVOIR QUALITY SIMULATION DISSOLVED OXYGEN (MG/L)

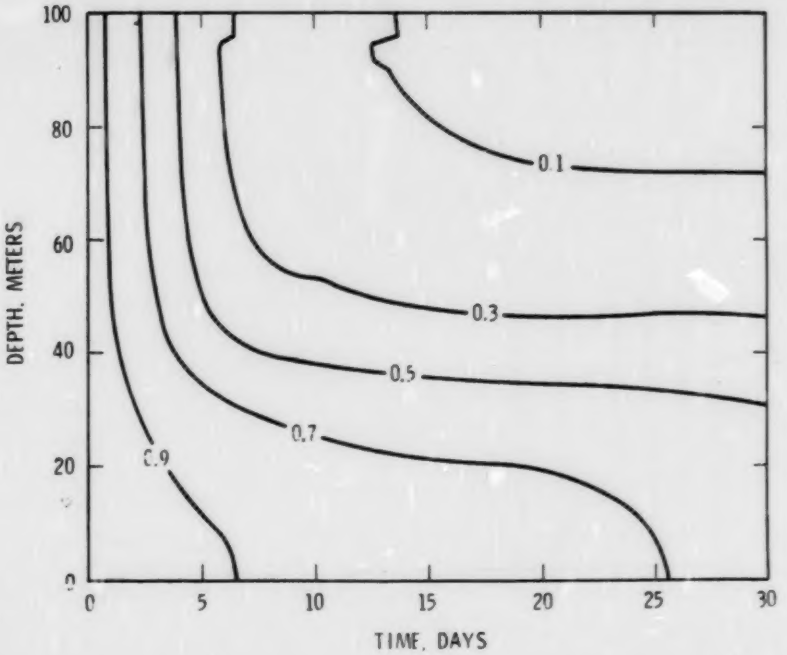

FIGURE 44. RESERVOIR QUALITY SIMULATION CARBONACEOUS BOD (MG/L)

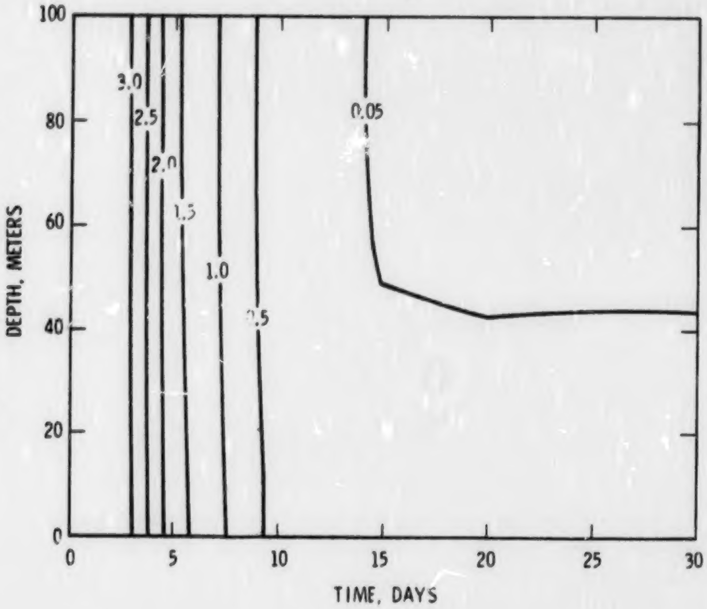

FIGURE 45. RESERVOIR QUALITY SIMULATION PHYTOPLANKTON (MG/L)

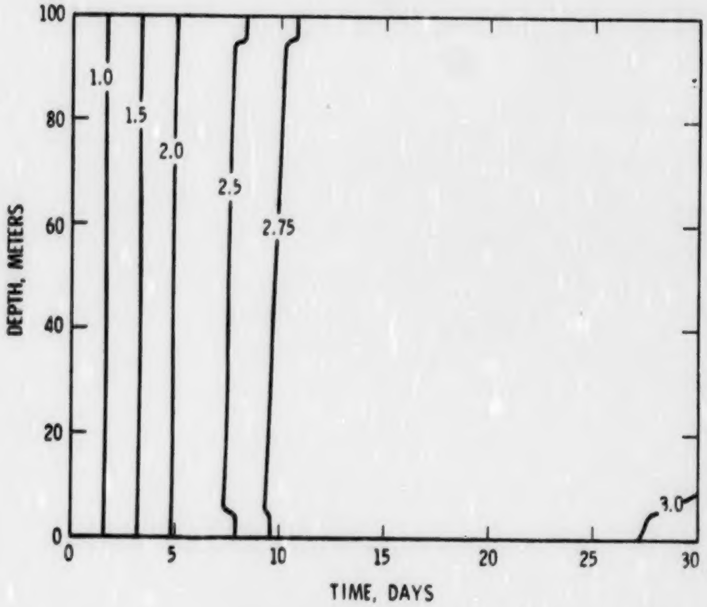

FIGURE 46. RESERVOIR QUALITY SIMULATION ZOOPLANKTON (MG/L)

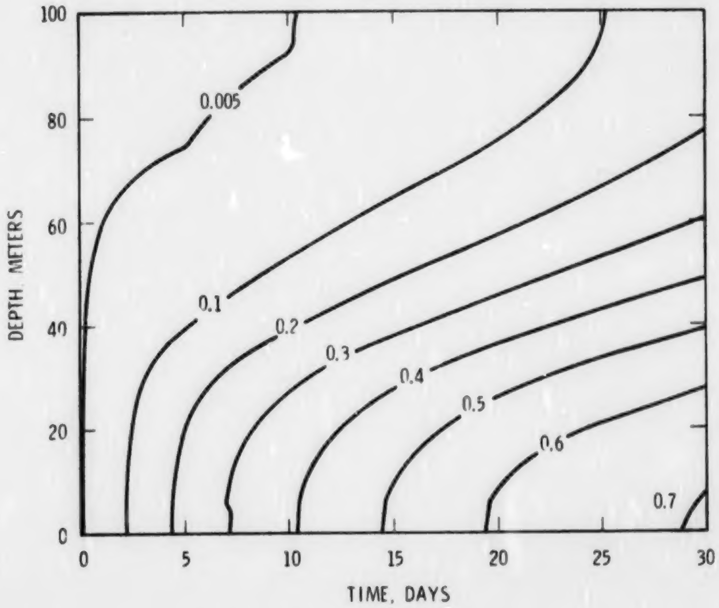

FIGURE 47. RESERVOIR QUALITY SIMULATION TOXIC COMPOUND (MG/L)

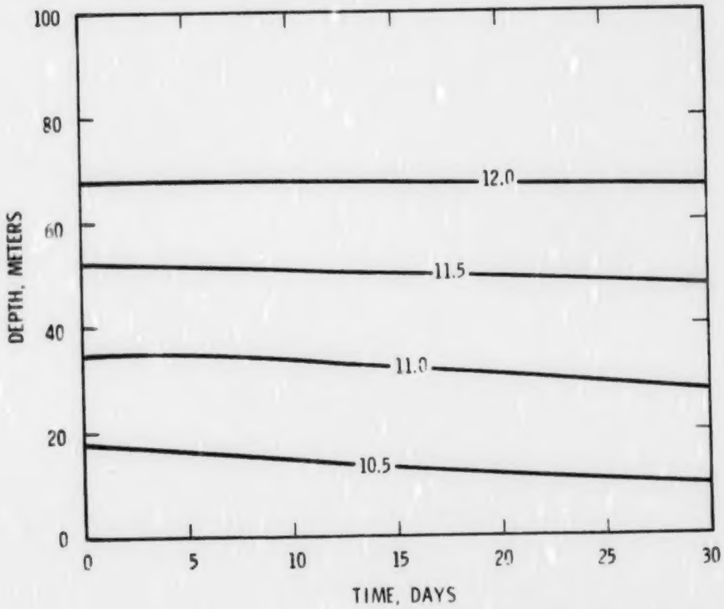

FIGURE 48. RESERVOIR QUALITY SIMULATION TEMPERATURE (°C)

SECTION IX

PROGRAM SYNOPSIS, CAPABILITIES AND LIMITATIONS

The individual hydraulic and water quality models discussed above have been coded in FORTRAN V to operate on most present-day digital computers. Of the two major components of EXPLORE-I, one models river and estuary systems and one models thermally stratified reservoirs. Each of these is a separate general-purpose computer code.

The river basin program is capable of modeling one-dimensional open channel flow in streams and rivers and two-dimensional flow in shallow lakes and estuaries. It consists of a hydraulic code which calculates the required water velocities, depths, and flows and a quality code which evaluates the quality parameter reactions and routes the constituents through the system. The reservoir program predicts temperature, flow patterns, and the distribution of water quality parameters in deep reservoirs.

The capabilities and limitations, the input requirements, and the expected results of each program will be summarized here. A more detailed explanation is provided in the user's manual.

RIVER BASIN PROGRAM

The river basin program is a river and estuary model designed to allow the user to study the effects of various river flows, different,waste discharge locations, and numerous treatment facilities on the water quality levels in a river basin. The rivers, shallow lakes, and estuary portions of the basin are modeled as a series of junctions connected by channels. The locations of these junctions are selected by the user in consideration of:

- locations of major point waste sources;
- distribution of diffuse waste sources;
- major hydraulic sources;
- changes in stream or river characteristics which affect input data;
- locations of available quality and hydraulic data; and
- desired accuracy and computer run times.

Preceding page blank

The physical data which must be supplied by the user include elevations, widths, depths, channel lengths, surface areas, and Manning coefficients of the channels. In addition, the values for the constants which describe the quality parameter reactions and temperatures must be input for each river reach in the basin. The program has been designed so that the input data are simple to organize and use. Constant or time varying hydraulic additions or withdrawals can be made at each node and constant or time varying waste discharges can be located at each node. The program allows both tidal cycles and diurnal cycles to be considered simultaneously.

Operation of the hydraulic code is separate from that of the quality code. The results of the hydraulic code, the flows, velocities, volumes and elevations needed by the quality model, are printed out on the lineprinter and on magnetic tape. After the tape has been made, the quality code uses hydraulic data to route the water quality parameters. The quality calculations give the concentration history of each water quality parameter at each node in the system. A special printing routine allows the user to search for specific results and to obtain printout of items of interest only.

RESERVOIR SIMULATION PROGRAM

The primary function of the Deep Reservoir simulation program is the prediction of temperatures, flows, and water quality changes. The computer program basically solves the mass transport (advection-diffusion) equations and the water reactions (water quality models) for the equilibrium concentrations. Predicted chemical changes in quality due to the dynamic interactions between dissolved oxygen, biochemical oxygen demand, algal populations, and the principal nutrients are superimposed onto the calculated changes due to advective-diffusive transport.

A layered discretization is used to represent the water body so that the geometry of a reservoir is idealized as a composite segment consisting of finite horizontal elements. Several of the existing thermal-hydraulic codes for stratified reservoirs use this type of discretization. Simulation with the Deep Reservoir Thermal code is prerequisite to application of the Deep Reservoir Quality simulation program. Temperature and flow profiles are essential inputs, as are horizontal surface areas which characterize the geometry. Input-output modifications must be made to other thermal-hydraulic codes for proper interface with the Deep Reservoir Quality code. Basically, data such as horizontal and vertical flow rates, temperatures, wind speed, number of layers (element), areas, etc. must be output to a magnetic tape file for later use by the quality module. Other intrinsic input requirements of the reservoir quality code related to the specific quality models: rate constants, decay contstants, effective diffusion constants, time steps, etc.

Quality predictions are output by the program at specified print intervals in the form of concentration profiles for each quality parameter. Concentration histories are printed at the specified print time interval.

APPLICATION OF THE EXPLORE-I MODEL

The EXPLORE-I model is a versatile and useful scientific tool for evaluation of alternative strategies of water quality management. In the hands of experienced analysts and decision-makers, this model can be efficiently used to find sound and economical solutions to complex water pollution problems in many different types of water systems including estuaries and bays, streams and river networks, lakes and reservoirs, and combinations of these. Application of EXPLORE-I is relatively inexpensive, far less than for large-scale sampling programs.

REFERENCES

1. O'Connor, D. J. and W. E. Dobbins. "Mechanism of Reaeration in Natural Streams." Transactions of ASCE, Vol. 123, p. 641, 1956.

2. Dobbins, W. E. "BOD and Oxygen Relationships in Streams." ASCE, Proc. Journal of the Sanitary Engineering Division, Vol. 90, No. SA3, Part 1, Paper 3949, pp. 53-78, June 1964.

3. Thackston, E. L. and P. A. Krenkel. "Reaeration Predictions in Natural Streams." ASCE, Proc. Journal of the Sanitary Engineering Division, Vol. 95, No. SA1, Paper 6407, pp. 65-94, February 1969.

4. Feigner, K. D. and H. S. Harris. "Documentation Report: FWQA Dynamic Estuary Model." U.S. Department of the Interior, Federal Water Quality Administration, July 1970.

5. Callaway, R. J., K. V. Byram and G. R. Ditsworth. "Mathematical Model of the Columbia River from the Pacific Ocean to Bonneville Dam - Part I." Federal Water Pollution Control Administration, Pacific Northwest Water Laboratory, pp. 155, November 1969.

6. Metcalf & Eddy, Inc. "Storm Water Management Model." Vol. 1-4. Palo Alto, California; University of Florida, Gainesville, Florida; and Water Resources Engineers, Inc. Walnut Creek, California.

7. "Prediction of Thermal Energy Distribution in Streams and Reservoirs." Prepared for the State of California Department of Fish and Game by Water Resources Engineers, Inc., Walnut Creek, California, Revised Edition, August 1968.

8. "Mathematical Models for Prediction of Thermal Energy Changes in Impoundments." Prepared for the Water Quality Office, Environmental Protection Agency, by Water Resources Engineers, Inc., Walnut Creek, California, December 1969.

9. Clay, H. M. and E. G. Fruh. "Selective Withdrawal at Lake Livingston: An Impoundment Water Quality Model Emphasizing Selective Withdrawal." Progress Report EHE 70-18 CRWR 66, University of Texas at Austin, Department of Civil Engineering, November 1970.

Preceding page blank

References (continued)

10. Ryan, P. J. and D. R. F. Harleman. "Prediction of the Annual Cycle of Temperature Changes in a Stratified Lake or Reservoir: Mathematical Model and User's Manual." Massachusetts Institute of Technology, Department of Civil Engineering, Ralph W. Parsons Laboratory for Water Resources and Hydrodynamics, Technical Report No. 137.

11. Markofsky, M. and D. R. F. Harleman. "A Predictive Model for Thermal Stratification and Water Quality in Reservoirs." Massachusetts Institute of Technology, Department of Civil Engineering, Ralph W. Parsons Laboratory for Water Resources and Hydrodynamics, Technical Report No. 134.

12. "Mathematical Models for the Prediction of Thermal Energy Changes in Impoundments - Computer Application Supplement." Presented to FWPCA, Columbia River Thermal Effects Project, by Water Resources Engineers, Inc., Walnut Creek, California.

13. Carnahan, B., H. A. Luther, J. O. Wilkes. Applied Numerical Methods. John Wiley and Sons, Inc., New York, 1969.

14. Price, H. S., J. C. Cavendish, R. S. Varga. "Numerical Methods of Higher-Order Accuracy for Diffusion - Convection Equations." SPE Journal, pp. 293-303, Sept. 1968.

15. River Mile Index, Willamette River and Tributaries. Prepared by the Hydrology Subcommittee, Columbia Basin Inter-Agency Committee.

16. 1967 Water Resources Data for Oregon, Part 1. Surface Water Records, United States Department of the Interior Geological Survey - Water Resources Division.

17. 1967 Water Resources Data for Washington, Part 1. Surface Water Records, United States Department of the Interior Geological Survey - Water Resources Division.

18. Willamette River Basin. State Water Resources Board, Salem, Oregon, June 1967.

19. Lower Willamette River Basin. State Water Resources Board, Salem, Oregon, June 1965.

20. Middle Willamette River Basin. State Water Resources Board, Salem, Oregon, June 1963.

References (continued)

21. Swift, C. H. III. "Appraisal of Streamflow in the Tualatin River Basin, Washington County, Oregon." United States Department of the Interior Geological Survey - Water Resources Division, 1971.

22. "Velocity, Average Depth and Cross-Sectional Area Versus Willamette River Mile from Willamette Falls to the Middle Fork of the Willamette."

23. Dempster, G. R. Jr. and G. A. Lutz. "Water Discharge Determinations for the Tidal Reach of the Willamette River from Ross Island Bridge to Mile 10.3, Portland, Oregon." United States Department of the Interior, Portland, Oregon, 1967.

24. Detroit Reservoir Project - Water Quality Data. NPD, Portland, Oregon, February 1968.

25. Parker, F. (personal communication), Dept. of Civil Engineering, Vanderbilt University, Nashville, Tennessee, May 13, 1972.

26. Anderson, J. (personal communication), Dept. of Civil Engineering, Vanderbilt University, Nashville, Tennessee, May 13, 1972.

27. Tichnor, B. (personal communication), EPA, Water Quality Laboratory, Corvallis, Oregon, May 12, 1972.

28. King, D. (personal communication), Bureau of Reclamation, Denver, Colorado, May 15, 1972.

29. Personal communication to L. Rosener from Water Resources Engineers, Inc., Walnut Creek, California.

30. Chan, C. W. and G. T. Orlob. "Ecologic Simulation for Aquatic Environments." Prepared for the Office of Water Resources Research, U. S. Dept. of Interior by Water Resources Engineers, Inc., December 1972.

ACKNOWLEDGMENTS

The Battelle-Northwest study team wishes to express its sincere appreciation to the State and Federal agencies which facilitated this investigation and to the many individuals whose cooperation and advice contributed to the successful completion of the work. The help of Mr. Kenneth Feigner, project officer, and the able staff of the Environmental Protection Agency, Planning Assistance Branch is particularly appreciated. Special thanks are extended to Dr. Warren Westgarth (Director of Laboratories and Applied Research for the State of Oregon) for his generous provision of field data and his extensive understanding of the Willamette River Basin.

The authors wish to extend their grateful appreciation to Leila Counts for her excellent contributions in editing and preparing the final report and to thank Jan Greenwell, Velva Harris, Loretta Howard, and Chris Jacobsen for typing the final draft.